Pharmacological treatment of Autoimmune Polyendocrine Syndrome type I with Rapamycin, a mTOR inhibitor

Master thesis in Pharmacy

Solveig Henriette Einevoll

Centre for Pharmacy,
Department of Clinical Science and
KG Jebsen Centre for Autoimmune Diseases

University of Bergen

May 2020

List of content

Acknowledgement

First, I would like to express my sincere gratitude to my supervisors Anette Susanne Bøe Wolff, Bergithe Eikeland Oftedal, and Eirik Bratland for never-ending enthusiasm and feedback through the writing process. Especially thanks to Anette Susanne Bøe Wolff and Bergithe Eikeland Oftedal for amazing guidance throughout the learning process and in technical training, their patience and encouragement has been outstanding!

I am also very grateful to all the members of the lab group, led by professor Eystein Sverre Husebye, creating an inclusive work environment and for being highly interested and helping. Special thanks to Lars Ertesvåg Breivik for teaching me the ELISA method and for feedback on my writing, and to Alexander Hellesen for guidance in the performing of ELISA. I would also like to thank the lab technicians Hajirah Muneer and Elisabeth Halvorsen for valuable technical help, always patiently answering my questions. I would also like to thank fellow master student in pharmacy Thea Sjøgren and PhD. candidates Sigrid Aslaksen and Amund Holte Berg for useful advises in the lab and for sharing your thoughts.

I would like to thank my family and friends, for always being loving and supporting. A special thanks to my partner Eirik Wiese for your endless patience and support, and for keeping me company through this special time.

This project took place in the period August 2019- May 2020. Funding for the project was provided by the Kristian Gerhard Jebsen foundation, the University of Bergen and the Western Norway Health Authority, and carried out at the lab facilities at Department of Clinical Science.

Solveig Henriette Einevoll
May 2020

UNIVERSITY OF BERGEN

HELSE BERGEN
Haukeland universitetssjukehus

Abstract

Autoimmune polyendocrine syndrome type 1 (APS-1) is a rare autoimmune disease, where the T cells fail to distinguish between self and non-self, due to mutations in the *Autoimmune Regulator, AIRE*, gene. To ensure self-tolerance, the regulatory T cell linage (T_{reg}) plays a crucial role, and *AIRE* is thought to be important in their development in the thymus. Patients with APS-1 display a wide variety of autoimmune manifestations and the treatment options are limited. Hence, there is a great need of studies on targeted treatment. As studies have found that T_{reg} are reduced in numbers and function in APS-1 patients, we hypothesized that the autoimmunity in patients with APS-1 is affected by a deficiency in the development or differentiation of T_{reg} modulated by the mTOR pathway.

We here aim to establish a cell-based drug screening system to study the effect of the mTOR-inhibitor rapamycin, in cell culture of PBMC from APS-1 patients and healthy controls. First, we investigated the expression of mTOR-related genes in blood from patients and controls to select genes of interest to study in our cell-based system. Then, we established an *in vitro* assay using PBMCs to study the effect of rapamycin in patients and controls.

From the mTOR signaling pathway analysis, two genes (*INS* and *mTOR*) were selected in addition to *CTLA-4,* for follow-up in the *in vitro* assay. Overall, no large differences between patients and controls were found, although a trend toward decreased expression was observed after treatment with rapamycin. From the *in vitro* assay, we found that both cell proliferation and IFN-γ production decreased after treatment with rapamycin. At the protein level, significant differences of the expression of CD31, a marker for recent thymic migration, and CD39, a marker for T_{reg} function, were observed. The frequency of T_{reg} in APS-1 patients and controls were comparable, with a decreasing trend when treated with rapamycin.

We did observe an immunosuppressive effect of rapamycin in our *in vitro* assay. But with a limited number of APS-1 patients we are unable to draw any firm conclusions from this study. However, we have successfully established an *in vitro* cell culture system to analyze the effect of rapamycin, which can be used for screening of other potential drugs on APS-1 patient cells in the future.

Abbreviations

21-OH: 21-hydroxylase

APC: Antigen-presenting cell

AIRE: Autoimmune regulator

APECED: Autoimmune polyendocrinopathy-candidasis-ectodermal dystrophy

APS-1: Autoimmune polyendocrine syndrome 1

BCR: B cell receptor

BSA: Bovine serum albumin

CD: Cluster of differentiation

CsA: Cyclosporine A

cT: Conventional T cell

cTEC: Cortical thymic epithelial cell

CTL: Cytotoxic T cell

CTLA-4: Cytotoxic T-lymphocyte-associated antigen 4

DC: Dendritic cell

DMSO: Dimethyl sulfoxide

DN: Double-negative

DP: Double-positive

ELISA: Enzyme-Linked Immuno-Sorbant Assay

G-ß-L: G protein ß-subunit-like protein

GF: Growth factor

FKBP-12: FK binding protein-12

FOXP3: Forkhead box P3

Ig: Immunoglobulin

IFN: Interferon

IL: Interleukin

INS: Insulin

IPEX: Immune dysregulation, polyendocrinopathy, enteropathy, X-linked syndrome

iTreg: Induced regulatory T cell

MHC: Major histocompability complex

mTEC: Medullary thymic epithelial cell

mTOR: Mammalian target of rapamycin

mTORC1: Mammalian target of rapamycin complex 1

mTORC2: Mammalian target of rapamycin complex 2

Nrp-1: Neuropilin-1

NK: Natural killer

nT$_{reg}$: Natural regulatory T cell

PPR: Pattern recognition receptor

PAMP: Pathogen-associated molecular pattern

PBS: Phosphate-buffered saline

PBMC: Peripheral blood mononuclear cell

PI3K: Phosphoinositide 3-Kinase

PKB: Protein Kinase B

PTEN: Phosphatase and tensin homolog

RA: Rheumatoid arthritis

ROAS: Register for organ specific autoimmune diseases

S6K: Protein 6 kinase

SLE: Systemic lupus erythematosus

SP: Single-positive

STAT: signal transducer and activator of transcription

TCR: T cell receptor

T$_H$ cell: Helper T cell

TGF-b**:** Transforming growth factor b

TLR: Toll-like receptor

TRA: Tissue-restricted antigen

T$_{reg}$: Regulatory T cell

1. Introduction

The immune system protects the host from a wide range of viruses, bacteria and fungi that we are all exposed to in our daily life. When such pathogens invade an organism, it has to overcome several hindrances to settle in the host and cause disease. To prevent this, we are dependent on a rapid immune response. In vertebrates, the immune system is divided in two, the innate and the adaptive, each part consisting of a wide range of cells and molecules with effector functions (figure 1.1) [1, 2]. Cooperation between these two systems through cell-contact, cytokines and chemokines is crucial for their protective mechanisms [3]. This demands a strict control to prevent damage of tissue and providing a tolerance to "self", where the suppressor T cell linage, regulatory T (T_{reg}) cells, is considered a key controller. If this control is not maintained, an imbalance in immunological defence and self-tolerance can cause autoimmunity [4]. There exists over 80 autoimmune diseases, where some are rarer than others [5]. An example of a rare, monogenic autoimmune disease is autoimmune polyendocrine syndrome type 1 (APS-1). After onset of APS-1, the symptoms are managed by replacing hormones and suppressing the mechanisms driven by aberrant immunity [6]. APS-1 is a T cell mediated disease, and to provide a better care, the search for new treatment is needed. In the following, a brief introduction of the innate and adaptive immunity is given, to further focus on APS-1, the function of T_{reg} in immune response, and how enhancing T_{reg} function potentially provides a better management of autoimmunity in APS-1.

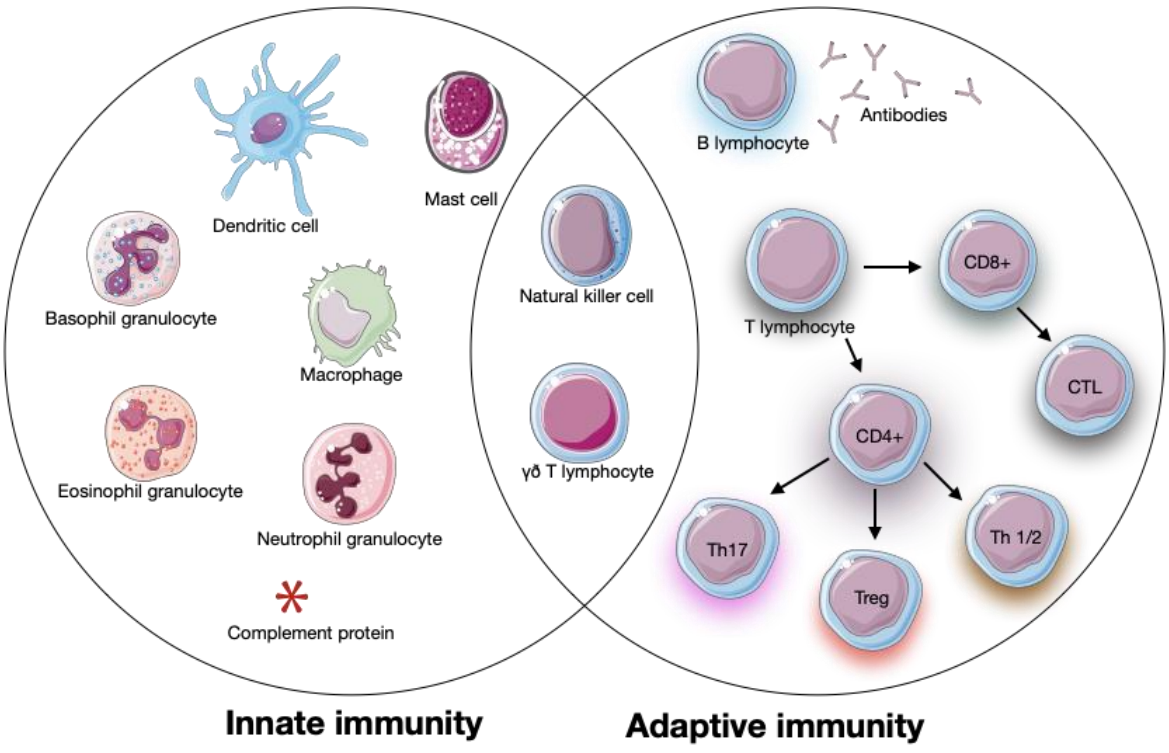

Figure 1.1: The cells involved in innate and the adaptive immunity. *The precursors of all immune cells are hematopoietic stem cells from the bone marrow that differentiate into a wide range of cells with different protection functions. The innate immune response is mediated by granulocytes (neutrophil, eosinophil and basophil) together with mast cells, dendritic cells, NK cells and macrophages. The adaptive immune response is mediated by T and B cells, that further divide into different subclasses. The cells in the interface between the two systems are involved in the interaction between the systems, together with other cells, such as antigen presenting cells in the innate immune system. Modified from Oliveira et. al.[7] using Servier Medical Art.*

1.1 Innate immunity

The innate immune system is the host's first line of defence. This is a fast acting, natural and non-specific response to invaders consisting of epithelial barriers and multiple defending cells, that do not develop memory of the invader [8]. These cells, such as natural killer cells (NK) and dendritic cells (DCs) (figure 1.1), rely on recognition of pathogen-associated molecular patterns (PAMPs) presented on the pathogen´s surface. PAMPs are recognized by pattern recognition receptors (PRRs) on the surface of the immune cells, such as toll-like receptors (TLR) [9]. Effector mechanisms like phagocytosis can then start immediately, and chemokines and cytokines are produced to induce additional protective mechanisms [10]. In addition to cells, there are numerous circulating plasma proteins and protein fragments with an effector function in innate immunity. About 30 of these constitute the complement system, a highly efficient effector mechanism leading to a cascade of reactions. The compliment system is activated directly by pathogens or by antibodies released from B cells bound to the bacteria [11, 12].

Although the innate immune system is an immediate response, these immune cells do not recognise or manage to protect the host from all invaders and sometimes need help from the adaptive immune system. The crosstalk between these two systems occurs by antigen presenting cells (APCs), such as DCs, and signalling molecules [10, 13]. When an invader is recognised by PRRs on the surface of DCs, the invader is engulfed through phagocytosis and a peptide representing the invader is brought to the surface, bound to major histocompatibility complex (MHC) molecules. Further, cells of the adaptive immune system can recognise this peptide by binding to MHC and start an immune response [14, 15]. An example of this is when DCs migrate to lymphoid tissues to present antigens to T-lymphocytes that in turn initiate an antigen specific immune response [16].

1.2 Adaptive immunity

The adaptive immune system is the host´s second line of defence, an acquired and specific response to foreign substances. Although the response is slower than for innate immunity, immunological memory is developed. This part consists of lymphocytes divided in two subsets, T and B lymphocytes responsible for cell mediated and humoral immunity, respectively [1, 17]. Both T and B lymphocytes arise in the bone marrow, where the B cells also mature before migrating to lymphatic organs. The precursor T cells emerge to the thymus to mature before entering the lymphatic system [1].

1.2.1 B cells

B cells mature in the bone marrow where they go through clonal deletion, and self-reactive B cells die by apoptosis. They further migrate to the peripheral lymphoid tissue to mature into subsets of B cells when activated [18, 19]. This activation occurs when B cells recognize antigens through the B cell receptor (BCR), consisting of membrane bound immunoglobulins (Igs) [20]. Further, B cells differentiate into plasma- and memory-cells [21]. These subclasses are specialized to attack invaders, specially extracellular pathogens and toxic compounds, where memory cells rapidly respond when re-exposed to the specific antigen [17]. Plasma cells release specific antibodies, with the same antigen-specificity as their BCR, that neutralize the specific pathogen to further be phagocytosed by macrophages and neutrophils, also leading to activation of the complement system [11, 12]. To do so, B cells are dependent on activation by cluster of differentiation (CD)4^+ T cells through recognition of antigenic peptides, presented in MHC class II on the B cell [22].

1.2.2 T cells

T cells go through a strict process in the thymus, involving multiple proliferative selection events resulting in mature naïve T-lymphocytes, committed to either CD8 or CD4, also known as cytotoxic T cells (CTLs) and effector T helper (T_H) cells, respectively (figure 1.1) [23]. These conventional T (cT) cells are involved several protective mechanisms. CTLs are involved in destruction of virus-infected cells and cancerous cells. They directly and specifically attack the infected cell by lysis, thereby preventing further replication of the pathogenic agent [24, 25]. T_H are involved in activation of both CTLs and B-cells by receptor contact and the release of a wide range of cytokines [16, 26]. Furthermore, T_H can differentiate into the subclasses T_{H1}, T_{H2}, T_{H17} and T_{reg} cells depending on the signal of initiation (figure 1.1) [27].

1.2.3 T cell development

In the thymus, T cells go through a strict process where they differentiate into subclasses and are tested for functionality and autoreactivity. Precursor T cells reach the thymus through the blood vessels, entering the thymic stroma in a double negative (DN) state, $CD4^-CD8^-$. Further, these thymocytes go through multiple stages in the outer cortex where the TCR are rearranged to develop TCRs, consisting of a α- and β-chain or the variation of a γ- and δ-chain [28, 29].

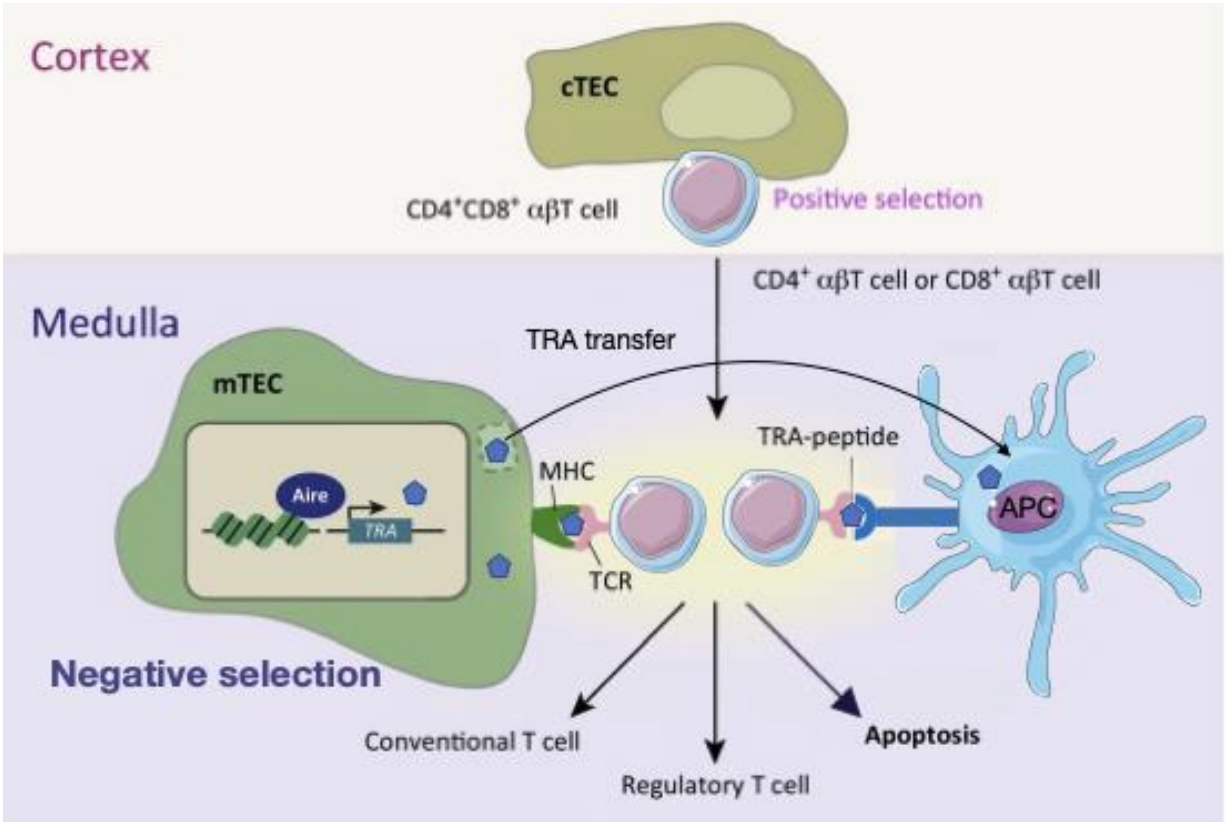

Figure 1.2: **T cell development in the thymus**. *The developing T cell goes through a positive selection in the cortex, before moving into the medulla going through negative selection, where a wide range of tissue restricted antigens (TRAs) are presented to the T cells by medullary thymic epithelial cells (mTECs). These antigens are induced by the autoimmune regulator (AIRE), ensuring self-tolerance. Some of the peptides are transferred to antigen presenting cells (APC), such as dendritic cells (DCs), also presenting them to the T cell. Modified from Takaba et. al. [30] using Servier Medical Art.*

During positive selection, the DN thymocytes which interact with cortical thymic epithelial cells (cTECs) with specificity to a host MHC-peptide complex on cTECs, will be kept and exit the cortex as $CD4^+CD8^+$ (DP) cells, where all other cells will die by apoptosis (figure 1.2). To enter a single positive (SP) stage where the cells commit to either the $CD4^-CD8^+$ or $CD4^+CD8^-$

-lineage, the cells goes through a subsequent selection, called negative selection. When entering the medulla, the thymocytes that bind with too high affinity against the host peptide presented by MHC on the surface of medullary thymic epithelial cells (mTECs) are autoreactive thymocytes and will go through apoptosis. Thymocytes with no or low affinity towards self-antigens proceed to the periphery as mature T cells (figure 1.2) [29, 31].

As a part of the negative selection, the transcription factor Autoimmune Regulator (AIRE) control the expression of tissue-restricted antigens (TRAs), found in mTECs (figure 1.2) [32]. TRAs pose a self-shadow of proteins found in the hosts´ organs and cells. This process is essential for the development of the T cell repertoire and the acquisition of self-tolerance [31, 33, 34]. It is further suggested that AIRE also has a pivotal role in thymic selection of regulatory T cells (T_{reg}) which control the activity of T_H cells in the peripheral tolerance [33, 35, 36]. The development of T_{reg} is suggested to occur when the immature thymocytes recognize TRAs with an intermediate strength, where the expression of Forkhead boxP3 (FoxP3) commits the T cell to a T_{reg} fate [37].

1.2.4 T cell activation

Both naïve and memory T cells continuously patrol secondary lymphoid organs [23], searching for pathogens presented by an APC. By cell mediated immunity, the TCR complex consisting of CD3 together with the co-receptor CD4 or CD8, can interact with MHC glycoproteins; CD4 interacts with MHC class II, and CD8 with MHC class I (figure 1.3) [16]. Peptides fits in specialised binding sites of MHC glycoproteins, and a specific immune response is initiated towards the protein that the peptide is derived from [38, 39]. In addition to these interactions, other co-stimulatory signals are needed for activation of the immune response. Such signals are induced by CD28, a protein presented on the T cell to interact with CD80/CD86 presented on APCs (figure 1.3). This occurs when the affinity between the TCR and MHC is strong enough, if not, CD28 will not be presented on the T cell and it goes into anergy, a state where T-cells fail to respond and are unable to be re-stimulated [40-42].

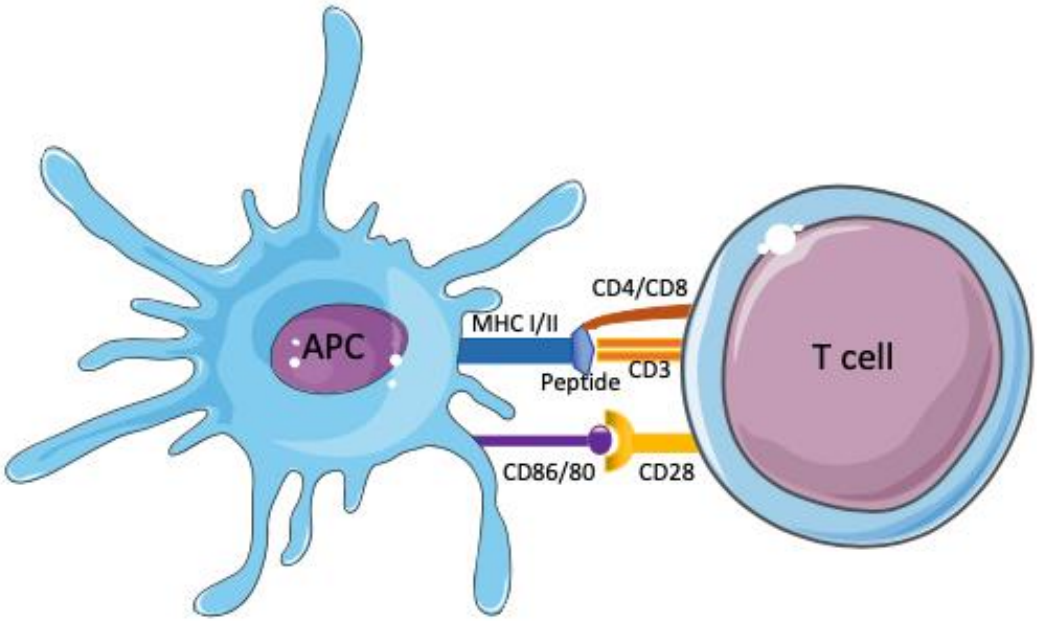

Figure 1.3: Activation of T cells by an antigen presenting cell (APC). *The activation of T cells goes through several signals. A peptide bound MHC on the surface of the APC is presented to the T cell and binds to CD3 and CD4 or CD8, dependent on the T cell, in addition to co-stimulatory signals through CD86/80 and secretion of cytokines. Modified from [43] using Servier Medical Art.*

Finally, to complete the activation, a signal involving inflammatory cytokines such as interleukin (IL)-12, IL-2 and type I interferons (IFN) is needed [44]. CD28 also provides naïve T cells with a co-stimulatory signal for promoting IL-2 production and cell expansion, preventing anergy induction and cell death. In contrast, the cytotoxic T-lymphocyte-associated antigen 4 (CTLA-4), competes with CD28 for the binding of CD80/CD86, and "down-regulate" the effector mechanisms when bound [36]. The expression of CTLA-4 is strictly regulated and is localized both intracellular and extracellular. Further, it is suggested that the extracellular CTLA-4 receptor is upregulated upon activation of T cells [45]. The CTLA-4 receptor provides a suppressive function and is associated with T_{reg}, where it is constitutively expressed [43, 46].

1.2.5 Regulatory T cells

T_{reg} are also known as suppressor T cells and are a subpopulation of T_H cells, playing a role in maintaining peripheral tolerance to self-antigens, and constitutes between 5-10% of the peripheral $CD4^+$ T cell pool [47]. Attention is given to this specific subpopulation for their ability to control inflammation and autoimmune responses, to promote the growth of tumour cells [48], and especially for its ability to suppress proliferation of self-reactive $CD4^+$ and $CD8^+$ T cells [49]. $CD4^+CD25^+$ T_{reg} can be divided in two subpopulations, naturally arising T_{reg} (nT_{reg})

and induced T_{reg} (iT_{reg}). nT_{reg} differentiate in the thymus before migrating to the periphery, whereas iT_{reg} diverges from T_H cells in the periphery [50].

To discriminate T_{reg} from other $CD4^+$ T cells in experimental studies, both extracellular and intracellular markers are used. FoxP3 as an intracellular marker was defined as the master transcriptional factor linked to the function of T_{reg} along with the α-chain of the extracellular IL-2 receptor (IL-2R), CD25 [48, 51]. Even though many T cells express CD25 upon activation, studies have shown that mice with IL-2 deficiency developed severe multi-organ autoimmunity due to a poor pool of $CD4^+CD25^+$ T cells [36]. Similar effects have also been shown for CD25 deficient mice, but these could be prevented by injecting them with $CD4^+CD25^+$ T cells from normal otherwise genetically identical mice [36, 52]. These two studies indicate that IL-2 and CD25 is crucial in preventing autoimmunity, and further suggested that IL-2 signaling is linked to the expression of FoxP3 in both nT_{reg} and iT_{reg} through the signalling pathways PI3K, Akt and mTOR [52]. IL-2 leads to inhibition of these signalling pathways and increases the expression of FoxP3 [53, 54], resulting in a larger pool of T_{reg}. Furthermore, studies in mice implicate that T cells with mTOR-deficiency differentiate into $FoxP3^+$ T cells [55].

To distinguish between nT_{reg} and iT_{reg} it has been suggested that the markers Helios, Neuropilin-1 (CD304) and CD31 can be used. Helios, a member of the Ikaros transcription factor family and an intracellular marker, is suggested to be restricted to nT_{reg}, and to have a role in maintaining stability and regulatory function of T_{reg} [48]. The extracellular marker CD304 is identified to be expressed in nT_{reg} [56], stabilizing the expression of FoxP3 by potentiating PTEN, a protein phosphatase negatively regulating PI3K [48]. CD31 is an extracellular marker with high expression in T cells recently emigrated from the thymus, while T cells with lower expression of CD31 are suggested to be aged T_H cells reflecting a reduced thymic output [57].

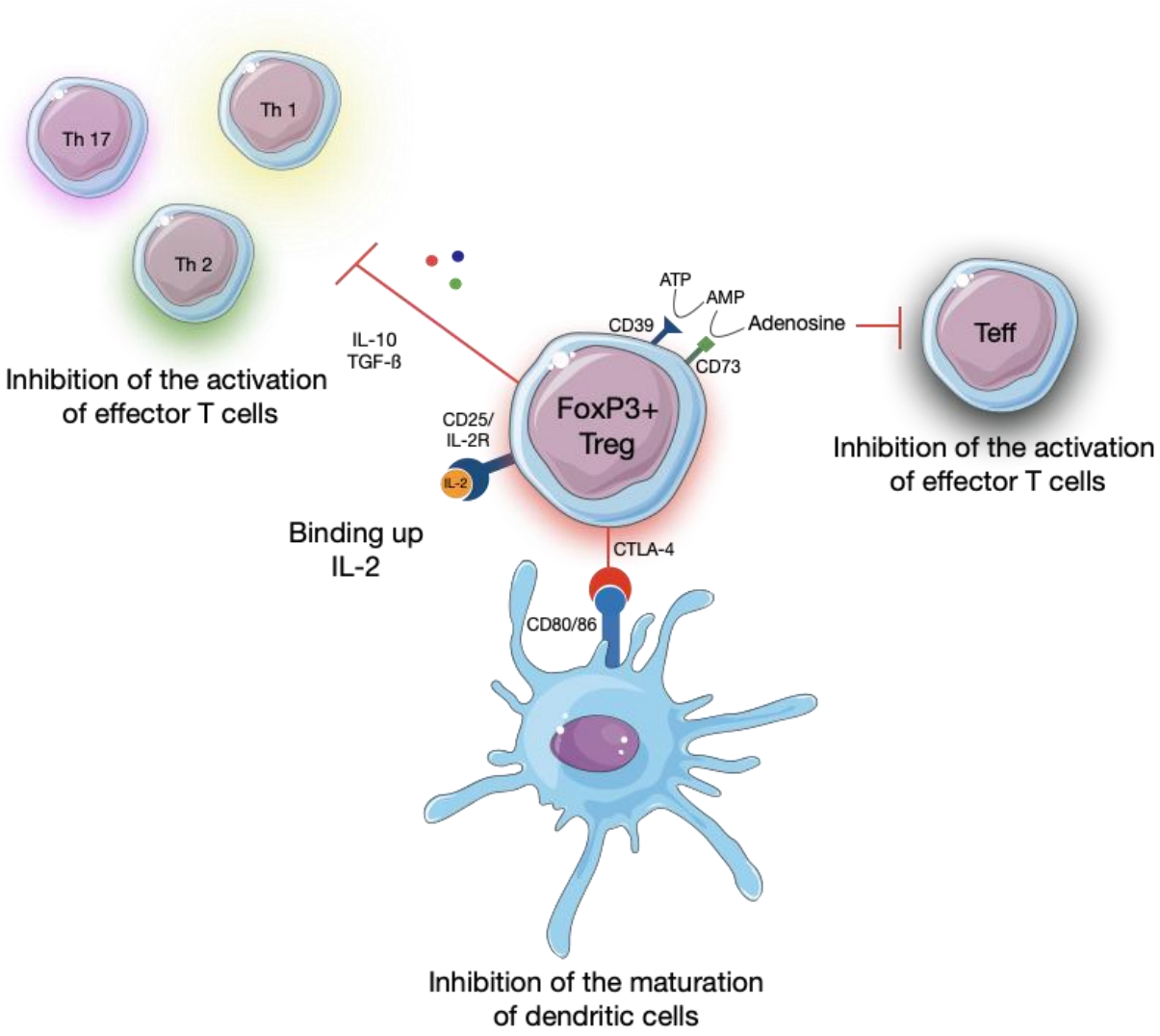

Figure 1.4: Regulatory T cell suppressive function. *Regulatory T cells have multiple suppressive functions, by producing the immune suppressive cytokines IL-10 and TGF-ß, and with the expression of IL-2R to bind up IL-2, making the cytokine less available for non-regulatory T cells. Furthermore, the expression of inhibitory molecules, CTLA-4 and CD39, inhibit maturation of DCs and activation of effector T cells, respectively. Bars represent inhibition. Modified from Braza et.al. [58] using Servier Medical Art.*

There are probably several modes of function for T_{reg} (figure 1.4). It is suggested that the high expression of CD25 on T_{reg} competes for the IL-2 produced by T_H cells , making it less available for nonregulatory T cells [59]. Furthermore, it has been shown that the immunosuppressive function of T_{reg} is dependent on CTLA-4. This surface receptor is important as a checkpoint inhibitor for autoreactive T cells as a homolog to CD28 with higher binding strength, which does not stimulate the production of cytokines. [43, 46]. Another receptor expressed on T_{reg} cells having immunosuppressive properties is the ectoenzyme CD39, which alternate the level of adenosine in the environment surrounding T_{reg} (figure 1.4) [60, 61].

In addition to interacting directly through cell-to-cell contact, T_{reg} produces the cytokines IL-10 and TGF-ß, which are central for their suppressive function (figure 1.4). IL-10 inhibits the production of other cytokines important for immune responses in T cells and have an anti-inflammatory and suppressive effect on most haematopoietic cells. TGF-ß has an immunomodulatory effect by suppressing the function in multiple cells [46, 62, 63], in addition to play a role in maintaining the peripheral T_{reg} population and suppressing IFN-γ, a proinflammatory cytokine produced by activated T cells [54, 64]. Furthermore, it has been shown in mice that TGF-ß inhibits the antigen-specific proliferation of naïve T cells [65].

With all mechanisms mentioned above, T_{reg} have a crucial role in maintaining peripheral tolerance, preventing autoimmunity. When this tolerance is broken either due to the lack of T_{reg} or dysfunction in this subpopulation it can cause severe autoimmunity [36, 37].

1.3 Autoimmunity

Up until the 1950s, the idea of the immune apparatus attacking self-antigens was questioned and considered absurd [66]. Now it is well established that autoimmunity occurs, even though the details of the pathogenesis and etiology of most autoimmune diseases is not fully understood [67]. When trying to understand the origin, researchers have suggested that autoimmunity can be influenced by genetics, gender, environment and medicines, and that viral infections can break down the tolerance to self and trigger an autoreactive cascade [68-70]. Autoimmune diseases affect approximately 8% of the general population, where women are most affected. What is clear is that autoimmunity is a result of an imbalance between effector and regulatory immune responses [71].

Based on the immune response, autoimmune disorders can be divided into two classes, organ-specific and systemic autoimmune diseases [72, 73]. An example of systemic autoimmunity is systemic lupus erythematosus (SLE), where almost any organ in the body could be a target for autoimmune inflammation. In SLE the targets for the immune response are typically ubiquitous expressed substances like DNA [74]. In contrast, tissue-restricted autoimmune disease is directed against self-antigens presented in one (or several) particular organ or tissue, such as type 1 diabetes or autoimmune primary adrenal insufficiency (Addison´s disease). When a person acquires more than one organ specific endocrine autoimmune disease, it is called an autoimmune polyendocrine syndrome [75].

1.4 Autoimmune polyendocrine syndrome type 1

Autoimmune polyendocrine syndrome type 1 (APS-1) is a rare condition also referred to as autoimmune polyendocrinopathy- candidiasis- ectodermal dystrophy (APECED) [76]. It has a prevalence of roughly 1:100.000 in most countries and is estimated to occur in about 1:90.000 in Norway [76, 77]. This polyglandular disorder is diagnosed when at least two of the three following manifestations is present; chronic mucosal candidiasis, chronic hypoparathyroidism and Addison´s disease, where the first signs of APS-1 usually occur early in childhood [78]. In addition to these manifestations, a number of other endocrine and non-endocrine symptoms also occur frequently such as enamel hypoplasia, enteropathy, pancreatic insufficiency pneumonitis, and primary ovarian failure (figure 1.5) [6, 76]. These patients have a high death and mortality rate, where most of the deaths occur before the age of 45 years, and the most common causes of death are due to the endocrinopathies, such as hypocalcemia and adrenal crisis [79].

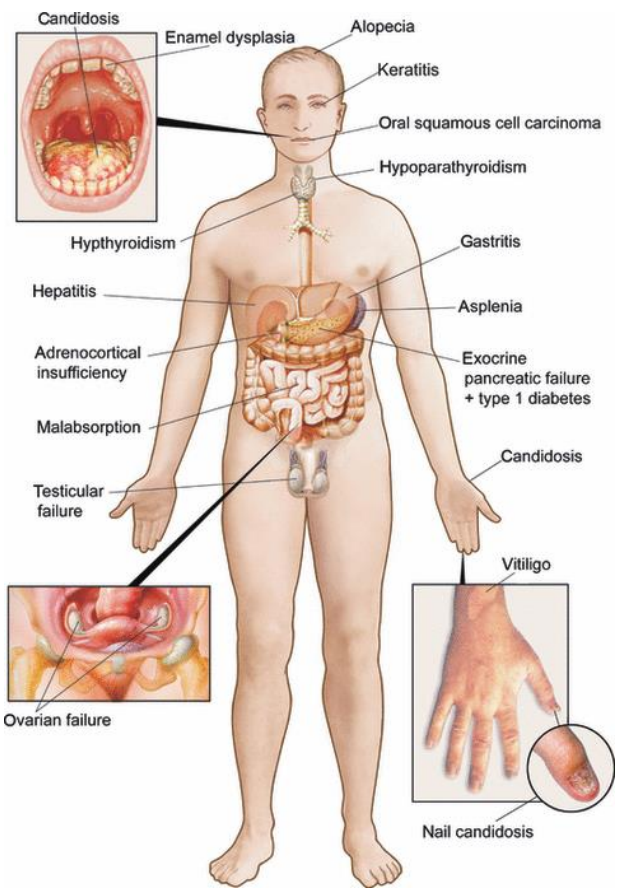

Figure 1.5: Clinical manifestations of APS-1
There are many potential manifestations and great variation among patients. Figure from Husebye et. al [6].

The disease is characterized by autoantibodies against several defined antigens, such as autoantibodies against the enzyme 21-hydroxylase (21-OH), expressed in the adrenal cortex [75]. Some autoantibodies appear early in the development of the disease, such as those against the immune mediators IFN-alpha (α) and especially IFN-omega (ω). These autoantibodies are apparently restricted to APS-1, making it possible to diagnose APS-1 early [80].

APS-1 is an autosomal recessive T cell mediated disease caused by loss of function of the AIRE protein. Mutations in the *AIRE* gene causes potentially autoreactive T cells to escape negative selection, further leading to autoimmune inflammation in selected organs [77]. This is thought to be a plausible explanation for why APS-1 patients have autoimmunity to multiple organs

[32]. In addition, the differentiation of T_{reg} seems to be affected [33]. A flow cytometry study of PBMC showed that the frequency of $CD4^+$ $CD25^+$ $FoxP3^+$ T_{reg} in APS-1 patients was significantly lower than in age- and sex-matched healthy controls [81]. The deficiency of T_{reg} in APS-1 patients could be due to the lack of both thymic development and peripheral activation [82]. In the periphery this could be due to lack of necessary activation signals, that T cells fail to upregulate FoxP3 upon activation [83], or that conventional T cells are resistant to the suppressive mechanisms of T_{reg} [84].

1.5 Pharmacological treatment of APS-1

Today the treatment of patients with APS-1 is based on their manifestations, where chronic mucocutaneous candidiasis generally is managed with oral nystatin (azole drug) and oral amphotericin B (polyene drug). Hypoparathyroidism is treated with oral vitamin D in combination with calcium and magnesium supplements, or parathyroid hormone [6]. Addison's disease is treated with cortisone acetate and fludrocortisone [76]. In the treatment of APS-1 patients there are several challenges, both due to the disease and the medication. Some patients have malabsorption leading to poor absorption of calcium and vitamin D [85]. On top of that, there are challenges with interactions between the drugs in the treatment, and that drugs are vulnerable to resistance. The azole drugs mechanism works by targeting ergosterol, the major sterol in the fungal plasma membrane [86]. By inhibiting the steroidogenesis, there is a risk of inducing adrenal insufficiency [6]. To avoid azole-resistance, azole drugs are combined with the polyene amphotericin B, an antifungal agent with another mechanism [76, 86].

Some patients are also treated with immunosuppressant cyclosporine A (CsA) to improve pancreatic insufficiency [85]. The mechanism of action of CsA is by blocking the transcription of cytokine genes such as IL-2 and IL-4, hence, inhibiting T cell activation [87]. Rituximab, another immunosuppressant has been reported to prevent pneumonitis and malabsorption [76]. Rituximab binds to CD20 on B-cells and induces cell death and B cell depletion [88]. To get a better treatment for patients with APS-1 the best target is yet to be identified, and there is a need for studies of drugs with possible beneficial immunosuppressant functions. A potential target for treating APS-1 could be expansion of T_{reg}, which seems to be central in the dysfunctional immune system in APS-1 patients.

1.6 The role of mTOR in autoimmunity and expansion of T_{reg}

The protein kinase mammalian target of rapamycin (mTOR) is a member of the phosphatidylinositol-3-OH kinase (PI3K)-related kinase family, a complex intracellular signaling pathway. mTOR consists of two multi-protein complexes, mTOR complex I (mTORC1) and mTOR complex II (mTORC2), put together with the regulatory associated proteins Raptor and Rictor, respectively, in addition to G protein ß-subunit-like protein (G-ß-L) (figure 1.6) [89, 90]. The role of mTOR is broad, having an impact in several mechanisms regulating cell growth and several cellular processes.

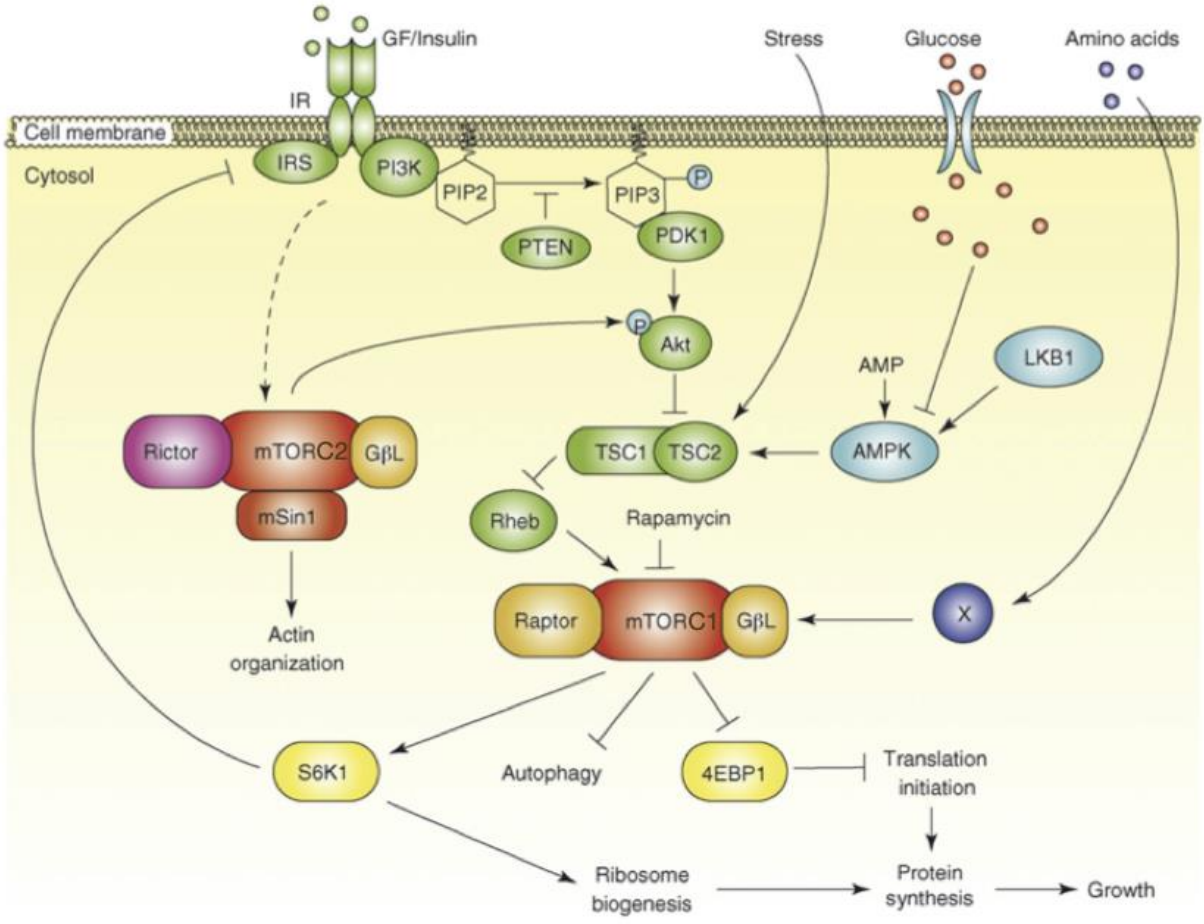

Figure 1.6: Signaling network of mTOR. *The role of mammalian target of rapamycin (mTOR) is broad, having a central role in cell growth and proliferation. The signaling network is complex, where activation and inhibition can be stimulated by several factors. Arrows and bars represent activation and inhibition, respectively. Figure modified from Tsang et. al. [91].*

mTOR is shown to be crucial for the function and development of T_{reg} and T_H cells. An increased signaling through mTOR can magnify the inflammatory environment in T_H cells. In T_{reg}, by contrast, the activity of mTOR has to be held back to maintain their suppressive function

[48]. Activation of mTOR goes through several mechanisms, where the enzyme phosphatidylinositol 3-kinase (PI3K) and Akt has central roles, in addition to loss of the tumor suppressor phosphatase and tensin homolog (PTEN) (figure 1.6) [90, 92].

IL-2 signaling through IL-2R and prolonged occupation of the TCR and CD28 surface molecule [93], or stimulation with growth factors (GF), can lead to activation of PI3K and a phosphorylation cascade activating Akt [90, 94]. mTORC1 is the major downstream component, regulating cell proliferation and metabolism (figure 1.6) [95]. Inhibition of mTORC1 is shown to increase the amount of T_{reg} in addition to suppress T cell activation and proliferation, hence giving a immunosuppressive effect promoting immune tolerance [96]. Moreover, $CD4_+$ T cells with a lack of mTOR were unable to differentiate into effector cells [89].

Drugs inhibiting the mTOR-signaling pathway are used in the treatment of cancer, allograft rejection and some autoimmune disorders. Such drugs are everolimus, temsirolimus and rapamycin [97].

1.7 Rapamycin, a mTOR inhibitor

Rapamycin, also known as Sirolimus, was first isolated in the early 1970s from a solid sample of Streptomyces hygroscopic discovered on the Easter Island, where this macrolide was found to be a potent anti-fungal agent (Figure1.7) [98]. Studies also showed that this inhibitor of mTOR has a strong immunosuppressive effect, as mTOR is an important regulator of T cells [99, 100], due to the mechanisms mentioned above (section 1.6).

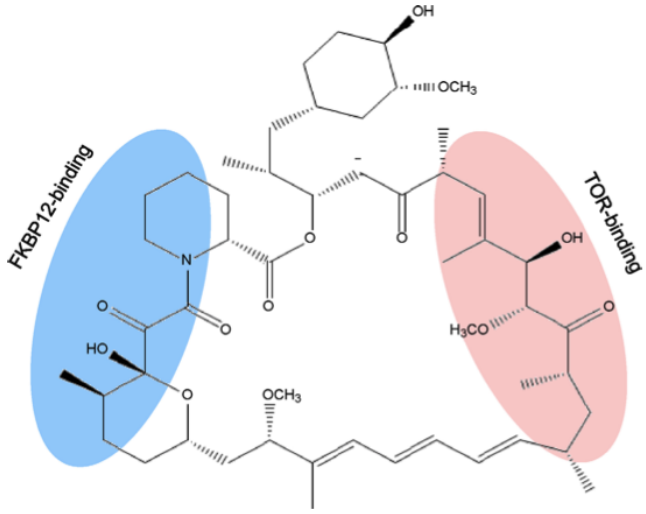

Figure1.7: Molecular structure of rapamycin. *The mTOR-binding domain is coloured in pink and the FKBP-12 binding domain is coloured in blue. Figure from Tsang et. al.* [91].

Rapamycin interacts with the immunophilin FK binding protein-12 (FKBP-12) to be biological active, making a complex inhibiting mTORC1 in a direct and potent way (figure 1.8) [91, 100, 101]. This leads to suppression of cT cells by blocking the cytokine-stimulated protein synthesis [95, 102], and inhibition of the T cell-cycle progression by blocking G1 to S phase after activation [103]. This also affects the differentiation of T_H cells, where mTORC1 activation is necessary for the differentiation of T_{H1} and T_{H17} cells, and mTORC2 in the case of T_{H2} cells [55, 89, 104]. In addition, rapamycin has been shown to stimulate the catabolic processes autophagy and cell death [91, 101, 105]. Further it is suggested that rapamycin promotes TCR-induced T cell anergy in the presence of co-stimulation, and blocks IL-2-induced proliferation without affecting the co-stimulation-dependent IL-2 production [103].

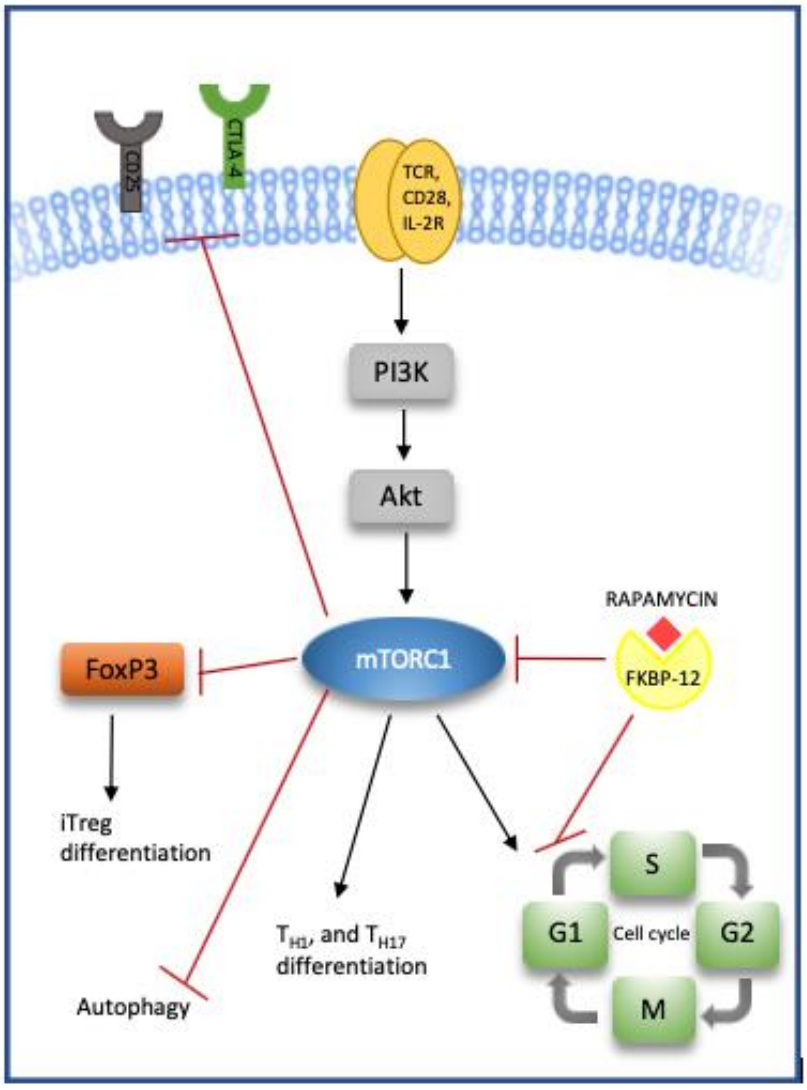

Figure 1.8: The effect of rapamycin on T cells. *Rapamycin binds to FKBP-12 making a complex inhibiting mTORC1 and blocks the cell cycle in G1 to S phase, thereby inhibiting the differentiation of T_{H1} and T_{H17}, and cell growth. Naturally mTOR downregulates the expression of FoxP3 and stops autophagy, in the presence of rapamycin these functions are blocked. Arrows and bars represent activation and inhibition, respectively. Modified from Mcmahan et. al. [96] and Chapman et. al [56].*

In contrast to cT cells, it is suggested that T_{reg} are less sensitive to rapamycin due to their high expression of PTEN, where IL-2 stimulation leads to JAK/STAT signaling regulating FoxP3 [96]. Others suggest that rapamycin promotes the function of T_{reg} due to stabilization of FoxP3 expression [48]. A study in cell culture has shown that T_{reg} treated with a pulse treatment of rapamycin had an increased expression of CD25 and CTLA-4, giving them an enhanced suppressive function compared to nontreated T_{reg} [106].

Not only has rapamycin an effect on T cells, it is suggested that rapamycin also has a suppressive effect on antigen-presenting cells, such as IL-4 dependent DC maturation, reducing DC-mediated antigen uptake and presentation, and consequently less activation of T cells [104].

1.8 Clinical use of rapamycin

The pharmaceutic rapamycin, mainly used to prevent transplant rejection, is thought to be a beneficial therapeutic in autoimmune diseases. Clinical studies have shown the effect of rapamycin in RA, a T cell mediated autoimmune disease, where the dysfunction of T cells is associated with activation of mTOR and a lack of peripheral T_{reg} [107]. Another example is SLE, where an open-label clinical trial suggests that the disease activity was reduced due to treatment with Rapamycin [108]. Interestingly, rapamycin has been shown to successfully control gastrointestinal and dermatologic symptoms and reduced the inflammatory reactions, in the monogenic autoimmune disease immunodysregulation polyendocrinopathy enteropathy X-linked syndrome (IPEX), a disease where the clinical picture has some overlap with APS-1. IPEX is a rare disease also being T-cell mediated, with a dysfunction in the transcription factor FoxP3 [6, 109, 110]. With the effects suggested in IPEX, RA and SLE, rapamycin could potentially have a positive effect on APS-1 patients, being a monogenic T cell mediated disease that can be associated to the mTOR-signaling pathway.

Even though rapamycin has several beneficial effects as an immunosuppressant, there are some side effects that have to be taken into consideration in treatment. The optimal dose varies in patients, and also does the likelihood of potential side effects, where weekly drug monitoring is required to titrate the dose [111]. Rapamycin is available in tablet form and oral solution. The oral absorption is poor, with an extensive uptake in erythrocytes [112]. In a clinical report, IPEX patients were treated with 0.15 mg/m^2 rapamycin daily with oral administration, and the serum levels were in the range 8-15 ng/mL [109]. Suppressing the immune system is likely to

predispose the host to viruses, infections, and even cancer. Studies have shown that some patients treated with rapamycin had higher cholesterol levels, and leuko-and thrombocytopenia were observed in others [113, 114]. In a long term treatment for five years of three IPEX patients using rapamycin, no significant side effects was reported [109, 110]. But as rapamycin is largely metabolized in the intestine and liver by cytochrome P450 (CYP) 3A4, an enzyme involved in the metabolization of several drugs, there is a risk of interaction with other treatments [112].

1.9 Research front

In the search for new targets to treat APS-1, mTOR was chosen for this project, due to a preliminary study performed by a previous master student, Marte Heimli. In the study, a significant increase in the expression of mTOR in patients with APS-1 compared with healthy controls was discovered. mTOR has an important role in the development of the T_{reg} linage, which has been shown to be reduced in APS-1 patients in comparison with age-and sex-matched healthy controls [81].

Furthermore, the research group is aware that clinical specialists in APS-1 have used the mTOR-inhibitor rapamycin in off label treatment of malabsorption in severe cases (personal communication). Rapamycin is also used in other diseases where there is a lack of T_{reg}, such as RA and SLE [107, 108]. In several IPEX and IPEX-like patients it was shown that rapamycin successfully controlled the gastrointestinal and dermatologic symptoms and reduced the inflammatory reactions for up to five years without significant side effects [109, 110].

By repurposing drugs, already validated and approved medication is investigated for the potential benefit in other disorders than its original intended use. This strategy to identify new treatment is both time- and cost-saving, and most importantly safer to use as the pharmacokinetics and pharmacodynamics of the drug is more familiar.

1.10 Hypothesis and aim

Our hypothesis is that the autoimmunity in patients with APS-1 is affected by a deficiency in the development or differentiation of T_{reg} modulated by the mTOR pathway. To explore this, we aimed to establish a cell-based drug screening system and specifically study the effect of treating PBMC from APS-1 patients with the mTOR-inhibitor, rapamycin.

The specific aims are:

1) Establish a cell-based system to test the outcome of different drugs at the KG Jebsen Centre for Autoimmune Diseases

2) Assess the gene expression pattern in the mTOR-signaling pathway at the RNA level in APS-1 patients and controls
    a. Assessment of the gene expression in whole blood from controls and patients, in order to select candidate genes to be further assessed in samples treated with rapamycin by qPCR.
    b. Determine the expression of the candidate genes (from 2 a) in activated PBMC treated or untreated with rapamycin in cell culture, from controls and patients by the use of qPCR.

3) Investigate the outcome of rapamycin treatment of PBMC at protein level
    a. Determine the expression of selected markers for T_{reg} in activated PBMC treated or untreated with rapamycin in cell culture, for controls and patients by the use of flow cytometry.
    b. Determine the levels of IFN-γ in activated PBMC treated with rapamycin in cell culture by ELISA, to assess the differences in samples treated with rapamycin and untreated samples.

2. Materials

2.1 Chemicals and reagents

Reagents and chemicals	Supplier	Ref.No.
Dulbecco's Phosphate Buffered Saline	Sigma Life Science	D8537
AB serum	Sigma Life Science	H4522
Dimethyl Sulphoxide (DMSO)	Sigma-Aldrich	D2650
FBS, Quaified, HI	Gibco	10500-064
PAXgene blood RNA-kit	Qiagen	762174
RNeasy micro plus kit	Qiagen	74034
RLT buffer	Qiagen	79216
BD Pharm Lyse	BD Biosciences	555899
b-mercaptoethanol	Aldrich chemistry	M6250
Absolutt Alkohol	Kemetyl Norge	200-578-6
RNeasy micro plus kit	Qiagen	74034
RT_2 Profiler PCR Array, Human mTOR Signaling	Qiagen	KD02-R1
Anti-CD3 V500, clone UCHT1	BD	561416
Anti-CD25 PE-Cy7	BD	335824
CellReace CFSE cell proliferation kit	Thermo Scientific	C34554
RPMI-1640 Medium	Sigma-Aldrich	R7388
L-glutamine	Sigma-Aldrich	G5792
Penicillin-streptomycin	Sigma-Aldrich	P4333
Rapamycin	Sigma-Aldrich	R0395
Live/dead Fixable Yellow Dead Cell stain kit	Life technologies	L34959
BSA		
Human Fc block	BD	564220
Anti-CD4 FITC, clone M-T466	Miltenyi Biotec	130-080-501
Anti-CD4 AF700, clone RPA-T4	BD	557922
Anti-CD8 PerCP-Cy5.5, clone SKI	BD	65310
Anti-CD25 PE, clone 4E3	Miltenyi Biotec	130-091-024
Anti-CD45RA APC-H7, clone HI100	BD	560674
Anti-CTLA4 BV421, clone BN13	Biolegend	369606
Anti-CD39 PE, clone ebioA1	Invitrogen	12-0399-42
Anti-CD31 BV786, clone L133.1	BD	744757
Anti-CD304/Neuropilin-1 BV650, clone U21-1283	BD	8297659
Anti-FOXP3 PE-CF594, clone 236A/E7	BD	9129576

Anti-CD127 APC, clone MB15-18C9	Miltenyi Biotec	130-098-121
Anti-Helios APC, clone 22F6	Biolegend	B260687
TaqMan Gene Expression Master Mix	Applied Biosystems	4369514
B2M, TaqMan gene expression assay (VIC)	Thermo Fisher	4448490
CTLA-4, TaqMan gene expression assay (FAM)	Thermo Fisher	4331182
mTOR, TaqMan gene expression assay (FAM)	Thermo Fisher	4331182
INS, TaqMan gene expression assay (FAM)	Thermo Fisher	4331182
RNA 6000 Pico Reagents	Agilent Technologies	5067-1513
High capacity RNA-to-cDNA kit	Applied Bisosystems	4387406
SuperScript III first-stand cDNA synthesis kit	Invitrogen	18080051
DEPC Treated Water	Invitrogen	AM9915G
Water Nuclease Free	VWR	436912C
MACS BSA Stock Solution	Miltenyi Biotec	130-091-376
Phosphate buffered saline 99.5%	Sigma Life Science	D8537
Superscript III first-strand synthesis system for rt-PCR	ThermoFisher	18080051
ELISA MAX Deluxe set for Human IFN- γ	BioLegend	430104
Tween 20	Sigma-Aldrich	9005-94-5
Sulfuric acid, (H_2SO_4)	Sigma-Aldrich	339741

2.2 Equipment

Equipment and consumables	**Supplier**	**Ref.no.**
CPT-tubes	BD	362753
PAXgene blood RNA tubes	BD	762165
Vortexer V1S000	IKA	4047700
5810R Centrifuge	Eppendorf	
Heraeus multifuge 3SR+	Thermo Fischer	
Kinetic energy 26 joules minicentrifuge	VWR	C1413V
Thermomixer	Eppendorf	
Disposable pipettes	VWR	1612-1613
ART Barrier reload insert pipette tips:	Molecular bio products	
10 µL		2139-RI
100 µL		2065-RI
200 µL		2069-RI
1000 µL		2179-RI

Clip-tips 300 µL	Thermo Scientific	94420513
Finnpipette F1 pipettes	Thermo Fischer	
Fastpette Pipetboy	Integra	
Pipette tips, 10 mL	Sterilin	475110
Centrifuge tubes 15 mL	VWR	21008-216
Centrifuge tubes 50 mL	VWR	21008-242
Polypropylene round-bottom tube, 5 mL	Falcon	352063
Safe-lock tubes 1.5 mL	Eppendorf	0030 120.086
Cryogenic vials 1.5 mL	Nalgene	5000-1020
MicroAmp 8-tube strip, 0.2 µL	Applied Biosystems	N8010580
MicroAmp 8-cap strip	Applied Biosystems	N8010535
MACSxpress separator	MiltenyiBiotec	130-098-308
LS Column	MiltenyiBiotec	130-042-401
MidiMACS separator	MiltenyiBiotec	130-042-302
Scepter sensor 40 um	EMD Millipore corporation	PHCC40050
MicroAmp Optical 96 well reaction	ThermoFisher	N8010560
384 Well Multiply PCR Plate	Sarstedt	72.1984.202
Load Cover	Qiagen	KH29
MicroAmp Optical Adhesive film	Applied Biosystems	4213663
QiaShredder Columns	Qiagen	79656
MicroAmp 8-tupe strip, 0.2 µL	Applied Biosystems	N8010580
MicroAmp 8-cap strip	Applied Biosystems	N8010535
Flowmi Cell Stainer 40 uM	Bel-Art H-B Instruments	J333189
Chip Priming station	Agilent Technologies	5065-4401
RNA Pico Chips	Agilent Technologies	5067-1530
IKA MS 3 S36 basic chip vortex	IKA	

2.3 Instruments

Instruments	**Supplier**
Scepter 2.0 cell counter	Merck
LSR Fortessa flow cytometer	BD
NanoDrop ND-1000 Spectrophotometer	Saveen Werner
ABI Prism 7900HT sequence detection system	Thermo Fisher
Agilent 2100 Bioanalyzer	Agilent technologies
Spectramax Plus	Molecular Divices
GeneAmp 9700 PCR system	Applied Biosystems

2.4 Software

Program	Supplier
ABI Prism 7900 HT SDS 2.3	Applied Biosystems
FlowJo 10	FlowJo, LLC
ND-1000 3.8	Thermo Fisher
2100 Expert	Agilent Technologies
GraphPad prism 8.0	GraphPhad Software
SoftMax Pro	Molecular Divices
Servier Medical Art (https://smart.servier.com)	Les Laboratories Servier, Suresnes, FR

3. Methods

3.1 Experimental pipeline

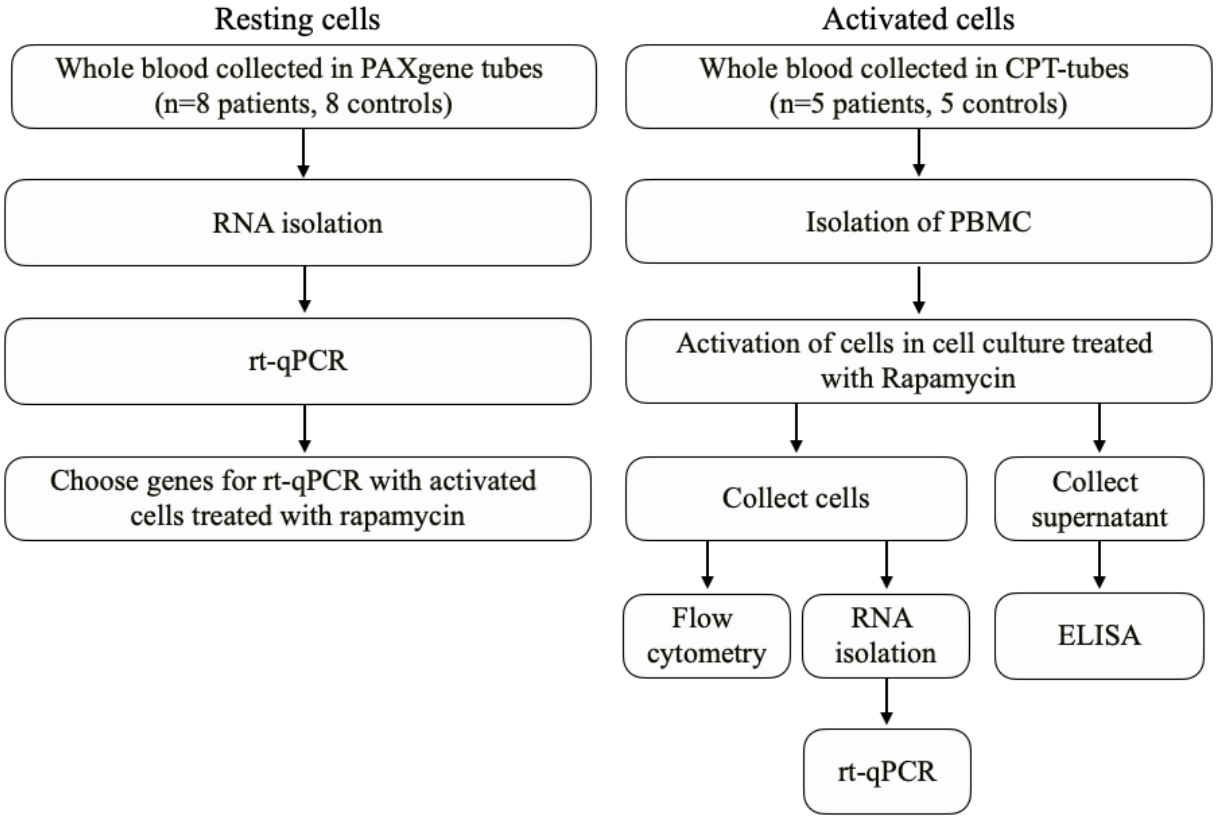

Figure 3.1: Overview of the experimental pipeline. *For the rt-qPCR of resting cells (left panel) RNA was isolated from whole blood collected in PAXgene tubes. For the experiments with activated cells (right panel) peripheral mononuclear cells (PBMC) were isolated from whole blood by density gradient centrifugation. RNA from PBMC and PBMC treated with rapamycin in cell culture were used for real-time qPCR. Flow cytometry of PBMC treated with rapamycin in cell culture was performed to assess the levels and phenotypes of* T_{reg} *in patients and controls. The supernatant from PBMC treated with rapamycin in cell culture were collected for assessment of IFN-* γ *production.*

The main experimental methods used in this project are cell culture, flow cytometry, real time quantitative polymerase chain reaction (rt-qPCR) and ELISA. The source to the material used to implement these methods is whole blood and peripheral mononuclear cells (PBMC) isolated from patients with APS-1 and healthy blood donors. The experimental pipeline is illustrated in figure 3.1.

3.2 Methodological considerations

Two of the main techniques used in this project are cell culture and flow cytometry. PBMC isolated from APS-1 patients and healthy controls were activated and treated with rapamycin to further grow in cell culture. Flow cytometry was chosen to assess the populations of activated cells and T_{reg} at protein level, where treated cells from cell culture were stained using fluorochrome-conjugated antibodies specific for the molecular target of interest. This laser-based technology analyzes single cells or particles by measuring fluorescence from the antibodies bound to the cell. When the cell passes the laser, the fluorochromes are excited to a higher level and spontaneously emits light (fluorescence) at a longer wavelength. The emitted light in the form of fluorescence is collected at selected wavelengths. This makes it possible to measure cell populations expressing specific proteins when antibodies against the proteins are labeled with different fluorophores [115]. In order to assess the proliferation of the cells carboxyfluorescein succinimidyl ester (CFSE) staining were used which measures the amount of cell divisions in the culture [116]. Calculations were performed by FlowJo software 10.6.2.

To investigate the change in expression of markers in controls and patients treated with rapamycin, the Δ Frequency of cells (formula 1) was calculated and differendes between patients and controls further determined statistically by a non-parametric Mann-Whitney test.

(Formula 1) $$\textit{Frequency of cells (untreated)} - \textit{Frequency of cells (treated with rapamycin)} = \Delta\,\textit{Frequency of cells}$$

Rt-qPCR is a method used to assess the expression level of selected genes at the mRNA level. The rt-qPCR methods were performed in four steps; extraction of mRNA from material, synthesise cDNA for mRNA by reverse transcription, amplification of a specific DNA sequence, and detection of the amplified product. The SYBR green technique was used to assess the gene expression in resting untreated cells, to choose the genes of interest for further analysis downstream in activation- and rapamycin treatment experiments. In the method, the SYBR Green dye fluoresces when attached to the double-stranded DNA, generated during the PCR reaction [117].

To assess the gene expression in cells treated with rapamycin the TaqMan technology was chosen, as it is considered a highly sensitive method, and even more specific than SYBR Green.

Here, a TaqMan probe binds to the single-stranded DNA, where a fluorescent reporter and a quencher are attached to the 5´and 3´ends of a TaqMan probe. During polymerization, the DNA polymerase cleaves the reporter dye from the probe, leading to emission of fluorescence. Common for both methods is that the more double-strand product produced, the more fluorescence is detected, and for each cycle the number of templates for each gene investigated is duplicated, and the earlier the signal reaches a threshold the more gene is expressed. For each method the output is given in the form of a C_t-value, a fractional PCR cycle number which is determined when the reporter fluorescence exceeds a given minimal threshold [118, 119].

The raw C_t-values were used to calculate the relative quantification, using the $\Delta\Delta C_t$ method. The target of interest was normalized to a housekeeping gene (HK) (formula 2). Further, the difference in ΔC_t between the sample and calibrator was calculated giving $\Delta\Delta C_t$ (formula 3). Finally, $\Delta\Delta C_t$ is used to calculate the fold-change, a relative expression value of the gene of interest (formula 4) [120].

(Formula 2) C_t *(target)* - C_t *(HK)* = ΔC_t

(Formula 3) ΔC_t *(sample)* - ΔC_t *(calibrator)* = $\Delta\Delta C_t$

(Formula 4) $2^{-\Delta\Delta Ct}$ = *Fold-change*

As an approach to normalize the $\Delta\Delta C_t$ for the samples treated with rapamycin, the untreated samples were used as calibrator.

Enzyme-Linked Immuno-Sorbant Assay (ELISA) is a sensitive technology used to measure the amount of proteins in a sample. In this project it was used to detect the amount of IFN- γ in the supernatant from the cell culture, produced by cells in cell culture treated with rapamycin (+) compared with untreated (-) cells. The selected approach was a commercial sandwich ELISA, where capture antibodies attached to the bottom of a well captures the protein of interest, while the secondary antibody linked to an enzyme provides detection and an amplification factor [121].

3.3 Patients and controls

The APS-1 patient samples were supplied from the world´s largest registry and biobanks of samples from patients with organ specific autoimmune diseases (ROAS), collected by the Endocrine Medicine research group at the Department of Clinical Science, University of Bergen/Haukeland University hospital. The biobank includes samples from patients with Addison´s diseases, where about 50% have an autoimmune polyendocrine syndrome (APS) and about 6% (N=48) are APS I-patients with mutations in *AIRE*. This unique biobank contains PBMCs, EDTA blood and sera.

The control samples were obtained from healthy blood donors from the local blood bank at Haukeland university hospital (HUS). In this project 12 patients (4 females, 8 males, 30-72 years old) and 14 controls were used, matched in both sex and age ($\pm$ 8 years). Detailed information about patients and controls are listed in appendix (table A.1 and A.2). Patient and control samples 1-5 and control 14 was included in the study with treatment of PBMC with rapamycin, while the patient samples 1 and 6-12, and control samples 6-13 was included in the study identifying gene expression in the mTOR signalling pathway.

3.4 Ethical aspects

All patients and controls included in this project have given written consent to use their samples in research. This project goes under the research projects “Immunological and genetic causes of organ specific autoimmune diseases” (project number: 2018/1417), “Autoimmune polyendocrine syndrome type 1” (project number: 2009/2055), and is approved by the Regional Ethical Committee of Western Norway. Biobank project number: 2013/1504.

3.5 PBMC isolation using vacutainer cellular preparation tubes (CPT)

Fresh blood (6-8 mL) was collected in CPT-tubes, containing heparin and Ficoll, and centrifuged at 1800 x g for 15 minutes at 20°C. The layer of mononuclear cells was collected to a separate tube filled up with PBS to a total volume of 15 mL to be centrifuged at 300 x g for 15 minutes at 20°C. The supernatant was removed, the pellet diluted in 10 mL PBS and counted using a scepter handheld cell counter from Merck. Further, the cells were centrifuged at 300 x g for 10 minutes, the supernatant was removed, and the cells resuspended in 500 µL

with AB serum 10% (v/v) DMSO. The samples were frozen gradually to -80°C for 24-72 hours, and subsequently stored at -150°C until use.

3.6 Cell culture and validation of rapamycin concentration

To determine a suitable concentration of rapamycin, serial dilutions was prepared in preliminary cell culture experiments with the concentrations 0.05 nM, 0.1 nM, 1 nM, 2 nM and 4 nM. Each concentration was prepared with DMSO/medium as described below. The concentration of 4 nM rapamycin was decided to be used for the rest of the project.

Wells were coated with anti-CD3 (1 μL/mL) and incubated for 2 hours at 37 °C, or overnight at 4 °C. PBMC were quickly thawed before diluted in 10 mL medium (37 °C) and centrifuged at 300 x g for 10 minutes. MACS dead cell removal kit was used to remove dead cells, following the producer's protocol and live cells were counted using the Scepter handheld cell counter from Merc. The cells were washed with 10 mL RPMI medium (10% FBS, 1% L-glutamine, 1% penicillin-streptomycin) at 300 x g for 10 minutes, the supernatant removed, and the cells resuspended in 1 mL PBS (37°C). The cells were stained with CFSE (5 mM) and incubated for 10 minutes at 37°C. To finish the staining, 2 mL FBS (4°C) were added and the cells incubated on ice for 5 minutes. After incubation, medium (37°C) were added to a total volume of 15 mL and the samples were centrifuged at 300 x g for 10 minutes, the supernatant removed, the pellet resuspended in medium (2 million cells/mL) and anti-CD28 (5 μL/mL) was added. Further, 100 μL cell suspension was added to each well in triplets or more, depending on the number of cells. Rapamycin were dissolved in 1 mL DMSO to a concentration on 25 nM, to further be diluted in medium to the chosen concentration. Rapamycin was diluted in 100 μL medium before added to the cells, while untreated cells received 100 μL medium. The cells were incubated for three days at 37°C with 5% CO2 before being split in to two wells and further incubated for two days and collected at day five.

3.7 RNA isolation from PBMC

RNA from PBMC treated with rapamycin in cell culture from patient and control 1-5 (section 3.6), was purified using RNeasy micro plus kit from Qiagen, following the manufacture´s protocol. Briefly, the sample was collected and resuspended in 350 μL RLT lysis buffer and added to a Qiashredder spin column and centrifuged at max speed for two minutes. The lysate was transferred to a gDNA eliminator spin column and centrifuged for 30 seconds at 10_4 rpm.

The flow through was collected, added 70% ethanol and mixed well, added to the RNeasy MiniElute spin column and centrifuged for 15 seconds at 10_4 rpm, the flow-through were discarded. 700 µL RW1 buffer was added to the RNeasy MiniElute spin column and centrifuged for 15 seconds at 10_4 rpm. The flow-through was discarded and 500 µL RPE buffer was added to the column and centrifuged for 15 seconds a 10_4 rpm. The flow-through was discarded and 500 µL 80% ethanol was added to the column and centrifuging for two minutes at 10_4 rpm. The flow-through was discarded and the column centrifuged with open lid for five minutes at full speed to dry the membrane. At the last step the column was placed in a new collection tube and added 14 µL RNase-free water and centrifuged for one minute at full speed to elute the RNA. The RNA was stored at -80°C if not used immediately.

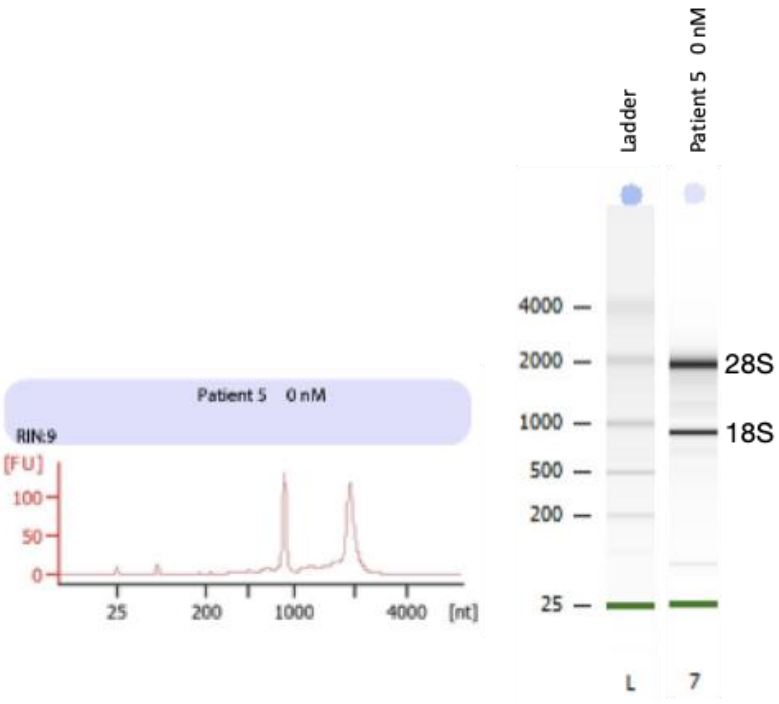

Figure 3.2: Example of Agilent bioanalyzer output for an RNA sample. *The sample from Patient 5 was isolated from activated PBMC in cell culture and used for rt-qPCR with activated cells. The RNA integrity number (RIN) of 9 reflects a high RNA quality (left panel). The simulated gel image for the sample shows two distinct bands for 28S and 18S (right panel).*

The RNA quality was assessed by the Agilent Bioanalyzer, using the Agilent 6000 Pico kit according to manufacturer's protocol (figure 3.2). The RNA concentration was determined by use of a NanoDrop ND-1000 Spectrophotometer, and the samples were stored at -80°C until use.

3.8 RNA isolation from whole blood

Whole blood was collected in PAXgene blood RNA tubes, and the RNA was purified using a PAXgene blood RNA-kit from Qiagen, following the manufactures protocol. Briefly, whole blood was collected in PAXgene blood RNA tubes, washed and centrifuged for 10 minutes at 3000-5000 x g, the pellet resuspended in 350 µL resuspension buffer and transferred to a microcentrifuge tube. 40 µL Protein kinase K and 300 µL binding buffer was added to the tube and incubated for 10 minutes at 55°C using a shaker-incubator at 400-1400 rpm. The lysate was directly transferred to a PAXgene shredder spin column and centrifuged for 3 minutes at 14 000 rpm. The supernatant of flow-through was transferred to a micro centrifuge tube, added 350 pure ethanol µL (96-100%), centrifuged briefly, loaded on a PAXgene RNA spin column and centrifuges for 1 minute at 8000-20000 x g. Then, 350 µL wash buffer was added to the column, centrifuged and the flow-through discarded. 10 µL DNase was added to 70 µL DNA digestion buffer in a microcentrifuge tub, mixed and centrifuged briefly, before 80 µL of the residual liquid was added to the PAXgene RNA spin column and placed on the bench for 15 minutes. 350 µL wash buffer was added to the column and centrifuged. The following step was then performed twice: the spin column was placed in a new processing tube and 500 µL wash buffer was added and the column, centrifuged, the flow-through discarded. The PAXgene RNA spin column was placed in a new microcentrifuge tube, added 40 µL elution buffer and centrifuged. Further, the eluate incubated for five minutes at 65°C and was immediately placed on ice. The RNA was stored at -80°C if not used immediately.

3.9 Real-time quantitative PCR of candidate genes in the mTOR signaling pathway

Whole blood was collected in PAXgene blood RNA tubes, and the RNA was purified using a PAXgene blood RNA-kit from Qiagen (section 3.8). For the cDNA synthesis the manufactures protocol for the RT_2 first strand kit in format E was followed. A genomic DNA elimination mix was made, containing RNA (400 ng), 2 µL buffer GE and RNase-free water to a total volume of 10 µL. This was further incubated for five minutes at 42°C and immediately placed on ice for at least 1 minute. A reverse-transcription mix was made containing: 4 µL 5x BC3 buffer, 1 µL control P2, 2 µL RE3 reverse transcriptase mix and 3 µL RNase-free water to a total volume of 10 µL for each sample. The reverse-transcription mix was added to the genomic DNA elimination mix to a total volume of 20 µL and mixed well. The mix incubated at 42 °C for 15 minutes and the reaction was stopped by incubation at 95 °C for 5 minutes. 91 µL RNase-free

water was added to each reaction and mixed well by pipetting. The reaction was placed on ice in prior to proceed following the real-time PCR protocol in format E. PCR components mix was made in 5 mL tubes, containing: 650 µL 2x RT_2 SYBR green mastermix, 102 µL cDNA synthesis reaction and 548 µL RNase-free water to a total volume of 1300 µL. For each 384-well custom RT_2 profiler PCR array, four samples were added in the amount of 10 µL to each well, analyzing 96 genes per sample including housekeeping genes, genomic DNA control, reverse-transcription control and positive PCR control. The plate was sealed and centrifuged at 1000 g for 1 minute to remove bubbles. The plate was run in an ABI prism 7900HT sequence detection system using the following program: 95 °C for 10 minutes then 40 cycles of 95°C for 15 seconds and 60°C for 1 minute.

3.10 Real-time quantitative PCR of chosen genes

RNA was purified using RNeasy micro plus kit from Qiagen, following the manufactures protocol (section 3.7). Further the Superscript III First-Strand Synthesis System for rt-PCR kit from Thermo Fisher was used to synthesize cDNA from RNA, following the manufactures protocol. For the first-strand synthesis a master mix was made for each sample containing: 0.35 µL random hexamer (50 ng/ µL), 0.35 µL oligo(dT)20 (50 µM), 0.35 µL dNTP mix (10 mM), 0.5 µL DEPC-treated water. 5 µL RNA from each sample was added and mixed by pipetting to a total volume 6.5 µL before incubating at 65 °C for 5 minutes. For the cDNA synthesis a master mix was made, each sample containing: 1 µL RT-buffer (10x), 2 µL $MgCl_2$ (25mM), 1 µL DTT (0.1 M), 0.5 µL RNase out (40 U/ µL), 0.5 µL SuperScript III RT (200 U/µL), 1.5 µL DEPC-treated water. 6.5 µL of the cDNA synthesis a master mix was added to the mix containing RNA to a total volume of 13 µL. The samples were run at the following program in a thermal cycler: 25°C for five minutes, 50°C for 60 minutes, 55°C for 15 minutes, 70°C for 15 minutes. Each sample was diluted 1:1 with DEPC-treated water and used for rt-qPCR. Rt-qPCR was performed using TaqMan gene expression assay. For each sample a mix of 1.65 µL probe/primer, 1.65 µL TaqMan enzyme (2x), 9.35 µL DEPC-treated water was added to 5 µL of the RNA sample (1:2 in DEPC-treated water). The reaction mixture was transferred in triplicates to a clear 384 well plate, 10 µL to each well. A negative control was prepared for each gene expression assay and a housekeeping gene (B2M) was added to each sample. The plate was run in the ABI prism 7900HT sequence detection system at the following grogram: 50 °C for 2 minutes, 95°C for 10 minutes, then 45 cycles of 95°C for 15 seconds and 60°C for 1 minute.

3.11 Flow cytometry

The PBMC from cell culture was collected at day 5 and directly centrifuged at 300 x g for 10 minutes (section 3.6). The supernatant was collected for later use (ELISA), and the pellet resuspended in 1mL PBS with dead cell stain and incubated for 20 minutes in room temperature. After incubation the cells were washed with 1 mL flow cytometry buffer (PBS with 0.5% BSA) and centrifuged at 300 x g for 10 minutes at 4 °C. The supernatant was removed, and the pellet resuspended in 100 µL flow cytometry buffer (PBS with 0.5% BSA) and added Fc block (0.5 mg/mL) for 20 minutes in room temperature before washed as previously described. The supernatant was removed, and the pellet resuspended in 100 µL flow cytometry buffer (PBS with 0.5% BSA). The cells were then stained with surface markers (table 3.1). After incubating for 20 minutes at 4°C protected from light the cells were washed with 2 mL flow cytometry buffer (PBS with 0.5% BSA) by centrifuging 300 x g for 10 minutes at 4 °C. To stain with the intracellular markers, fixation and permeabilization was performed by the anti-human FoxP3 staining set, following the manufacture´s protocol. The cells were added 1 mL perm/fix buffer and incubated at 4 °C protected from light overnight. The day after, the cells were washed with 1 x permeabilization buffer by centrifuging 500 x g for 5 minutes at 20 °C, the supernatant discarded, and the cells resuspended in 100 µL permeabilization buffer. The cells were stained with antibodies against the intracellular markers FoxP3 and Helios (table 3.1), and incubated for 30-60 minutes at 4 °C. Further the cells were washed with 1 x permeabilization buffer by centrifuging 500 x g for 5 minutes at 20 °C and kept on ice until the flow cytometry was performed using the BD LSR Fortessa, at the Flow Cytometry Core Facility, Department of Clinical Science, University of Bergen. To analyze the results FlowJo software 10.6.2 were used.

Table 3.1: Flow cytometry panel. *Overview of targets, fluorochromes, dilution factor and wavelengths used for excitation and collection of emittances.*

Target	Fluorochrome	Dilution factor	Excitation (nm)	Filter for emittance (band pas)
CD3	V500	1:20	407	670/30
CD4	Alexa Fluor 700	1:160	640	730/45
CD8	PerCP-Cy5.5	1:20	488	695/40
CD25/IL2RA	PE-Cy7	1:40	561	780/60
CD45RA	APC-H7	1:80	640	780/60
CD152/CTLA-4	BV421	1:20	407	450/50
CD39/ENTPD-1	PE	1:500	561	582/15
CD31/PECAM-1	BV785	1:160	407	780/60
CD304/Neuropilin-1	BV650	1:80	407	670/30
FoxP3	PE-CF594	1:10	561	610/20
Helios/IKZF2	APC	1:40	640	670/14
Dead cell stain	q-dot585	1:1000	407	585/42
CFSE	FITC	1:10	488	530/30

3.12 Cytokine enzyme-linked immunosorbent assay (ELISA)

ELISA was used to quantify the amount of IFN- γ in the supernatant from the activated PBMC harvested for flow cytometry (section 3.11), using an ELISA MAX Deluxe set for Human IFN-γ delivered from BioLegend, following the manufacture´s protocol. All chemicals were diluted as described in the manufacture´s protocol.

Briefly, supernatant was collected from the cells in cell culture, both untreated and treated with rapamycin. At day one, a 96 well plate was coated with 100 µL capture antibody (1:200), sealed, and incubated over night at 2°C-8°C. The day after, all reagents were brought to room temperature before use and the coated plate washed with at least 300 µL washing buffer. 200 µL assay diluent A (1:5) was added to each well to block non-specific binding and reduce background, the plate was sealed and incubated at room temperature for 1 hour with shaking.

The standard cure was made with 1000 µL of the top standard diluted in assay diluent A (1:5) to a concentration of 500 pg/mL. A six two-fold serial dilution of the 500 pg/mL top standard was performed, and assay diluent A diluted (1:5) was used as the zero standard at 0 pg/mL.

The plate was washed 4 times, and 100 µL of each standard and sample was added to the plate in triplets, the samples were diluted in assay diluent A (1:5) with the dilution factors: 1, 1:25 and 1:100. The plate was sealed and incubated at room temperature for 2 hours with shaking. The plate was washed 4 times with wash buffer, before adding 100 µL detection antibody (1:200) and incubated for 1 hour at room temperature with shaking. The plate was washed 4 times with washing buffer and 100 µL Avidin-HRP solution (1:1000) was added to each well, sealed and incubated for 30 minutes in room temperature with shaking. Further the plate was washed 5 times, where it was soaked in wash buffer for 30 seconds between each wash. Freshly mixed TMB substrate solution was added to each well in the amount of 100 µL and incubated for 20 minutes protected from light. Wells containing IFN-γ now turned blue in color. To stop the reaction, 100 µL stop solution (H_2SO_4, 0.2 M) was added to each well, which turned the positive blue wells into yellow. The absorbance was then read at 450 nm within 15 minutes using Spectramax Plus. The IFN- γ concentration (pg/mL) was calculated from four parameter logistic (4-PL) curve-fit.

3.13 Statistical analysis

For statistical analysis of the rt-qPCR, flow cytometry and ELISA results, both non-parametric two-tailed Mann-Whitney test and parametric paired t-test was used. A non-parametric two-tailed Mann-Whitney test was chosen in the comparison of patients and controls. Two-tailed nonparametric tests were chosen due to the low number of samples avoiding an assumption of a normal distribution, using the median value for the central tendency. In the comparison of treated and untreated samples a two-tailed paired parametric t-test was chosen, as a non-parametric paired test is not suitable for $N<5$ with a significance threshold set at $P<0.05$. Results were found significant if $P < 0.05$ in the flow cytometry results, ELISA results and the rt-qPCR of activated cells. The rt-qPCR results with resting cells were found significant if $P <0.01$ to correct for multiple testing. All analysis was performed by using GraphPad software, prism 8.

4. Results

4.1 Real-time quantitative PCR assessment of genes in the mTOR signaling pathway in resting cells

Isolated RNA from whole blood from patients (patient 1 and 7-12) and controls (control 6-13) were assessed for the expression level of genes in the mTOR signaling pathway (86 genes), all genes are listed in appendix (table A.4). The plates used for rt-qPCR were analysing genes in the mTOR signalling pathway, commercially available by Qiagen. The RNA from patients and controls had a RIN-values ranging from 7.8-9.1 and concentration in the range 63-164 ng/µL. Each sample was only analysed once for gene expression due to limited material available. The cut-off was defined at 40 cycles and the threshold at 0.2; those samples who were undetectable were removed. For the gene *Insulin*, only three of the controls (6,7 and 9) and three of the patients (6,8 and 9) reached the threshold; the others were therefore removed. This was also observed in other samples for nine other genes, but all samples passed the internal controls including housekeeping genes, positive PCR control, RT control and human genomic DNA contamination.

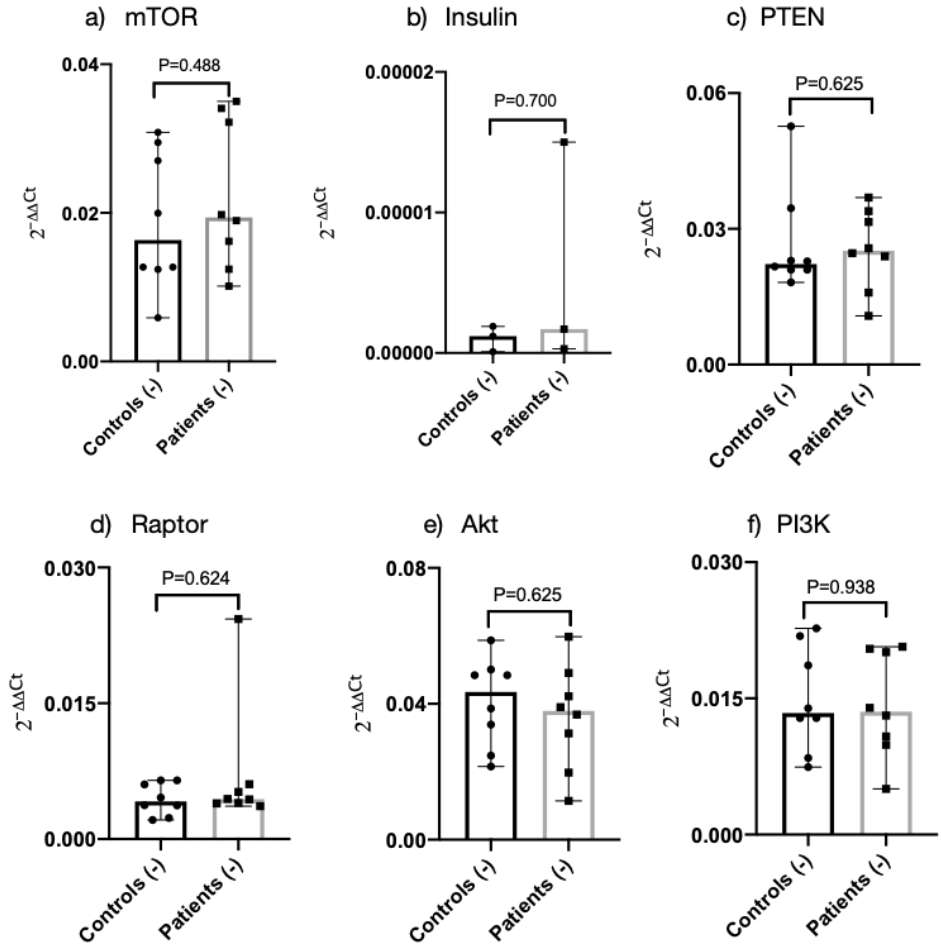

Figure 4.1: Comparing the fold change in patients and controls. *The fold change were calculated using the $2^{-\Delta\Delta Ct}$-formula, showing a relative expression level of the target. The bars illutrates the median fold change value and the error bars shows the 95% CI. (-) means that the cells are not treated with rapamycin. The p-value was calculated using non-parametric Mann-Whitney test, samples were found significant if P<0.01. For insulin only 3 of the controls (6,7 and 9) and 3 of the patients (6,8 and 9) reached treshold, the others are therefore removed.*

For each sample and gene, the fold change was calculated using the $2^{-\Delta\Delta Ct}$-formula, where the fold change for the housekeeping gene is taken into account. No significant difference in controls or patients was observed for any of the genes using the RT^{2}Profiler PCR Array Data Analysis Webportal, nor calculations of the p-value in GraphPad, using a non-parametric Mann-Whitney test (table 4.1). No differences were observed in the expression of genes comparing patients and controls, but a slightly increased expression could be seen for *mTOR* (P=0.488) in the patients (figure 4.1 a, table 4.1). For *Insulin* (P=0.700), one of the patients had a notable expression (figure 4.1 b, table 4.1); this was also observed for *Raptor* (P=0.624) (figure 4.1 d, table 4.1). Some of the other genes *PTEN* (P=0.625), *Akt* (P=0.625) and *PI3K* (P=0.938) (figure 4.1 c, e, f, table 4.1) which are also important in the regulation of mTOR [91], did not show any changes in the expression comparing patients and controls.

Table 4.1: Comparison of the fold change ratio of the relative gene expression between patients and controls in some of the genes in the mTOR signaling pathway.

Gene	Fold change $(\frac{\text{Patient}}{Control})$	Median fold change, controls	95% CI, controls	Median fold change, patients	95% CI, patients	P-value*
mTOR	1.22	0.0163	0.035, 0.007	0.0193	0.035, 0.001	0.488
Insulin	3.41	$1.2 \cdot 10^{-6}$	$6.27 \cdot 10^{-6}$, $-4.13 \cdot 10^{-6}$	$1.7 \cdot 10^{-6}$	$5.22 \cdot 10^{-5}$, $-4.08 \cdot 10^{-5}$	0.700
PTEN	0.94	0.0222	0.041, 0.013	0.0252	0.036, 0.015	0.625
Raptor	1.35	0.0042	0.007, 0.002	0.0044	0.016, -0.002	0.624
Akt	0.85	0.0435	0.052, 0.030	0.0379	0.049, 0.023	0.625
PI3K	0.94	0.0134	0.020, 0.010	0.0135	0.019, 0.010	0.938
IGF1	0.62	$1.4 \cdot 10^{-5}$	$2.36 \cdot 10^{-5}$, $8.49 \cdot 10^{-6}$	$9.0 \cdot 10^{-6}$	$1.63 \cdot 10^{-5}$, $3.70 \cdot 10^{-6}$	0.322
PDPK1	1.43	0.0148	0.025, 0.011	0.0205	0.053, 0.007	0.266

**Non-parametric Mann-Whitney test, results were found significant if P < 0.01.*

When comparing the mean foldchange in patients and controls calculated by RT$_2$ Profiler PCR Array Data Analysis Webportal, *Insulin* had a fold change (patient/control) 3.41 greater for the

patients than for the controls, indicating a 3.41 times larger expression in the patients (table 4.1). Even though only one of the patients had a great expression of *Insulin*, this gene was chosen for further analysis in the assessment of gene expression using RNA from activated cells treated or untreated with rapamycin (section 4.2). The other genes had a fold changes (patient/control) in the range 0.62-1.43 (table 4.1). *mTOR* and *CTLA-4* was also chosen for further analysis, as *mTOR* is the target of rapamycin, and *CTLA-4* is important for the suppressive function in T_{reg} [58, 91]. Fold change (patient/control) for all genes included are listed in appendix (table A.4).

4.2 Real-time quantitative PCR assessment of chosen genes in activated PBMC treated with rapamycin in cell culture

To assess the expression of the genes *mTOR*, *Insulin* and *CTLA-4* in PBMC activated with anti-CD3 and -CD28 and treated with rapamycin in cell culture, RNA was isolated from PBMC after 5 days in cell culture from patient and control 1-5. The RNA used had a RIN-values ranging from 3.7-9.0 and concentrations ranging from 1.7-96.6 ng/µL. When looking at the resulting raw Ct values, the expression of the housekeeping gene *B2M*, run in the same tube as for candidate genes, was observed in all samples with a threshold put to 0.3540 Ct. For the genes of interest, the thresholds for *CTLA-4* and *Insulin* were put to 0.0147 Ct, and for *mTOR* to 0.0195 Ct, reflecting low expression in the selected genes. Due to the low expression of *Insulin* in the treated samples for control 1 and patient 2, they did not reach threshold and was therefore removed.

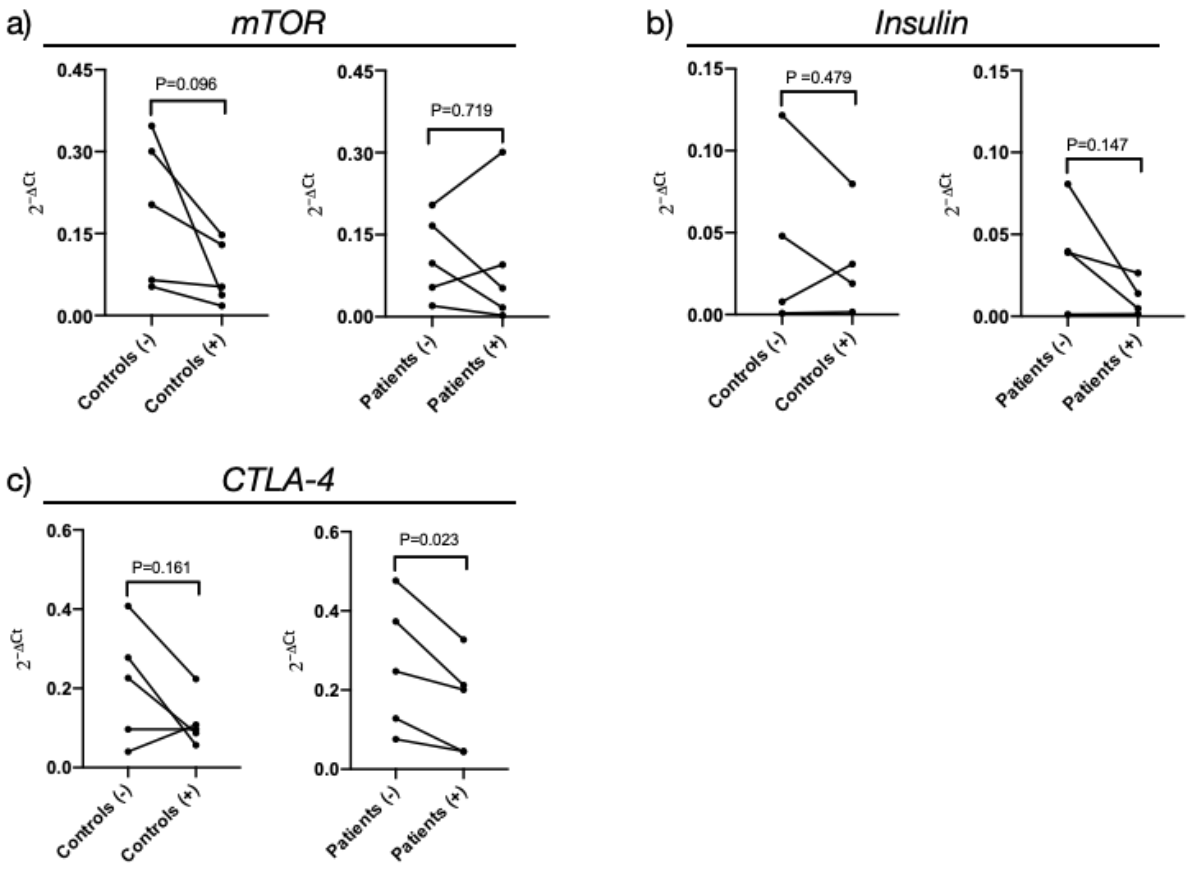

Figure 4.2: Normalized gene expression comparing treated and untreated controls and patients. *The lines show the change in gene expression, comparing untreated (-) and treated (+) samples. The p-value were calculated using a parametric paired t-test, samples were found significant if P<0.05. For Insulin, patient 2 and control 1 were removed since they did not reach treshold.*

To assess the difference in treated and untreated samples for patients and controls a normalized gene expression was used (figure 4.2). When comparing the untreated and treated samples, in the patient and control group, only the expression of *CTLA-4* in the patients (untreated patients median: 0.25± 0.47, 0.05 median treated patients: 0.20± 0.32, 0.016, P=0.023) had a significant decrease when treated with rapamycin (figure 4.2 c). However, a trend was observed, for most samples, where the expression of the respective genes decreased after addition of rapamycin. Interestingly, two of the patients had an increase in the expression of *mTOR* when treated with rapamycin (figure 4.2 a). This was also observed for one control in the expression of *Insulin* (figure 4.2 b) and *CTLA-4* (figure 4.2 c).

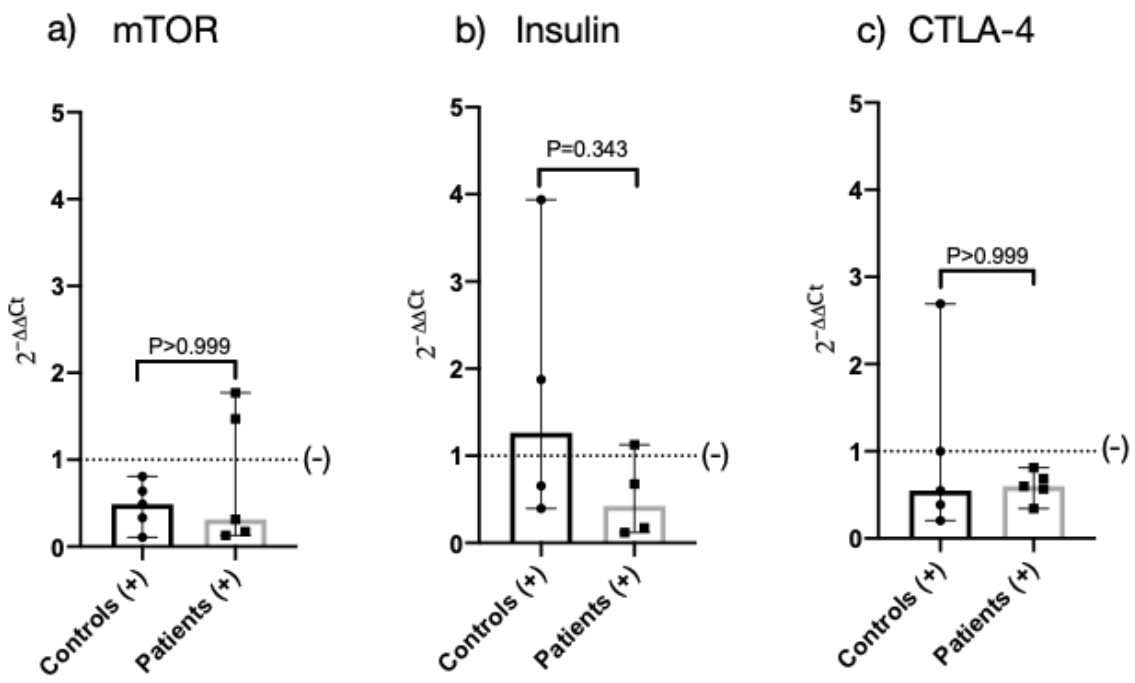

Figure 4.3: Gene expression comparing control and patient. *The bars show the gene expression in treated samples (+) and the error bar shows the 95% CI, untreated samples are represented by the stipled line at 1 (-). The p-value were calculated using a non-parametric Mann-Whitney test, samples were found significant if P<0.05. For Insulin patient 2 and control 1 were removed since they did not reach treshold. The column shows the median with 95% CI.*

To further look at the effect of rapamycin on the expression of the respective genes, the gene expression in the treated samples for controls and patients was normalized relative to the untreated samples. For all the genes investigated, the spread between individuals were relatively large and the differences between APS-1 patients and controls were small for *mTOR* and *CTLA-4*, while a larger difference occurred for *Insulin* (figure 4.3). Still, a trend was observed, that expression level of all three genes were decreased in the treated samples, except for *Insulin* in the treated controls where the median showed an increase (figure 4.3 c). There was also some samples that did not follow the trend, with an increased expression after the treatment with rapamycin. However, no significant difference was observed comparing the patients and controls using a non-parametric Mann-Whitney test, where the difference was found significant if $P<0.05$.

4.3 Validation of rapamycin concentration and assessment of activated cells and T_{reg} with flow cytometry

Flow cytometry was used to determine the optimal concentration of rapamycin and to assess the frequency of activated cells, defined as $CD3^+$ $CD4^+$ $CD25^+$, and T_{reg}, defined as $CD25^{high}$ $FoxP3^+$, in patients and controls. PBMC was isolated from patient and control 1-5, activated with anti-CD3 and -CD28, treated with rapamycin in cell culture for five days, and stained with extracellular and intracellular markers prior to flow cytometry.

4.3.1 Gating strategy

The gating strategy is shown by a representative sample in figure 4.4 (activated cells), 4.5 (subpopulations within activated cells) and 4.6 (subpopulations within T_{reg}). All samples followed the same gating strategy.

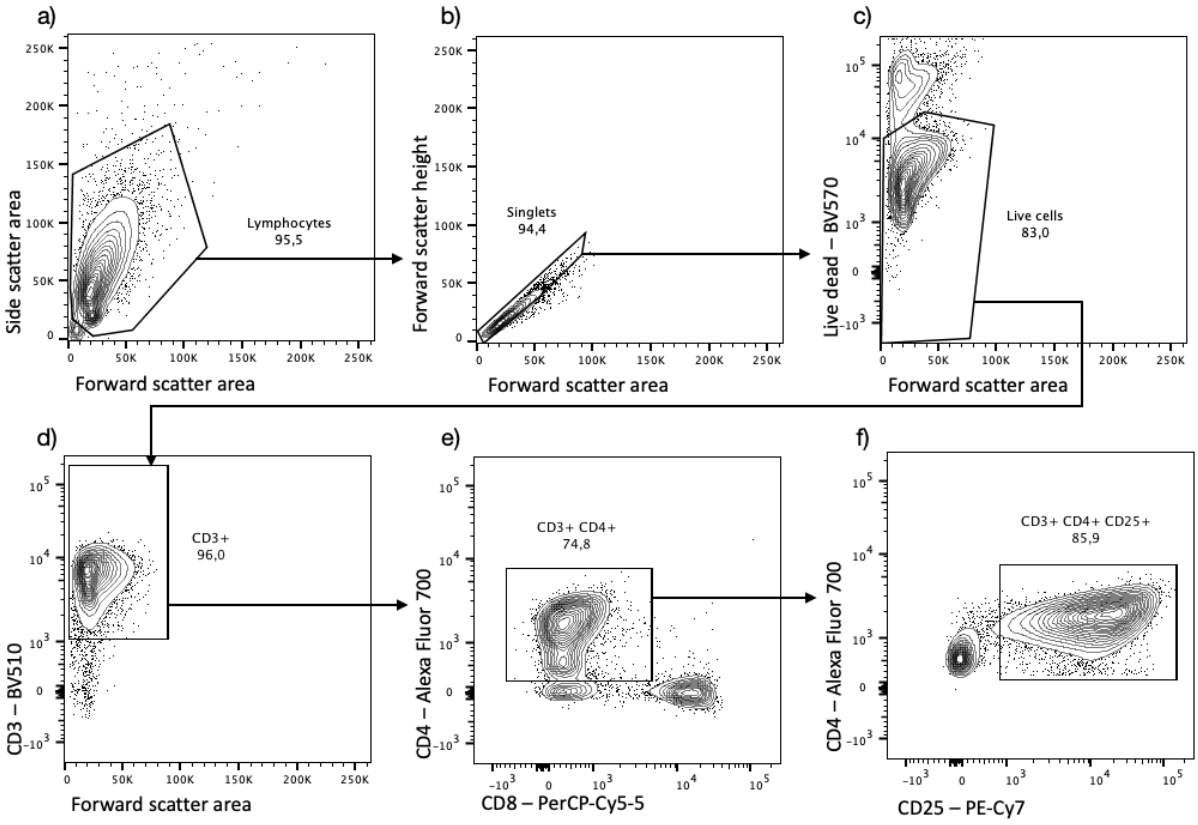

Figure 4.4: Gating strategy in FlowJo, untreated control 1. *A plot of forward scatter area versus side scatter area is used to gate for lymphocytes (a), further gating for singlets (b) with forward scatter area versus forward scatter height. Live cells (c) were gated with forward scatter area versus BV570 fluorescence. To gate for T cells, defined as $CD3^+$ (d) a gate with forward scatter area versus BV510 was made. Further a gate with PerCP-Cy5-5 versus Alexa Fluor 700 was used to gate for $CD4^+CD8^-$ cells (e), and finally activated cells defined as $CD3^+$ $CD4^+$ $CD25^+$ (f) was gated with PE-Cy7 versus Alexa Fluor 700.*

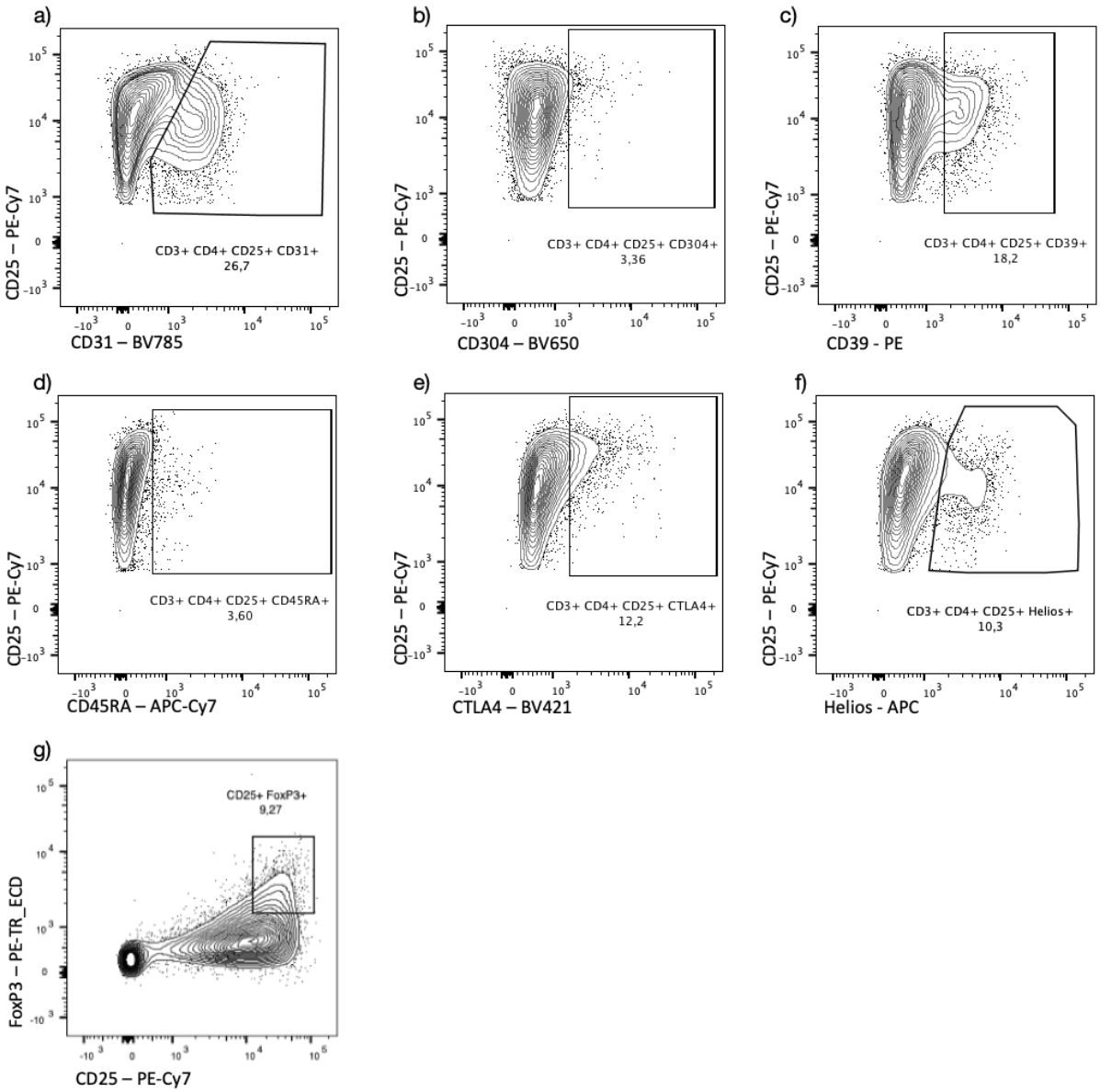

Figure 4.5: Gating strategy in FlowJo, populations of cells within CD3+ CD4+ CD25+ cells, untreated control 1. *To gate for subpopulations within activated cells, defined as CD3+ CD4+ CD25+, the gate for CD3+ CD4+ CD25+ cells defined in figure 4.4 (f) was used for a)-f). The respective markers for a) – f) at the y-axis was gated with PE-Cy7 to define subpopulations. To gate for T_{reg}, defined as CD3+ CD4+CD25$_{high}$FoxP3+(g) the gate for CD4+CD8- cells defined in figure 7.4 (e) was used to directly plotting PE-Cy7 versus PE-TR_ECD.*

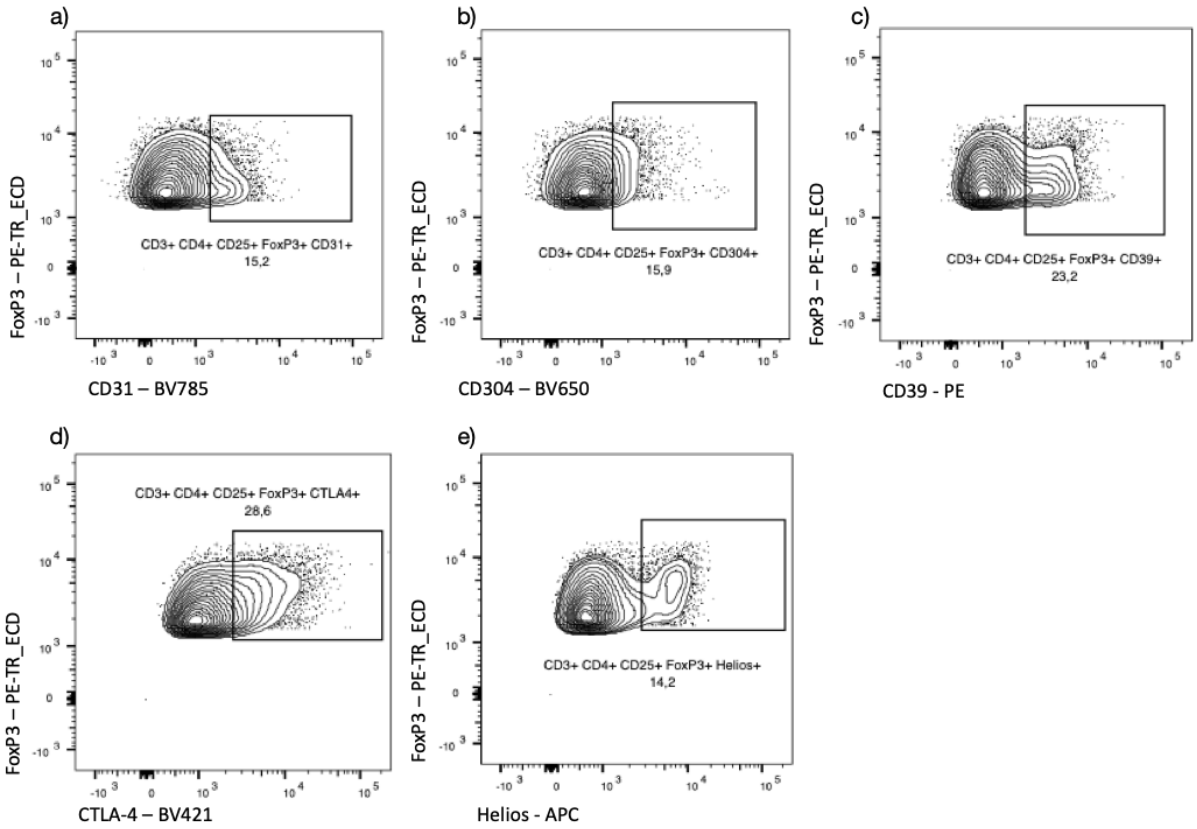

Figur 4.6: Gating strategy in FlowJo, populations of cells within T_{reg}, defined as $CD25_{high}$ $FoxP3^{+}$ cells, untreated control 1. *To gate for subpopulations within T_{reg}, the gate for $CD25_{high}$ $FoxP3^{+}$ defined in figure 4.6 (g) was used. The respective markers for a) – e) at the x-axis versus PE-TR_ECD was used to gate for subpopulations.*

4.3.2 Determination of rapamycin concentration

In order to investigate the effect of rapamycin on PBMC from patients and controls, an appropriate concentration of the drug had to be determined. Two titration lines were prepared, and flow cytometry was used to analyze the proliferation of the cells. We wanted to choose a concentration with an inhibiting effect but that would not kill too many cells, due to the low number of cells available. The number of cells is listed in appendix (A.3). The first titration line included the concentrations; 0.05 nM, 0.1 nM, 1 nM and 2 nM performed on control 14, and the second titration line included 2 nM and 4 nM performed on patient and control 1. The choice of 4 nM for use in all samples was based on the small difference between the cells ability to divide compared with the concentration at 2 nM. Results are listed in appendix (A.5).

4.3.3 Cell proliferation after treatment with rapamycin

When comparing the percentage of live cells in samples treated with rapamycin with the respective untreated sample, a decreasing trend was observed for the treated samples. There was one odd control, in which a small increase was observed (figure 4.7 a). The same was observed for the proliferation index (figure 4.7 b), except for one of the patient samples, which had an increase in the cell proliferation when treated with rapamycin, compared with the untreated sample. When performing a parametric paired t-test, only the proliferation in the controls had a significant decrease after treatment with rapamycin. Still, a trend was observed in most samples, with a decrease in live cells and proliferation after treatment with rapamycin.

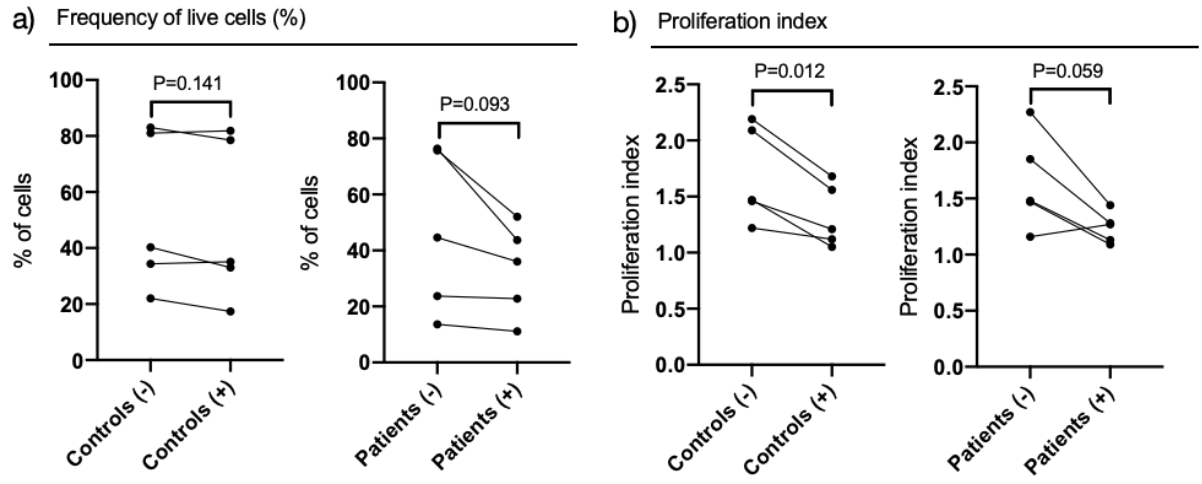

Figure 4.7: Frequency of live cells and proliferation index for controls and patients, treated with rapamycin and untreated. *The lines shows the change in frequency comparing samples treated with rapamycin (+) and untreated (-). The p-value were calculated using a parametric paired t-test, samples were found significant if P<0.05.*

The median proliferation index and median frequency of live cells show the same trend as mentioned above (table 4.2). The median frequencies of live cells in activated cells and T_{reg} are listed in appendix (A.6 and A.7).

Table 4.2: Median (range) proliferation index and median frequency of live cells for samples treated with rapamycin (+) and untreated (-) samples, for patients and controls.

	Controls (-) (95% CI)	Controls (+) (95% CI)	P-value*, comparison controls (-) and controls (+)	Patients (-) (95% CI)	Patients (+) (95% CI)	P-value*, comparison patients (-) and patients (+)
Median proliferation index	1.47 (1.16, 2.22)	1.21 (0.98, 1.67)	**0.012**	1.48 (1.12, 2.18)	1,27 (1.07, 1.41)	0.059
Median frequency of live cells (%)	40.3 (17.3, 87.0)	35.1 (13.0, 85.4)	0.141	44.6 (10.9, 82.7)	36,0 (12.8, 53.4)	0.093

**parametric paired t-test, results were found significant if P < 0.05.*

When all untreated samples were compared with the treated samples, patients and controls combined using a parametric paired t-test, the frequency of live cells (untreated samples median: 42.45 (95% CI: 68.8, 30.14), treated samples median: 35.55 (95% CI: 58.2, 24.10), P= 0.042) and the proliferation (untreated samples median: 1.47 (95% CI: 1.95, 1.38), treated samples median: 1.24 (95% CI: 1.44, 1.13), P= 0.001), had a significant decrease in the treated samples, indicating that rapamycin had an effect on both cell death and the cells ability to proliferate.

4.3.4 The effect of rapamycin in subpopulations of $CD4_+$ cells upon activation

To assess the level of the chosen markers within activated cells, the gates in figure 4.5 was used. For all markers the median frequency of cells decreased in the samples treated with rapamycin, for both patients and controls, where some reached statistical significance (table 4.3). In both patients (P=0.0193) and controls (P=0.0357) the frequency of activated cells ($CD3_+CD4_+CD25_+$) had a significant decrease when treated with rapamycin. This was also observed for the markers CD31 and CD39 (table 4.3). However, the markers CD304 and CTLA-4 only had a significant decrease in the patients when treated with rapamycin (table 4.3). The other markers Helios and FoxP3 also had a decreased frequency when treated with rapamycin, but not reaching statistical significance.

Table 4.3: Median frequency of cells within $CD3^+CD4^+CD25^+$ for samples treated with rapamycin (+) and untreated (-) samples, for patients and controls.

Markers	Controls(-) Median(%) (95% CI)	Controls(+) Median(%) (95% CI)	P-value*, comparison controls(-) and controls(+)	Patients (-) Median(%) (95% CI)	Patients(+) Median(%) (95% CI)	P-value*, comparison patients(-) and patients(+)
$CD3^+$	97.2 (93.9, 99.8)	98.1 (91.1, 101)	0.5385	98.2 (94.7, 99.8)	97.0 (93.52, 99.0)	0.3865
$CD3^+CD4^+CD8^-$	64.7 (47.6, 75.7)	61.0 (47.8, 74.9)	0.8233	67.5 (39.4, 81.9)	66.5 (34.8, 83.0)	0.2105
$CD3^+CD4^+CD25^+$	21.6 (-6.43, 93.13)	6.69 (-12.9, 70.4)	**0.0193**	56.5 (9.64, 95.8)	39.7 (5.21, 55.1)	**0.0357**
Markers within $CD3^+CD4^+CD25^+$						
$CD31^+$	22.7 (12.9, 28.6)	9.86 (3.79, 15.8)	**0.0002**	15.9 (10.9, 27.0)	8.40 (2.29, 21.4)	**0.0003**
$CD304^+$	6.03 (2.90, 12.6)	1.38 (-1.90, 8.06)	0.0618	7.85 (1.90, 16.0)	1.34 (-1.61, 7.28)	**0.0455**
$CD39^+$	18.2 (13.5, 27.9)	1.93 (-3.00, 15.8)	**0.0123**	44.6 (20.5, 66.1)	4.58 (-0.46, 19.0)	**0.0036**
$CTLA\text{-}4^+$	9.31 (1.23, 21.5)	3.63 (-0.74, 13.0)	0.0742	10.7 (6.19, 14.1)	2.27 (1.08, 5.35)	**0.0151**
$Helios^+$	11.7 (-1.53, 42.4)	10.7 (-0.30, 37.2)	0.3331	12.5 (-1.36, 33.0)	8.22 (-1.63, 25.4)	0.1234
$FoxP3^+$	9.22 (3.35, 12.0)	1.18 (-1.19,9.03)	0.2198	9.93 (0.13, 27.2)	7.43 (2.22, 10.9)	0.1247

**Parametric paired t-test, results were found significant if $P < 0.05$.*

Comparison of the difference between untreated and treated cells in patients and controls was performed by normalizing the samples treated with rapamycin relative to the untreated sample (table 4.4). This was done due to a great variation observed among the samples.

Table 4.4: Comparison of median difference between untreated (-) and treated (+) cells in patients and controls for the respective markers.

Markers	Median difference between untreated (-) and treated (+) cells, controls (95% CI)	Median difference between untreated (-) and treated (+) cells, patients (95% CI)	P-value*
$CD3^+$	-0.3 (-2.63, 4.31)	1.4 (-1.90, 3.94)	0.730
$CD3^+CD4^+CD8^-$	-1.3 (-2.98, 3.54)	0.7 (-1.49, 4.92)	0.421
$CD3^+CD4^+CD25^+$	14.91 (3.90, 25.31)	16.8 (2.48, 42.68)	0.310
Markers within $CD3^+CD4^+CD25^+$			
$CD31^+$	11.6 (8.68, 13.26)	7.2 (5.41, 8.86)	**0.016**
$CD304^+$	5.04 (-0.37, 9.74)	5.9 (0.20, 11.98)	0.548
$CD39^+$	12.24 (5.12, 23.41)	40 (18.6, 49.47)	**0.032**

CTLA-4+	2.52 (-0.81, 11.23)	5.14 (2.21, 11.67)	0.310
Helios+	1 (-3.03, 7.01)	4.05 (-1.68, 9.60)	0.691
FoxP3+	1.86 (-3.43, 10.96)	2.36 (-3.08, 17.3)	0.548

**Non-parametric Mann-Whitney test, results were found significant if P < 0.05.*

The difference between the treated and untreated samples in the controls compared with the patients was analyzed by performing a non-parametric Mann-Whitney test, where significance was shown for CD31 (P=0.016) and CD39 (P= 0.032) (table 4.4). This indicates a greater decrease in the frequency of $CD31^+$ cells in the controls, and a greater decrease in the frequency of $CD39^+$ cells in the patients (table 4.4). None of the other markers had a significant difference in the comparison of patients and controls, where all markers had a decreasing trend in the samples treated with rapamycin. When gating for activated cells within $CD3^+$ $CD8^+$ cells, the same pattern was observed (data not shown), indicating that rapamycin suppresses both CD^+CD25^+ and $CD8^+$ T cells.

4.3.5 The effect of rapamycin on T_{reg} and subpopulations of cells within T_{reg}

To assess the frequency of T_{reg} cells, the gate in figure 4.5 g) was used. The respective markers within T_{reg}, were gated as shown in figure 4.6 a)-e). Comparison of the percentages of the respective markers in cells treated with rapamycin and untreated cells was performed using a parametric paired t-test (figure 4.8 b, and 4.9). For most samples a trend was observed, the median frequency of cells decreased after treatment with rapamycin, where some of the markers reached a significant decrease (figure 4.9, table 4.5).

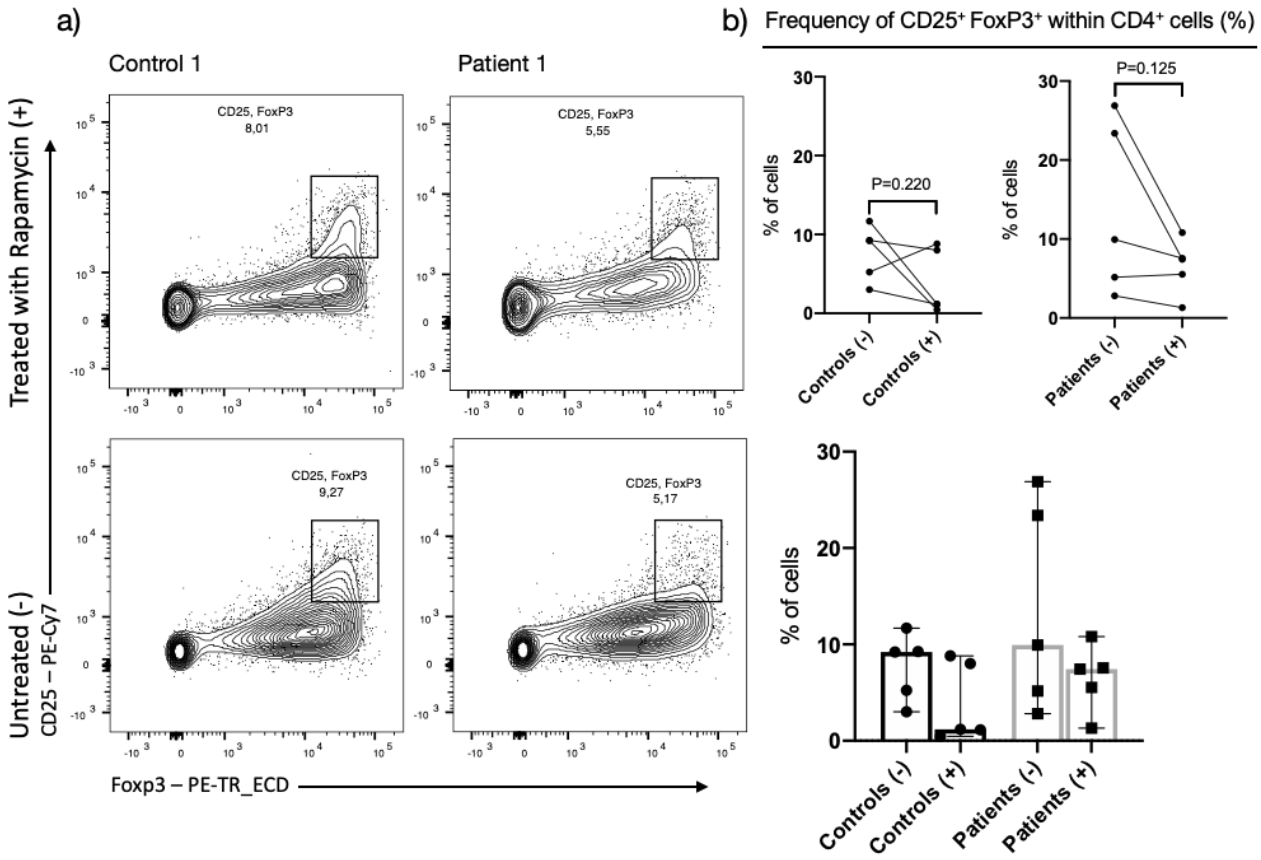

Figure 4.8: Comparison of the frequency of T_{reg}, defined as $CD25_{high}$ $FoxP3^{+}$, in PBMC treated with rapamycin and untreated for patients and controls. *a) Shows the gating in FlowJo for both treated (+) and untreated (-) samples in control and patient 1. b) Shows the change in frequency in patients and controls, illustrated by the lines (upper part). The bars shows the median frequency of positive cells and the error bar shows the 95% CI (lower part). The p-value were calculated using a parametric paired t-test, samples were found significant if P<0.05.*

When gating for the T_{reg} population (figure 4.8 a), great variations could be seen among the different samples. Interestingly, for two of the patients and two controls, the frequency of T_{reg} only had a small decrease when treated with rapamycin, and for one control and one patient only a small increase occurred. The rest of the samples had a more distinct decrease of T_{reg} when treated with rapamycin (figure 4.8 b). When comparing the median for controls and patients treated with rapamycin a greater decrease in frequency of T_{reg} was observed in the controls (figure 4.8 b).

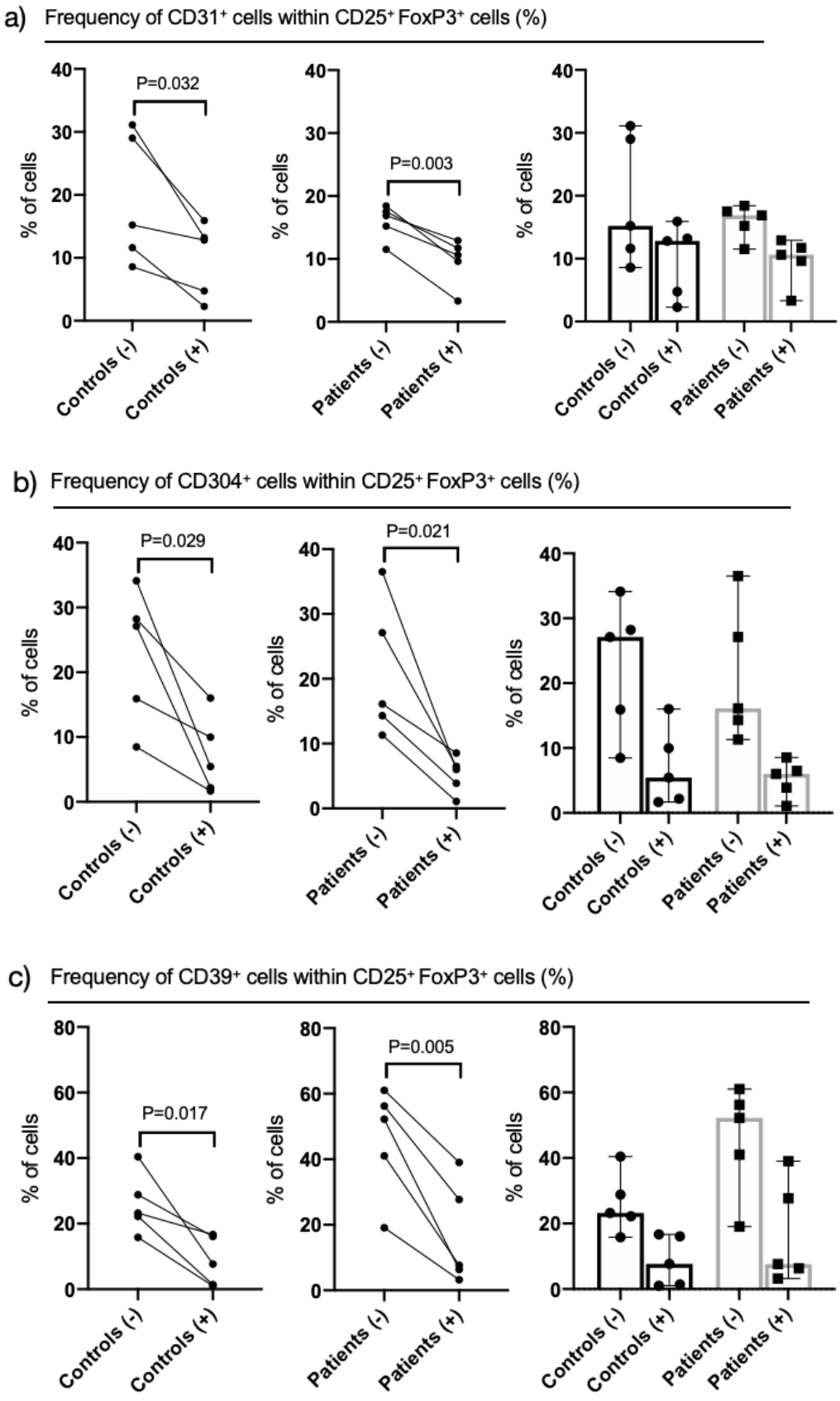
a) Frequency of CD31+ cells within CD25+ FoxP3+ cells (%)
P=0.032
P=0.003
% of cells
Controls (-)
Controls (+)
Patients (-)
Patients (+)
b) Frequency of CD304+ cells within CD25+ FoxP3+ cells (%)
P=0.029
P=0.021
c) Frequency of CD39+ cells within CD25+ FoxP3+ cells (%)
P=0.017
P=0.005

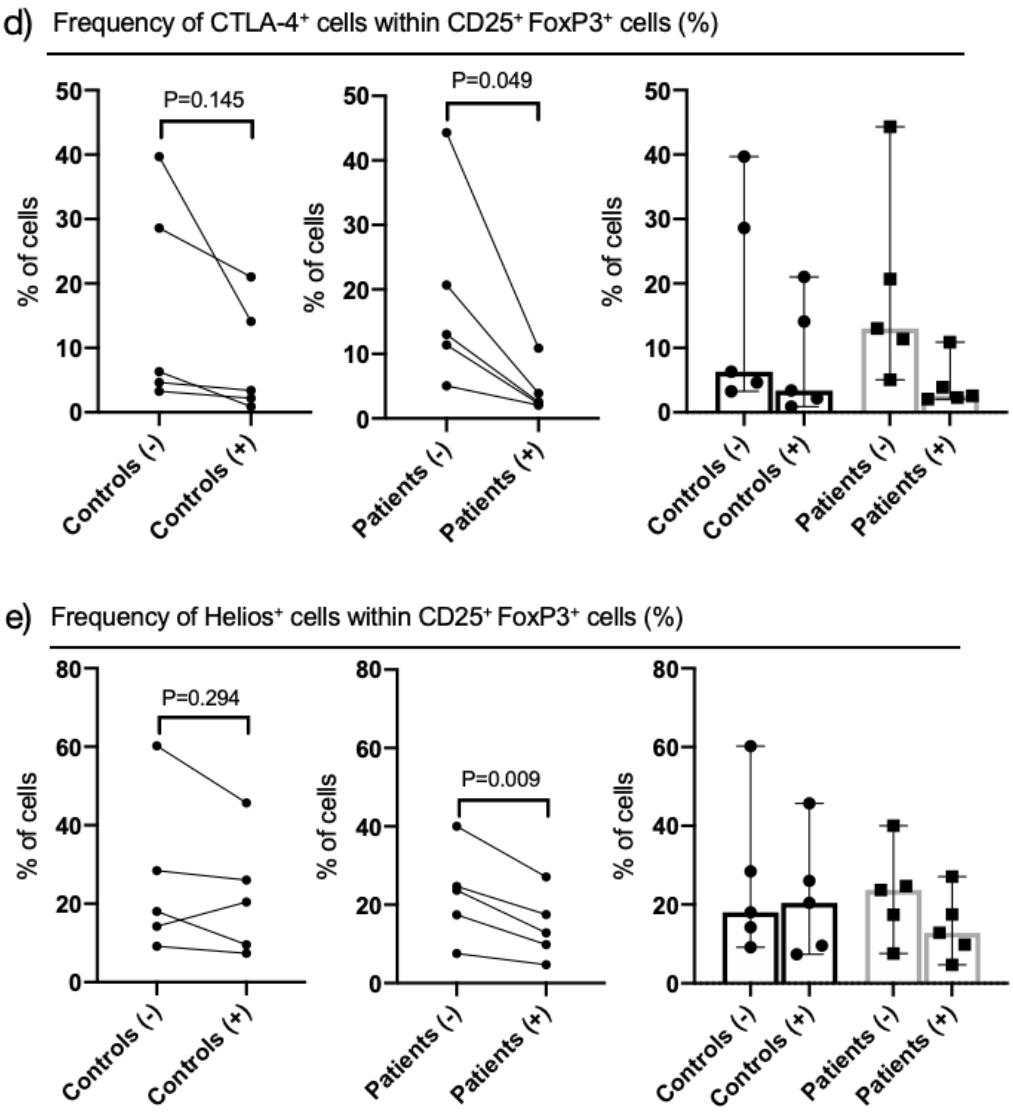

Figure 4.9: Comparison of the frequency of positive cells for the respective markers within T_{reg} ($CD25^{high}$ $FoxP3^{+}$) in PBMC treated with rapamycin and untreated for patients and controls. *The respective markers within T_{reg} are represented in a) – e). The lines between treated and untreated samples shows the change in frequency (left and middle part), the bars shows the median frequency of positive cells within the respective population and the error bar shows the 95% CI (right part). (+) means that the sample were treated with rapamycin and (-) means that the sample were untreated. The p-value were calculated using a parametric paired t-test, samples were found significant if P<0.05.*

The frequency of $CD31^{+}$ cells, a marker which expression indicates a recent thymic emigration [57], had great variation among the controls, whereas the frequency in the patients samples had less variation. However, for both control and patients a significant decrease of CD31 was observed when treated with rapamycin (figure 4.9 a, table 4.5). For Helios, a marker suggested for nT_{reg} [48], no great difference in the controls were observed, where the median had a slight increase when treated with rapamycin. In the patients, on the other hand, the samples had a

significant decrease in frequency when treated (figure 4.9 e, table 4.5). Interestingly, for these two markers most samples seemed to only have a small decrease when treated with rapamycin. When comparing the frequency of CD304 (neuropilin-1), a marker for $nT_{reg.}$ [56], a great variation among the samples occurred in both the patients and controls, also her both patients and controls had a significant decrease in frequency when treated with rapamycin (figure 4.9 b, table 4.5). The frequency of CD39, a marker with inhibitory properties expressed on T_{reg} [60], had a greater decrease in the patient samples treated with rapamycin compared with the treated controls, where the patients had a higher expression in the untreated sample compared with the untreated control (figure 4.9 c, table 4.5). But both patients and controls had a significant decrease.

When staining the cells, CTLA-4 staining was performed prior to permeabilization; therefore, only extracellular CTLA-4 was detected. The expression of this marker varies in both controls and patients, where the patient samples had a significant decrease when treated with rapamycin. The control also had a decreased expression, but not reaching statistical significance (figure 4.9 d, table 4.5).

Table 4.5: Median frequency of cells within T_{reg} ($CD25_{high}$ $FoxP3_{+}$) for samples treated with rapamycin (+) and untreated (-) samples, for patients and controls.

Markers within $CD25_{high}FoxP3_{+}$	**Controls(-) Median(%) (95% CI)**	**Controls(+) Median(%) (95% CI)**	**P-value*, comparison controls(-) and controls(+)**	**Patients (-) Median(%) (95% CI)**	**Patients(+) Median(%) (95% CI)**	**P-value*, comparison patients(-) and patients(+)**
CD31	15.2 (6.31, 31.9)	12.8 (2.44, 17.1)	**0.032**	16.90 (12.5, 19.3)	10.60 (4.98, 14.3)	**0.003**
CD304	27.10 (9.92, 35.6)	5.45 (-0.39, 14.5)	**0.029**	16.1 (8.03, 34.1)	6.03 (1.68, 8.73)	**0.021**
CD39	23.2 (14.6, 37.6)	7.73 (-0.85, 18.0)	**0.017**	52.2 (25.2, 66.6)	7.60 (-2.75, 36.3)	**0.005**
CTLA-4	6.31 (-4.13, 37.1)	3.38 (-2.64, 19.3)	0.145	13.0 (-0.05, 37.8)	2.55 (-0.30, 8.98)	**0.049**
Helios	18.0 (0.68, 51.3)	20.4 (2.66, 40.9)	0.294	23.7 (7.97, 37.4)	12.8 (3.86, 24.9)	**0.009**

**Parametric paired t-test, results were found significant if $P < 0.05$.*

When performing the same comparison in patients and controls for the markers in T_{reg} as described for activated cells (section 4.3.4), none of the markers had a significant difference in the frequency comparing controls and patients (table 4.6). However, a greater decrease in the controls for CD31 and a greater decrease in the patients for CD39 was observed in the treated samples, the same trend as was observed within activated cells (section 4.3.4).

Table 4.6: Comparison of median difference between untreated (-) and treated (+) cells in patients and controls in the respective markers within T_{reg} ($CD25_{high}$ $FoxP3^{+}$)

Markers within $CD25_{high}$ $FoxP3^{+}$	Median difference between untreated (-) and treated (+) cells, controls (95% CI)	Median difference between untreated (-) and treated (+) cells, patients (95% CI)	P-value*
$CD31^{+}$	9.33 (1.31, 17.3)	5.80 (3.63, 8.92)	0.691
$CD304^{+}$	12.20 (2.68, 28.72)	10.41 (3.96, 27.75)	0.841
$CD39^{+}$	14.79 (5.19, 14.9)	28.50 (14.9, 43.34)	0.095
$CTLA\text{-}4^{+}$	5.40 (-4.38, 20.8)	10.45 (0.12, 28.98)	0.222
$Helios^{+}$	2.40 (-5.49, 13.84)	7.56 (3.50, 13.07)	0.421

**Non-parametric Mann-Whitney test, results were found significant if $P < 0.05$.*

A parametric paired t-test was performed for the markers within T_{reg} ($CD25_{high}$ $FoxP3^{+}$) cells in all untreated samples, both controls and patients together, paired with their treated samples. This showed a highly significant decrease in frequency for all markers (table 4.7), and indicates that the frequency of cells with the respective markers, within T_{reg}, decreases when treated with rapamycin.

Table 4.7: Comparison of positive cells with the respective markers within $CD25_{high}$ $FoxP3^{+}$ cells for all untreated and treated samples, including both patients and controls.

Markers within $CD25_{high}$ $FoxP3^{+}$	Median frequency (%) in untreated samples (-) (95% CI)	Median frequency (%) in treated samples (+) (95% CI)	P-value*
$CD31^{+}$	16.05 (12.28, 22.72)	11.15 (6.37, 13.04)	**0.0006**
$CD304^{+}$	21.60 (14.9, 28.96)	5.74 (2.89, 9.37)	**0.0005**
$CD39^{+}$	34.60 (24.20, 47.77)	7.67 (3.81, 21.57)	**0.0002**
$CTLA\text{-}4^{+}$	12.20 (6.90, 28.49)	2.97 (1.52, 11.13)	**0.0088**
$Helios^{+}$	20.85 (13.02, 35.65)	15.15 (9.26, 26.94)	**0.0109**

**Parametric paired t-test, results were found significant if $P < 0.05$.*

4.4 IFN-γ production by activated PBMC treated with rapamycin in cell culture analysed by ELISA

The supernatant from the activated PBMC was collected when the cells were harvested for flow cytometry, to assess the production of IFN-γ, a proinflammatory cytokine produced by activated T cells [64]. To determine the concentration of IFN-γ, a standard curve was made (figure 4.9), with a top concentration at approximately 500 pg/mL using ELISA MAX Deluxe kit.

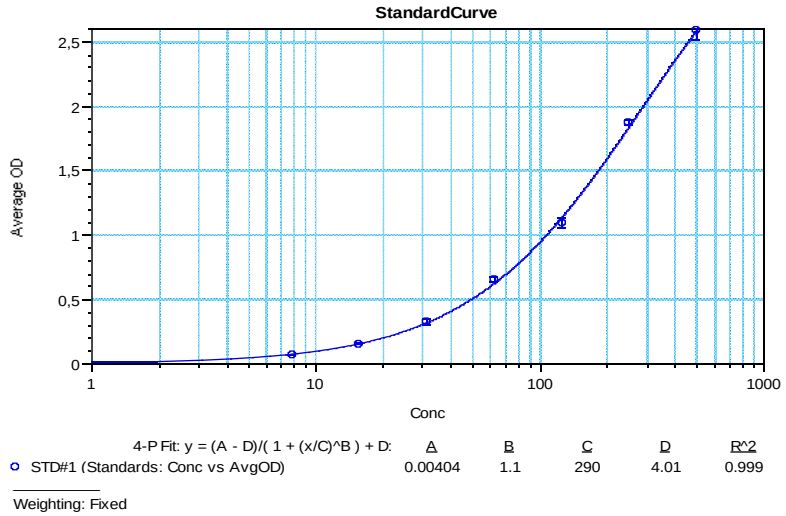

Figure 4.9: Standard curve. *A six two-fold serial dilution of the 500 pg/mL top standard was performed to make the standard curve. The x-axis presents the average concentration and the y-axis the average optical density (O.D).*

There was a great variation among the samples, and some samples needed to be diluted with the dilution factors 1:25 and 1:100 to fit the standard curve. Control 3 did still not fit in the standard curve; hence the measured amount is likely to be much higher than detected.

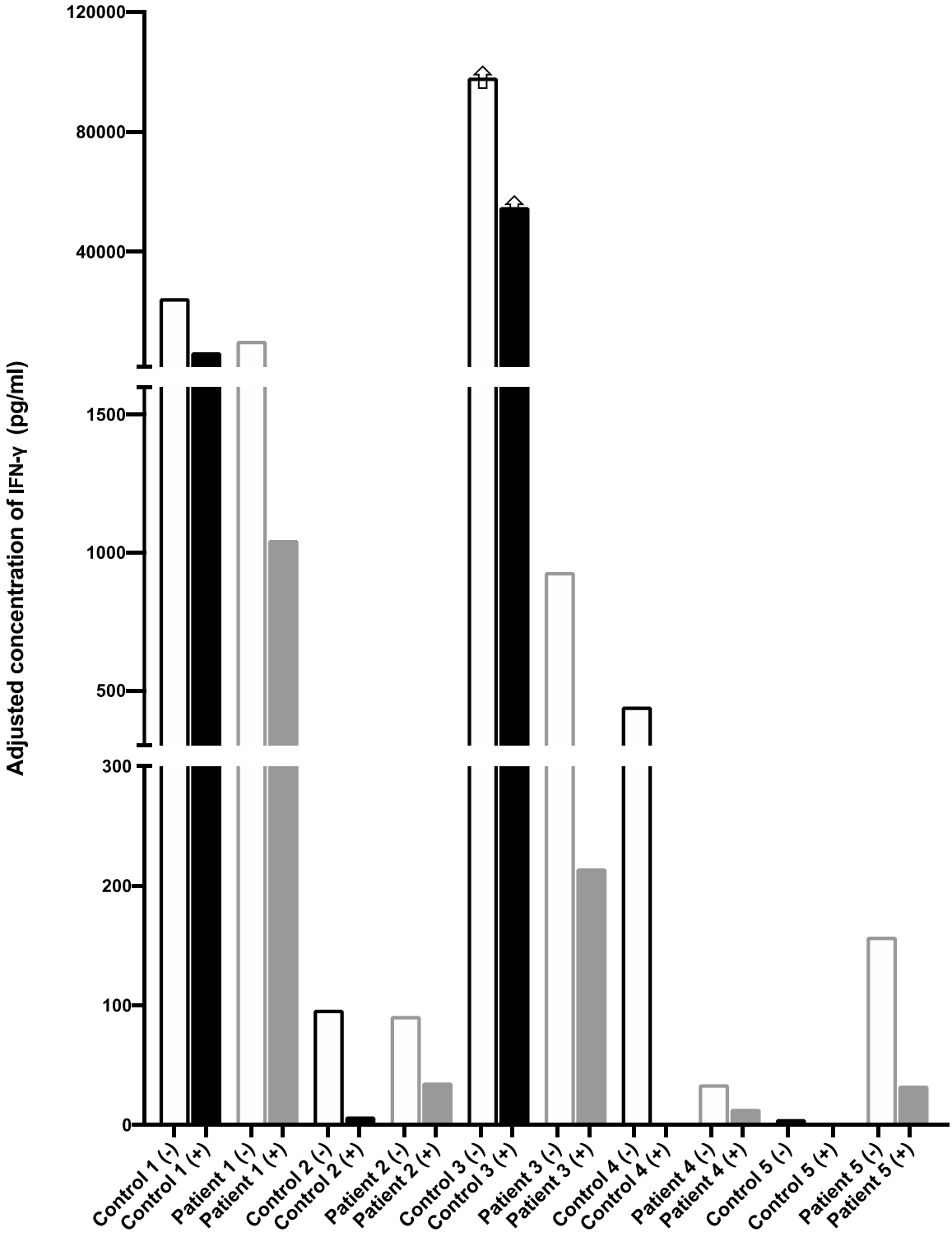

Figure 4.10: The adjusted concentration of IFN-γ (pg/mL) for each individual sample. *The bars present the mean adjusted concentration of IFN-γ in each individual sample. (+) means that the sample were treated with rapamycin and (-) means that the sample were untreated. The bars marked with arrows illustrates the samples that did not fit the standard curve (figure 4.9), where the amount of IFN-γ were higher than measured.*

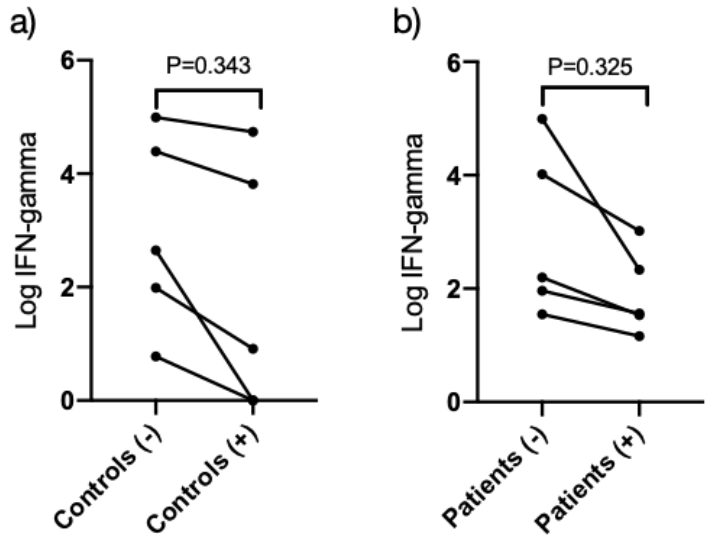

Figure 4.11: Comparison of the amount IFN-γ in treated and untreated samples for controls and patients using log-values. *The lines show the change in the amount of IFN-γ, comparing untreated samples (-) and samples treated with rapamycin (+). Using a parametric paired t-test comparing the amount of IFN-γ in patients (-) and (+) (P=0.325), and control (-) and (+) (P=0.343) gave no significance, results were found significant if P < 0.05.*

The results illustrated in figure 4.10 indicates great variation between all samples in both controls and patients. Using a parametric paired t-test comparing the amount of IFN-γ in patients treated with rapamycin and untreated (untreated patients median:157.5 (95% CI: -31529, 75045) treated patients median: 35.6 (95% CI: -280.4, 817.4) P=0.325), and control treated with rapamycin and untreated (untreated controls median: 442.3 (95% CI: -20653, 61105), treated controls median: 7.164 (95% CI: -24735, 57551), P=0.343) gave no significant decrease. When performing the same test with all samples treated with rapamycin, paired with their respective untreated sample, combining patients and controls, the result gave a no significant decrease in the amount of IFN-γ in the treated samples (untreated samples median: 299.9 (95% CI: -4810, 46794), treated samples median: 34.27 (95% CI: -8597, 25273), P=0.223). However, a trend was observed, where all samples treated with rapamycin had a decrease in the amount of IFN-γ for both controls and patients (figure 4.11).

5. Discussion

APS-1 is a rare disease characterized by the three main manifestations of Addison´s disease, hypoparathyroidism and chronic mucocutaneous candidiasis. In addition, there are several other symptoms observed affecting organs and tissue of both endocrine and non-endocrine origin. The present treatment accordingly includes hormone-replacement, oral azole drugs and in some cases the immune suppressants, such as CsA. These patients suffer from an earlier death, and lower quality of life compared to the general population [79, 122]. In the treatment regimens there are challenges due to interactions and drug resistance, and there is a great need of studies on new targeted treatments of APS-1. Studies have found that the differentiation of the T_{reg} lineage seems to be affected in these patients [33], in addition to a reported lower frequency of T_{reg} in APS-1 patients in comparison with age-and sex-matched healthy controls [81]. An important regulator of metabolism and proliferation in the development of T_{reg} is the gene *mTOR*, encoding a protein kinase with the same name [48]. The mTOR inhibitor rapamycin is mainly used to prevent allograft rejection but is suggested to have effect in autoimmune diseases as well. The mechanism of action has similarities with CsA as they both bind to FKBP-12, but instead of inhibiting TCR-induced calcineurin activity, rapamycin inhibits mTORC1 [103], where studies have indicated that rapamycin promotes the generation of T_{reg} cells or enhances their activity [48].

5.1 Establishing an experimental cell-based system to investigate the effect of rapamycin on PBMC

In this project we succeeded to establish a cell-based system to assess the effect of rapamycin on PBMC from APS-1 patients compared to healthy controls. However, the setup had some limitations, the major ones being limited patient material and few patients. For example, even though we already form the beginning had a limited amount of PBMCs from each individual, we had to use frozen cells and we chose to use a magnetic bead-based kit to remove dead cells prior to the cell culture. This introduced even larger challenges with low and variable numbers of cells, but this procedure was considered a necessity to further be able to assess the effect of rapamycin on cell death and proliferation. To simulate an activation of the cells, plate bound anti-CD3 and -CD28 were added, before the cells were to be further treated with rapamycin in cell culture. Based on the response in cell culture and the assessment by flow cytometry, the activation of the cells was successful also in the presence of rapamycin. Activation using anti-

CD3 and CD28 was performed because this is known to have a large T cell specific stimulation [123], which we needed in our approach.

As rapamycin has low solubility in water [112], DMSO were used as dissolvent. However, there may be some complications with diluting rapamycin in DMSO. Studies has found that the concentration of compounds diluted in DMSO were variable after distribution of the diluted stock solution, and that the concentration of the diluted compound was below the expected value [124]. We were unable to assess the concentration of rapamycin after each dilution, which may affect the results due to a possible variable concentration in the different assays. Also, a distribution of the stock solution was considered necessary to avoid the need of freezing and thawing, which may affect the stability of the compound.

When performing this experiment for the various samples, great variation occurred. This may be due to biological variations or the performance on the day it was completed, although the attempt was made to carry out the experiment equally. We took care to always include one patient and one control each time we performed the cell assay. Despite these limitations we succeeded in the development of a protocol to further be used to assess the effect of rapamycin or other drugs on PBMC.

5.2 A possible immunosuppressive effect of rapamycin in controls and patients

To assess the effect of rapamycin at RNA level, we first searched for candidate genes in the mTOR signaling pathway using rt-qPCR with resting blood cells that were not treated with rapamycin. No great differences in the gene expressions comparing patients and controls were observed (figure 4.1), but *mTOR* was chosen for downstream applications, being the target of rapamycin. Furthermore, *Insulin* was chosen, as mTOR is dependent on stimulation of nutrients to be activated [91], and the fold change comparison of patients and controls showed a higher expression of *Insulin* in patients compared to healthy individuals. Finally, *CTLA-4* was chosen as it is suggested to be crucial for the suppressive mechanisms of T_{reg} [58].

Only *CTLA-4* in the patients had a significant change in the gene expression of activated cells treated with rapamycin for the chosen genes using rt-qPCR (figure 4.2 c). Still, a trend occurred for all genes in most samples, where the gene expression decreased when the cells were treated with rapamycin, in both patients and controls. However, there were exceptions where some

samples did not follow the trend, e.g. only 3/5 patients had a decrease in the expression of *mTOR* (figure 4.3 a). Interestingly, 2 patients had an increase in the expression of *mTOR*, hence one might speculate that some APS-1 patients may be resistant or less sensitive to treatment with rapamycin. Previous findings have shown a downregulation of *mTOR* after treatment with rapamycin, however that study were performed on other cell lines at a protein level [125]. A study in yeast suggested that mutations in mTOR and FKBP-12 can cause resistance to rapamycin treatment, by preventing an interaction between mTOR, FKBP12 and rapamycin [126]. Other studies have speculated on how different cells may be resistant or less sensitive to rapamycin, where rhabdomyosarcoma cancer cell lines were more sensitive than colon cancer cell lines [127]. Mutations or genetic variation in *mTOR* itself have not been investigated in these APS-1 patients.

The expression of *CTLA-4* decreased in most samples for both patients and controls, where only the patient samples had a significant decrease (figure 4.2 c). This corresponds with our observations at protein level using flow cytometry, where also only the patient samples had a significant decrease in the frequency of CTLA-4 (table 4.3, figure 4.9 d). A study using flow cytometry identified that T_{reg} had a higher expression of CTLA-4 after treatment with rapamycin [106], this do not correspond with our findings. However, in our study PBMC was used, hence not being able to assess the specific expression of *CTLA-4* in T_{reg}. Also, *Insulin* had a decreasing trend after the treatment with rapamycin, but two of the controls had an increase in the expression after treatment with rapamycin (figure 4.3 b). Notably, other studies have found that rapamycin increased insulin sensitivity in healthy men, and increased the insulin dependent glucose uptake [128]. There are factors that may affect the results. In the case of *CTLA-4* expression, an increased expression has been observed after infection [129]. Another important factor is variable concentration and integrity of the mRNA used in this project, where low quality mRNA affects the cDNA synthesis, making the results less reliable. However, we only had the material that we got from the cell cultures and had to perform our analysis on this limited material.

To assess the effect of rapamycin at the protein level, selected T cell markers were used for staining of activated PBMC treated with rapamycin from patients and controls prior to flow cytometry. CFSE staining was also performed prior to flow cytometry, to assess the effect of rapamycin on cell proliferation. We observed changes in the cells ability to proliferate in presence of rapamycin and a decrease in the number of live cells (figure 4.7). mTOR is crucial

for cell proliferation and the prevention of autophagy; when cells are exposed for metabolic and therapeutic stress, such as the mTOR inhibitor rapamycin, autophagy and cell death can be observed [130]. In a related study looking at how rapamycin affects the proliferation in PBMC similar findings were noted, where PBMC was treated with 10 nM rapamycin in cell culture [131]. This suggests that the rapamycin treated cells had a reduced proliferative capacity compared with the untreated samples. However, no significant decrease in live cells were found after treatment with rapamycin in neither the controls nor the patients (table 4.2), but a significant decrease in the proliferation was observed in the controls, but not for the patients (table 4.2). In our study the concentration of rapamycin was 4 nM, where a higher concentration possibly could have given a larger decrease in live cells and proliferation. When including both controls and patients in the same statistics to compare the samples treated with rapamycin with the untreated, a significant decrease in live cells and proliferation occurred. This suggests that the number of samples in the patient and control group are too few to give enough statistical power.

T cells are known to express CD25 upon activation, which has been shown to be suppressed by rapamycin upon CD3 activation [132]. This align with our results, where the frequency of activated cell ($CD3^+CD4^+CD25^+$) had a significant decrease in both patients and controls when treated with rapamycin, indicating that rapamycin inhibited the activation of T cells *in vitro*. This was also observed for the markers CD31 and CD39, and for the markers CD304 and CTLA-4 a significant decrease occurred only in the patients (table 4.3). As only extracellular staining was used to assess the expression of CTLA-4, we were not able to assess the intracellular expression. It would be interesting to look further into this, as it is suggested that the intracellular expression of CTLA-4 in T cells is constitutive [133]. However, no large difference between APS-1 patients and controls were found when comparing the median difference between untreated and treated cells in patients and controls (table 4.4). This implicates that the immunosuppressive effect of rapamycin on PBMC were not more favorable in the controls than the patients, or vice versa. An exception to this was in the comparison within activated cells where the expression of CD31 and CD39 had a significant difference between the APS-1 patients and controls (table 4.4). CD31 had a larger decrease in the controls than in APS-1 patients (table 4.4), where the same trend was observed for this marker within T_{reg}, but not reaching statistical significance (table 4.6). However, it is worth noticing that the untreated control samples had a higher frequency of $CD31^+$ cells than in the APS-1 patients within activated cells. This observed lack in CD31 in the APS-1 patients, a marker for recently

emerged T cells [57], could possibly reflect a lack of AIRE expression in the thymus, as other studies have observed a possible impairment of T_{reg} cells emerging from the thymus in APS-1 patients [82]. For CD39 within activated cells, a larger decreased in the APS-1 patients occurred (table 4.4), also here the same trend was observed within T_{reg} but not reaching statistical significance (table 4.6). This do not correspond with previous studies reporting that rapamycin gave an enhanced CD39 expression on iT_{reg}, but these studies were performed with isolated $CD4^+$ cells and T_{reg} [134, 135]. In our study the amount of iT_{reg} in the PBMC might not be large enough to show an increase in the expression of CD39. It would be interesting to look further into this phenomenon with isolated T_{reg}.

Our findings of a decreased amount of IFN-γ in all samples treated with rapamycin correspond with previous findings (section 4.4), where the production of IFN- γ decreased in PBMC in the presence of rapamycin [136]. IFN-γ is secreted by T cells such as T_{H1} [137], and Delgoffe et al. demonstrated that this T cell linage were dependent on mTORC1 to proliferate. Knockout of Rheb (an activator of mTORC1) in T cells decreased the differentiation of T_{H1} and T_{H17}, both implicated in promoting autoimmune diseases [89]. However, it is worth noticing that a possible reduced proliferation of T_{H17} may not be beneficial for APS-1 patients, ass this T cell subset produces IL-17, a cytokine reported to be involved in clearing Candida infections, a condition many APS-1 patients suffer from [138].

The decrease in both IFN-γ and CD39 within activated cells in all samples after treatment with rapamycin, possibly correspond with an observations in mice suggesting that $IFN\text{-}\gamma^+$ $CD4^+$ and $CD8^+$ T cells both express CD39 [139]. We also observed that the frequency of activated $CD8^+$ T cells decreased when treated with rapamycin, where a great decrease of $CD8^+CD39^+$ occurred (data not shown). One study have observed that $CD8^+CD39^+$ cells were associated with IFN-γ production [140]. However, we were not able to detect the IFN-γ producing cells, as the supernatant was collected for PBMC.

A previous study have found a decreased level of T_{reg} in PBMC in APS-1 patients compared with controls [81]. This do not correspond with our study where no large difference was observed, and patients had a larger frequency in the untreated sample compared with the controls. However, the cells in our study was incubated in cell culture for five days. Interestingly, the frequency of T_{reg}, for three of the patients and controls, only had a small decrease when treated with rapamycin, whereas two of the patients and controls had a more

distinct decrease (figure 4.8 b). Studies have found that rapamycin promotes expansion of functional T_{reg}, in PBMC from both healthy controls and patients suffering from autoimmunity [141, 142]. We were not able to determine the exact effect of rapamycin on T_{reg} in this regard, but it is worth noticing that Helios and CD31, suggested to be expressed on nT_{reg} [48, 57], in both patients and controls illustrates a smaller decrease when treated with rapamycin than some of the other markers (figure 4.9 a and e). However, a significant decrease of CD31 occurred for both patients and controls in the treated samples, but only for the patients in the case of Helios (table 4.5). Studies have suggested that rapamycin favor the proliferation of nT_{reg} [143]. However, the reliability of Helios as a marker for nT_{reg} are under debate [144]. It is also interesting that CD304 apparently had a larger decrease than Helios and CD31 (figure 4.9 b), as it is also suggested to be a marker for nT_{reg} [56].

Although some of the results reached a statistical significance, the reliability of these findings is weak, with the low number of samples in the patient and control group. Also, methods such as flow cytometry requires great caution in the analysis as small adjustments has a great impact, especially with low number of cells, and that there is disagreement in the reliability of markers used in flow cytometry [144].

5.3 Limitations and methodological optimization

One of the main limitations in this project was the availability of patient material, as APS-1 is a very rare disease. The low sample volume and variable number of cells, in addition to the small patient and control groups makes the results less reliable. To improve this, the frequency of sample collection or the amount of PBMC could have been increased. Also avoiding the freezing step could have improved the number of PBMC in the samples, as this step may induce cell death. But due to the limited time frame and the need to avoid frequent blood sampling of patients, this was not achievable. Other factors such as genetic background of both the patients and controls may also affect the results, and in this case the controls´ backgrounds were not known. Further, it is likely that the patients are treated with medications that might have influence on the results, but it was not possible to adjust for these factors. Finally, the presence of other cells than T cells in PBMC may affect these observations, as PBMC includes B cells, monocytes, NK cells in addition to T cells [145].

When comparing the methods used in this project with others who identified an expanded T_{reg} population in cell culture there were some differences. Other studies used isolated $CD4^+$ T cells or T_{reg} in cell culture [131, 143]. We used PBMC to study the effect of rapamycin due to the small number of cells, where an isolation of $CD4^+$ cells or T_{reg} would have decreased it even more. The concentration of rapamycin was also different in some studies, where some claimed that a low dose (1 nM-10 nM) of rapamycin did not expand the population of T_{reg}, but a concentration of at least 100 nM was needed [143]. On the other hand, some suggests that a concentration of 1 nM did induce an expansion of this population, but that 100 nM gave an even larger expansion [141]. These studies were performed on isolated T_{reg} in cell culture for 1-6 weeks, in some of the experiments the cells were re-stimulated several times in cell culture, with anti-CD3 and –CD28 and IL-2 [141, 142]. In our protocol the cells were only stimulated with anti-CD3 and-CD28 once together with the concentration of 4 nM rapamycin. Modification of the protocol could include a longer time in cell culture and a broader titration line with concentrations up to 100 nM. However, we were also afraid to go too high in concentration and induce unnecessary cell deaths. Another factor is the half-life of rapamycin, which in human it is about 57-63 hours [112], however this is not transferable to cell culture, in an *in vitro* environment. Still, it would be interesting to assess the effect after a second treatment during the time in culture.

The protocol used for flow cytometry was well established in the lab prior to this project, which was timesaving. However, additional markers for anergy and autophagy could have been useful to assess the effect of rapamycin. Studies have different opinions if rapamycin induces anergy or not. A study of alloreactive human T cells suggested that rapamycin do not induce anergy but inhibited the proliferative capacity, another study of autoreactive T cells suggested that rapamycin induced anergy due to blocking the cell cycle progression [146, 147]. A study of anergic cells in mice suggested that the cell surface markers PD-1, CD7, CD28 and CD4 could be used to identify anergic cells [148]. To detect the presence of autophagy, anti-LC3-II was used in a study looking at the rapamycin induced autophagy [149]. As rapamycin is suggested to induce T cell cycle arrest in G1 phase to S, a marker for this would also be helpful to assess the effect of rapamycin [103]. It is further possible that the choice of markers or gating strategy used did not manage to gate for a pure T_{reg} population, as T_{reg} represent a small cell population. A possible way to make it easier to assess the effect of rapamycin on T_{reg} could be to isolate this T cells population, or add additional markers, such as CD127, a marker suggested to be

expressed in a low frequency on T_{reg} [143]. However, T_{reg} isolation was not performed in this project due to the limited time frame, and limited numbers of available cells.

In the study of gene expression in activated cells, it could have been useful to look at the expression of *PTEN*, as high levels of *PTEN* have been observed in T_{reg}. *PTEN* is suggested to block the downstream event in the PI3K pathway in T_{reg}, thereby not being sensitive to rapamycin [141]. It could also be interesting to look at the expression of *S6K1* in the cells after treatment with rapamycin, as this gene is regulated by mTORC1 [91].

6. Concluding remarks

In this study, we aimed to investigate the effect of rapamycin on cells from APS-1 patients and to establish a cell-based system to assess the effect of drugs. We introduced rapamycin as a potential treatment of APS-1 and found only minor differences between the controls and patients. The only significant differences were the decrease of CD39 in the patients and decrease of CD31 in the controls. However, the immunosuppressive effect of rapamycin was similar in APS-1 patients and controls evidenced by the decreased cell proliferation for both groups.

With a limited number of APS-1 patients, the power of this study is not high enough do make any general conclusions. However, we here established an in vitro cell culture system to analyse the effect of rapamycin, which can also be used for screening of other potential drugs on patient cells in the future.

7. Future perspectives

We successfully established a cell-based system to treat PBMC *in vitro* with rapamycin. To further assess the effect of the drug, the use of phosphospecific flow cytometry would have been useful. This method allows for measuring the intracellular signaling pathway to follow the activation of the cell at a single-cell level [150, 151]. Also assessing the levels of IL-10 and TGF-b would have been helpful tools to identify a possible T_{reg} expansion, as other studies has identified an increased level of these cytokines after treatment with rapamycin [152]. It would further be interesting to assess the effect of other rapalogues and drugs expanding the T_{reg} population, such as Rabbit anti-thymocyte globulin (rATG) [153]. Humanized mouse models could be beneficial tools in pre-clinical testing of drugs and to further study the disease, in order

to get access to more relevant cells and tissue that are not available from patients, due to ethical reasons [154, 155]. As the symptoms in APS-1 patients has a variable onset, there is a need of early identification of the symptoms to slow it down. This brings challenges with the need to avoid frequent blood sampling and diagnostic procedures, to avoid putting individuals at risk.

Patients with APS-1 suffer from a rare disease with limited treatment options and the best target of treatment is yet to be identified. The use of T_{reg} therapy in autoimmune diseases is constantly being brought up to date as it has shown to provide a better treatment for other severe autoimmune conditions, such as IPEX and SLE [108, 109]. T_{reg} therapy may be a good option at the moment as the knowledge of this T cell population is rapidly expanding in the area of autoimmune diseases [156]. Novel approaches are needed for further progress in this area of medicine, with a need of targeted and personalized medicine, as there is a broad variation in symptoms. To achieve this there is a great need of specialized methods to understand the complexity of the diseases, where single cell technology has shown to improve the knowledge in diagnostic procedures in the field of autoimmunity [157, 158]. By using such methods, including polychromatic flow cytometry and gene sequencing techniques, the knowledge of endocrine immune diseases has improved, and even more advanced methods has made it possible to dig deeper into the complexity and perhaps identify therapeutic targets [159]. However, there are still a need for further identification of therapeutic targets in APS-1 and other autoimmune disorders.

8. References

1. Calder, P.C., *Fuel utilization by cells of the immune system.* Proceedings of the Nutrition Society, 1995. **54**(1): p. 65-82.
2. Medzhitov, R. and C.A. Janeway Jr, *Innate immune recognition and control of adaptive immune responses.* Seminars in Immunology, 1998. **10**(5): p. 351-353.
3. Janeway, C.A. and K. Bottomly, *Signals and signs for lymphocyte responses.* Cell, 1994. **76**(2): p. 275-285.
4. Sakaguchi, S., *Regulatory T Cells: Key Controllers of Immunologic Self-Tolerance.* Cell, 2000. **101**(5): p. 455-458.
5. Cho, J.H. and M. Feldman, *Heterogeneity of autoimmune diseases: pathophysiologic insights from genetics and implications for new therapies.* Nature Medicine, 2015. **21**(7): p. 730-738.
6. Ingelfinger, J.R.M.D., et al., *Autoimmune Polyendocrine Syndromes.* The New England Journal of Medicine, 2018. **378**(12): p. 1132-1141.
7. Oliveira, C., et al., *Recent advances in characterization of nonviral vectors for delivery of nucleic acids: Impact on their biological performance.* Expert Opinion on Drug Delivery, 2014. **12**.
8. Charles A. Janeway, J. and R. Medzhitov, *Innate Immune Recognition.* Annual Review of Immunology, 2002. **20**(1): p. 197-216.
9. Kumar, H., T. Kawai, and S. Akira, *Toll-like receptors and innate immunity.* Biochemical and Biophysical Research Communications, 2009. **388**(4): p. 621-625.
10. Bennouna, S., et al., *Cross-Talk in the Innate Immune System: Neutrophils Instruct Recruitment and Activation of Dendritic Cells during Microbial Infection.* The Journal of Immunology, 2003. **171**(11): p. 6052.
11. Carroll, M.C., *The complement system in regulation of adaptive immunity.* Nature immunology, 2004. **5**(10): p. 981-986.
12. Müller-Eberhard, H.J., *Molecular organization and function of the complement system.* Annual review of biochemistry, 1988. **57**(1): p. 321-347.
13. Guermonprez, P., et al., *Antigen Presentation and T Cell Stimulation by Dendritic Cells.* Annual Review of Immunology, 2002. **20**(1): p. 621-667.
14. Rosenthal, A.S. and E.M. Shevach, *Function of macrophages in antigen recognition by guinea pig T lymphocytes. I. Requirement for histocompatible macrophages and lymphocytes.* The Journal of experimental medicine, 1973. **138**(5): p. 1194-1212.
15. Freudenthal, P.S. and R.M. Steinman, *The distinct surface of human blood dendritic cells, as observed after an improved isolation method.* Proceedings of the National Academy of Sciences, 1990. **87**(19): p. 7698.
16. Hao, S., J. Yuan, and J. Xiang, *Nonspecific CD4+ T cells with uptake of antigen-specific dendritic cell-released exosomes stimulate antigen-specific CD8+ CTL responses and long-term T cell memory.* Journal of Leukocyte Biology, 2007. **82**(4): p. 829-838.
17. Bonilla, F.A. and H.C. Oettgen, *Adaptive immunity.* Journal of Allergy and Clinical Immunology, 2010. **125**(2, Supplement 2): p. S33-S40.
18. Hardy, R.R., et al., *Resolution and characterization of pro-B and pre-pro-B cell stages in normal mouse bone marrow.* Journal of Experimental Medicine, 1991. **173**(5): p. 1213-1225.
19. Hardy, R.R. and K. Hayakawa, *B Cell Development Pathways.* Annual Review of Immunology, 2001. **19**(1): p. 595-621.
20. Parker, D.C., *T cell-dependent B cell activation.* Annual review of immunology, 1993. **11**(1): p. 331-360.

21. Dörner, T. and A. Radbruch, *Selecting B cells and plasma cells to memory.* The Journal of experimental medicine, 2005. **201**(4): p. 497-499.
22. Scholl, P.R. and R.S. Geha, *MHC class II signaling in B-cell activation.* Immunology Today, 1994. **15**(9): p. 418-422.
23. MacIver, N.J., R.D. Michalek, and J.C. Rathmell, *Metabolic regulation of T lymphocytes.* Annual review of immunology, 2013. **31**: p. 259-283.
24. Lehmann-Grube, F., D. Moskophidis, and J. LÖHler, *Recovery from Acute Virus Infection.* Annals of the New York Academy of Sciences, 1988. **532**(1): p. 238-256.
25. Vose, B.M. and G.D. Bonnard, *Human tumour antigens defined by cytotoxicity and proliferative responses of cultured lymphoid cells.* Nature, 1982. **296**(5855): p. 359-361.
26. Tada, T., et al., *Two distinct types of helper T cells involved in the secondary antibody response: independent and synergistic effects of Ia- and Ia+ helper T cells.* The Journal of experimental medicine, 1978. **147**(2): p. 446-458.
27. Nurieva, R.I., et al., *Generation of T Follicular Helper Cells Is Mediated by Interleukin-21 but Independent of T Helper 1, 2, or 17 Cell Lineages.* Immunity, 2008. **29**(1): p. 138-149.
28. Wilson, A., J.-P. de Villartay, and H.R. MacDonald, *T Cell Receptor Delta Gene Rearrangement and T Early alpha (TEA) Expression in Immature alpha beta LineageThymocytes: Implications for alpha beta/gamma delta Lineage Commitment.* Immunity, 1996. **4**(1): p. 37-45.
29. Takahama, Y., *Journey through the thymus: stromal guides for T-cell development and selection.* Nature Reviews Immunology, 2006. **6**(2): p. 127-135.
30. Takaba, H. and H. Takayanagi, *The Mechanisms of T Cell Selection in the Thymus.* Trends in Immunology, 2017. **38**(11): p. 805-816.
31. Laufer, T.M., et al., *Unopposed positive selection and autoreactivity in mice expressing class II MHC only on thymic cortex.* Nature, 1996. **383**(6595): p. 81-85.
32. Anderson, M.S., et al., *Projection of an Immunological Self Shadow Within the Thymus by the Aire Protein.* Science, 2002. **298**(5597): p. 1395.
33. Anderson, M.S., et al., *The Cellular Mechanism of Aire Control of T Cell Tolerance.* Immunity, 2005. **23**(2): p. 227-239.
34. Liston, A., et al., *Aire regulates negative selection of organ-specific T cells.* Nature Immunology, 2003. **4**(4): p. 350-354.
35. Jordan, M.S., et al., *Thymic selection of CD4+CD25+ regulatory T cells induced by an agonist self-peptide.* Nature Immunology, 2001. **2**(4): p. 301-306.
36. Sakaguchi, S., *Naturally Arising CD4+ Regulatory T Cells for Immunologic Self-Tolerance and Negative Control of Immune Responses.* Annual Review of Immunology, 2004. **22**(1): p. 531-562.
37. Fontenot, J.D., M.A. Gavin, and A.Y. Rudensky, *Foxp3 programs the development and function of CD4+CD25+ regulatory T cells.* Nature Immunology, 2003. **4**(4): p. 330-6.
38. Doherty, P.C., *The function of γδ T cells.* British Journal of Haematology, 1992. **81**(3): p. 321-324.
39. Doherty, P.C., *Cell-Mediated Immunity in Virus Infections of the Central Nervous System.* Annals of the New York Academy of Sciences, 1988. **540**(1): p. 228-239.
40. Smith-Garvin, J.E., G.A. Koretzky, and M.S. Jordan, *T cell activation.* Annual review of immunology, 2009. **27**: p. 591-619.
41. Hogquist, K.A., et al., *T cell receptor antagonist peptides induce positive selection.* Cell, 1994. **76**(1): p. 17-27.

42. Jacobs, S.R., et al., *Glucose uptake is limiting in T cell activation and requires CD28-mediated Akt-dependent and independent pathways.* Journal of immunology (Baltimore, Md. : 1950), 2008. **180**(7): p. 4476-4486.
43. Buchbinder, E.I. and A. Desai, *CTLA-4 and PD-1 pathways: similarities, differences, and implications of their inhibition.* American journal of clinical oncology, 2016. **39**(1): p. 98.
44. Curtsinger, J.M. and M.F. Mescher, *Inflammatory cytokines as a third signal for T cell activation.* Current Opinion in Immunology, 2010. **22**(3): p. 333-340.
45. Iida, T., et al., *Regulation of Cell Surface Expression of CTLA-4 by Secretion of CTLA-4-Containing Lysosomes Upon Activation of CD4+ T Cells.* The Journal of Immunology, 2000. **165**(9): p. 5062.
46. Annacker, O., et al., *CD25+ CD4+ T Cells Regulate the Expansion of Peripheral CD4 T Cells Through the Production of IL-10.* The Journal of Immunology, 2001. **166**(5): p. 3008.
47. Itoh, M., et al., *Thymus and Autoimmunity: Production of CD25+CD4+ Naturally Anergic and Suppressive T Cells as a Key Function of the Thymus in Maintaining Immunologic Self-Tolerance.* The Journal of Immunology, 1999. **162**(9): p. 5317.
48. Kasper, I.R., et al., *Empowering Regulatory T Cells in Autoimmunity.* Trends in Molecular Medicine, 2016. **22**(9): p. 784-797.
49. O'Garra, A. and P. Vieira, *Regulatory T cells and mechanisms of immune system control.* Nature Medicine, 2004. **10**(8): p. 801-805.
50. Curotto de Lafaille, M.A. and J.J. Lafaille, *Natural and Adaptive Foxp3+ Regulatory T Cells: More of the Same or a Division of Labor?* Immunity, 2009. **30**(5): p. 626-635.
51. Sakaguchi, S., et al., *Immunologic self-tolerance maintained by activated T cells expressing IL-2 receptor alpha-chains (CD25). Breakdown of a single mechanism of self-tolerance causes various autoimmune diseases.* The Journal of Immunology, 1995. **155**(3): p. 1151.
52. Malek, T.R., et al., *CD4 Regulatory T Cells Prevent Lethal Autoimmunity in IL-2Rβ-Deficient Mice: Implications for the Nonredundant Function of IL-2.* Immunity, 2002. **17**(2): p. 167-178.
53. Sauer, S., et al., *T cell receptor signaling controls Foxp3 expression via PI3K, Akt, and mTOR.* Proceedings of the National Academy of Sciences of the United States of America, 2008. **105**(22): p. 7797-7802.
54. Haxhinasto, S., D. Mathis, and C. Benoist, *The AKT-mTOR axis regulates de novo differentiation of CD4+Foxp3+ cells.* The Journal of experimental medicine, 2008. **205**(3): p. 565-574.
55. Delgoffe, G.M., et al., *The mTOR kinase differentially regulates effector and regulatory T cell lineage commitment.* Immunity, 2009. **30**(6): p. 832-844.
56. Chapman, N.M. and H. Chi, *mTOR signaling, Tregs and immune modulation.* Immunotherapy, 2014. **6**(12): p. 1295-1311.
57. Kimmig, S., et al., *Two subsets of naive T helper cells with distinct T cell receptor excision circle content in human adult peripheral blood.* The Journal of experimental medicine, 2002. **195**(6): p. 789-794.
58. Braza, F., et al., *Regulatory T cells in kidney transplantation: new directions?* American Journal of Transplantation, 2015. **15**(9): p. 2288-2300.
59. de la Rosa, M., et al., *Interleukin-2 is essential for CD4+CD25+ regulatory T cell function.* European Journal of Immunology, 2004. **34**(9): p. 2480-2488.
60. Gu, J., et al., *Human CD39hi regulatory T cells present stronger stability and function under inflammatory conditions.* Cellular & Molecular Immunology, 2017. **14**(6): p. 521-528.

61. Deaglio, S., et al., *Adenosine generation catalyzed by CD39 and CD73 expressed on regulatory T cells mediates immune suppression.* Journal of Experimental Medicine, 2007. **204**(6): p. 1257-1265.
62. Roncarolo, M.G., et al., *Type 1 T regulatory cells.* Immunological Reviews, 2001. **182**(1): p. 68-79.
63. Wahl, S.M., et al., *Transforming growth factor-beta is a potent immunosuppressive agent that inhibits IL-1-dependent lymphocyte proliferation.* The Journal of Immunology, 1988. **140**(9): p. 3026.
64. Schoenborn, J.R. and C.B. Wilson, *Regulation of Interferon-γ During Innate and Adaptive Immune Responses*, in *Advances in Immunology*. 2007, Academic Press. p. 41-101.
65. Gilbert, K.M., et al., *Transforming growth factor-β1 induces antigen-specific unresponsiveness in naive t cells.* Immunological Investigations, 1997. **26**(4): p. 459-472.
66. Miescher, P.A., et al., *Autoimmune disorders: a concept of treatment based on mechanisms of disease.* Springer Seminars in Immunopathology, 2003. **25**(1): p. S5-S60.
67. Smith, H.R. and A.D. Steinberg, *Autoimmunity-a perspective.* Annual review of immunology, 1983. **1**(1): p. 175-210.
68. Hewagama, A. and B. Richardson, *The genetics and epigenetics of autoimmune diseases.* Journal of Autoimmunity, 2009. **33**(1): p. 3-11.
69. Bogdanos, D.P., et al., *Twin studies in autoimmune disease: Genetics, gender and environment.* Journal of Autoimmunity, 2012. **38**(2): p. J156-J169.
70. Herrath, M.G.v. and M.B.A. Oldstone, *Virus-induced autoimmune disease.* Current Opinion in Immunology, 1996. **8**(6): p. 878-885.
71. Fairweather, D. and N.R. Rose, *Women and autoimmune diseases.* Emerging infectious diseases, 2004. **10**(11): p. 2005-2011.
72. Streilein, J.W., M. Takeuchi, and A.W. Taylor, *Immune privilege, T-cell tolerance, and tissue-restricted autoimmunity.* Human Immunology, 1997. **52**(2): p. 138-143.
73. Shi, G., et al., *Systemic Autoimmune Diseases.* Clinical and Developmental Immunology, 2013. **2013**: p. 728574.
74. Wahren-Herlenius, M. and T. Dörner, *Immunopathogenic mechanisms of systemic autoimmune disease.* The Lancet, 2013. **382**(9894): p. 819-831.
75. Arlt, W. and B. Allolio, *Adrenal insufficiency.* The Lancet, 2003. **361**(9372): p. 1881-1893.
76. Husebye, E.S., et al., *Clinical manifestations and management of patients with autoimmune polyendocrine syndrome type I.* Journal of Internal Medicine, 2009. **265**(5): p. 514-529.
77. Wolff, A., et al., *Autoimmune Polyendocrine Syndrome Type 1 in Norway: Phenotypic Variation, Autoantibodies, and Novel Mutations in the Autoimmune Regulator Gene.* The Journal of clinical endocrinology and metabolism, 2007. **92**: p. 595-603.
78. Betterle, C., N.A. Greggio, and M. Volpato, *Clinical review 93: Autoimmune polyglandular syndrome type 1.* The Journal of clinical endocrinology and metabolism, 1998. **83**(4): p. 1049-1055.
79. Borchers, J., et al., *Patients With APECED Have Increased Early Mortality Due to Endocrine Causes, Malignancies and infections.* The Journal of clinical endocrinology and metabolism, 2020. **105**(6): p. dgaa140.
80. Meager, A., et al., *Anti-interferon autoantibodies in autoimmune polyendocrinopathy syndrome type 1.* PLoS medicine, 2006. **3**(7): p. e289-e289.

81. Wolff, A.S.B., et al., *Flow Cytometry Study of Blood Cell Subtypes Reflects Autoimmune and Inflammatory Processes in Autoimmune Polyendocrine Syndrome Type I.* Scandinavian Journal of Immunology, 2010. **71**(6): p. 459-467.
82. Koivula, T.T., et al., *Clonal Analysis of Regulatory T Cell Defect in Patients with Autoimmune Polyendocrine Syndrome Type 1 Suggests Intrathymic Impairment.* Scandinavian Journal of Immunology, 2017. **86**(4): p. 221-228.
83. Laakso, S.M., et al., *Regulatory T cell defect in APECED patients is associated with loss of naive FOXP3+ precursors and impaired activated population.* Journal of Autoimmunity, 2010. **35**(4): p. 351-357.
84. Mercadante, E.R. and U.M. Lorenz, *Breaking Free of Control: How Conventional T Cells Overcome Regulatory T Cell Suppression.* Frontiers in immunology, 2016. **7**: p. 193-193.
85. Ward, L., et al., *Severe Autoimmune Polyendocrinopathy-Candidiasis-Ectodermal Dystrophy in an Adolescent Girl with a Novel AIRE Mutation: Response to Immunosuppressive Therapy1.* The Journal of Clinical Endocrinology & Metabolism, 1999. **84**(3): p. 844-852.
86. Georgopapadakou, N.H., *Antifungals: mechanism of action and resistance, established and novel drugs.* Current Opinion in Microbiology, 1998. **1**(5): p. 547-557.
87. Matsuda, S. and S. Koyasu, *Mechanisms of action of cyclosporine.* Immunopharmacology, 2000. **47**(2): p. 119-125.
88. Weiner, G.J., *Rituximab: Mechanism of Action.* Seminars in Hematology, 2010. **47**(2): p. 115-123.
89. Delgoffe, G.M., et al., *The kinase mTOR regulates the differentiation of helper T cells through the selective activation of signaling by mTORC1 and mTORC2.* Nature immunology, 2011. **12**(4): p. 295-303.
90. Sarbassov, D.D., S.M. Ali, and D.M. Sabatini, *Growing roles for the mTOR pathway.* Current Opinion in Cell Biology, 2005. **17**(6): p. 596-603.
91. Tsang, C.K., et al., *Targeting mammalian target of rapamycin (mTOR) for health and diseases.* Drug Discovery Today, 2007. **12**(3): p. 112-124.
92. LoPiccolo, J., et al., *Targeting the PI3K/Akt/mTOR pathway: Effective combinations and clinical considerations.* Drug Resistance Updates, 2008. **11**(1): p. 32-50.
93. Colombetti, S., et al., *Prolonged TCR/CD28 Engagement Drives IL-2-Independent T Cell Clonal Expansion through Signaling Mediated by the Mammalian Target of Rapamycin.* The Journal of Immunology, 2006. **176**(5): p. 2730.
94. Jhanwar-Uniyal, M., et al., *Discrete signaling mechanisms of mTORC1 and mTORC2: Connected yet apart in cellular and molecular aspects.* Advances in Biological Regulation, 2017. **64**: p. 39-48.
95. Tong, M. and Y. Jiang, *FK506-Binding Proteins and Their Diverse Functions.* Current molecular pharmacology, 2015. **9**.
96. McMahon, G., et al., *The Evolving Role of mTOR Inhibition in Transplantation Tolerance.* Journal of the American Society of Nephrology, 2011. **22**(3): p. 408.
97. Palavra, F., C. Robalo, and F. Reis, *Recent Advances and Challenges of mTOR Inhibitors Use in the Treatment of Patients with Tuberous Sclerosis Complex.* Oxidative medicine and cellular longevity, 2017. **2017**: p. 9820181-9820181.
98. Vézina, C., A. Kudelski, and S.N. Sehgal, *Rapamycin (AY-22,989), a new antifungal antibiotic. I. Taxonomy of the producing streptomycete and isolation of the active principle.* The Journal of antibiotics, 1975. **28**(10): p. 721-726.
99. Thomson, A.W., H.R. Turnquist, and G. Raimondi, *Immunoregulatory functions of mTOR inhibition.* Nature reviews. Immunology, 2009. **9**(5): p. 324-337.

100. Zhang, Z., et al., *Low dose rapamycin exacerbates autoimmune experimental uveitis.* PloS one, 2012. **7**(5): p. e36589-e36589.
101. Thoreen, C.C., et al., *An ATP-competitive mammalian target of rapamycin inhibitor reveals rapamycin-resistant functions of mTORC1.* Journal of Biological Chemistry, 2009. **284**(12): p. 8023-8032.
102. Kunz, J. and M.N. Hall, *Cyclosporin A, FK506 and rapamycin: more than just immunosuppression.* Trends in Biochemical Sciences, 1993. **18**(9): p. 334-338.
103. Battaglia, M., A. Stabilini, and M.-G. Roncarolo, *Rapamycin selectively expands CD4+CD25+FoxP3+ regulatory T cells.* Blood, 2005. **105**(12): p. 4743-4748.
104. Fredriksson, K., et al., *Paradoxical effects of rapamycin on experimental house dust mite-induced asthma.* PloS one, 2012. **7**(5): p. e33984-e33984.
105. Castedo, M., K.F. Ferri, and G. Kroemer, *Mammalian Target of Rapamycin (mTOR): Pro- and Anti-Apoptotic.* Cell Death & Differentiation, 2002. **9**(2): p. 99-100.
106. Singh, K., et al., *Regulatory T Cells Exhibit Decreased Proliferation but Enhanced Suppression After Pulsing With Sirolimus.* American Journal of Transplantation, 2012. **12**(6): p. 1441-1457.
107. Wen, H.-Y., et al., *Low-Dose Sirolimus Immunoregulation Therapy in Patients with Active Rheumatoid Arthritis: A 24-Week Follow-Up of the Randomized, Open-Label, Parallel-Controlled Trial.* Journal of immunology research, 2019. **2019**: p. 7684352-7684352.
108. Lai, Z.-W., et al., *Sirolimus in patients with clinically active systemic lupus erythematosus resistant to, or intolerant of, conventional medications: a single-arm, open-label, phase 1/2 trial.* Lancet (London, England), 2018. **391**(10126): p. 1186-1196.
109. Bindl, L., et al., *Successful Use of the New Immune-suppressor Sirolimus in IPEX (Immune Dysregulation, Polyendocrinopathy, Enteropathy, X-linked Syndrome).* The Journal of Pediatrics, 2005. **147**(2): p. 256-259.
110. Yong, P.L., P. Russo, and K.E. Sullivan, *Use of Sirolimus in IPEX and IPEX-Like Children.* Journal of Clinical Immunology, 2008. **28**(5): p. 581.
111. Stenton, S.B., N. Partovi, and M.H.H. Ensom, *Sirolimus.* Clinical Pharmacokinetics, 2005. **44**(8): p. 769-786.
112. Mukherjee, S. and U. Mukherjee, *A comprehensive review of immunosuppression used for liver transplantation.* Journal of transplantation, 2009. **2009**: p. 701464-701464.
113. Murgia, M.G., S. Jordan, and B.D. Kahan, *The side effect profile of sirolimus: A phase I study in quiescent cyclosporine-prednisone-treated renal transplant patients.* Kidney International, 1996. **49**(1): p. 209-216.
114. Saunders, R.N., M.S. Metcalfe, and M.L. Nicholson, *Rapamycin in transplantation: A review of the evidence.* Kidney International, 2001. **59**(1): p. 3-16.
115. Aghaeepour, N., et al., *Critical assessment of automated flow cytometry data analysis techniques.* Nature Methods, 2013. **10**(3): p. 228-238.
116. Roederer, M., *Interpretation of cellular proliferation data: Avoid the panglossian.* Cytometry Part A, 2011. **79A**(2): p. 95-101.
117. Bookout, A.L. and D.J. Mangelsdorf, *Quantitative real-time PCR protocol for analysis of nuclear receptor signaling pathways.* Nuclear Receptor Signaling, 2003. **1**(1): p. nrs.01012.
118. Löseke, S., et al., *Differential expression of IFN-α subtypes in human PBMC: evaluation of novel real-time PCR assays.* Journal of Immunological Methods, 2003. **276**(1): p. 207-222.

119. Holland, P.M., et al., *Detection of specific polymerase chain reaction product by utilizing the 5´——3´ exonuclease activity of Thermus aquaticus DNA polymerase.* Proceedings of the National Academy of Sciences, 1991. **88**(16): p. 7276.
120. Schmittgen, T.D. and K.J. Livak, *Analyzing real-time PCR data by the comparative CT method.* Nature Protocols, 2008. **3**(6): p. 1101-1108.
121. Leng, S.X., et al., *ELISA and multiplex technologies for cytokine measurement in inflammation and aging research.* The journals of gerontology. Series A, Biological sciences and medical sciences, 2008. **63**(8): p. 879-884.
122. Bratanic, N., et al., *Clinical, Genetic and Immunological Characteristics of Paediatric Autoimmune Polyglandular Syndrome Type 1 Patients in Slovenia.* Zdravstveno varstvo, 2015. **54**(2): p. 112-118.
123. Kalamasz, H.D., et al., *Optimization of Human T-Cell Expansion Ex Vivo Using Magnetic Beads Conjugated with Anti-CD3 and Anti-CD28 Antibodies.* Journal of Immunotherapy, 2004. **27**(5): p. 405-418.
124. Popa-Burke, I.G., et al., *Streamlined System for Purifying and Quantifying a Diverse Library of Compounds and the Effect of Compound Concentration Measurements on the Accurate Interpretation of Biological Assay Results.* Analytical Chemistry, 2004. **76**(24): p. 7278-7287.
125. Rogers-Broadway, K.-R., et al., *Differential expression of mTOR components in endometriosis and ovarian cancer: Effects of rapalogues and dual kinase inhibitors on mTORC1 and mTORC2 stoichiometry.* International journal of molecular medicine, 2019. **43**(1): p. 47-56.
126. Lorenz, M.C. and J. Heitman, *TOR mutations confer rapamycin resistance by preventing interaction with FKBP12-rapamycin.* Journal of Biological Chemistry, 1995. **270**(46): p. 27531-27537.
127. Dilling, M.B., et al., *Rapamycin Selectively Inhibits the Growth of Childhood Rhabdomyosarcoma Cells through Inhibition of Signaling via the Type I Insulin-like Growth Factor Receptor.* Cancer Research, 1994. **54**(4): p. 903.
128. Krebs, M., et al., *The Mammalian Target of Rapamycin Pathway Regulates Nutrient-Sensitive Glucose Uptake in Man.* Diabetes, 2007. **56**(6): p. 1600.
129. Ayukawa, H., et al., *Expression of CTLA-4 (CD152) in peripheral blood T cells of children with influenza virus infection including encephalopathy in comparison with respiratory syncytial virus infection.* Clinical and experimental immunology, 2004. **137**(1): p. 151-155.
130. Fulda, S., et al., *Cellular Stress Responses: Cell Survival and Cell Death.* International Journal of Cell Biology, 2010. **2010**.
131. Hester, J., et al., *Low-Dose Rapamycin Treatment Increases the Ability of Human Regulatory T Cells to Inhibit Transplant Arteriosclerosis In Vivo.* American Journal of Transplantation, 2012. **12**(8): p. 2008-2016.
132. Woerly, G., N. Brooks, and B. Ryffel, *Effect of rapamycin on the expression of the IL-2 receptor (CD25).* Clinical and experimental immunology, 1996. **103**(2): p. 322-327.
133. Wang, X.B., et al., *Regulation of Surface and Intracellular Expression of CTLA-4 on Human Peripheral T Cells.* Scandinavian Journal of Immunology, 2001. **54**(5): p. 453-458.
134. Lu, Y., et al., *Rapamycin Regulates iTreg Function through CD39 and Runx1 Pathways.* Journal of Immunology Research, 2014. **2014**: p. 989434.
135. Passerini, L., et al., *Treatment with rapamycin can restore regulatory T-cell function in IPEX patients.* Journal of Allergy and Clinical Immunology, 2020. **145**(4): p. 1262-1271.e13.

136. Javorkova, E., et al., *The effect of clinically relevant doses of immunosuppressive drugs on human mesenchymal stem cells.* Biomedicine & pharmacotherapy = Biomedecine & pharmacotherapie, 2017. **97**: p. 402-411.
137. Assenmacher, M., J. Schmitz, and A. Radbruch, *Flow cytometric determination of cytokines in activated murine T helper lymphocytes: Expression of interleukin-10 in interferon-γ and in interleukin-4-expressing cells.* European Journal of Immunology, 1994. **24**(5): p. 1097-1101.
138. Eyerich, K., et al., *Patients with chronic mucocutaneous candidiasis exhibit reduced production of Th17-associated cytokines IL-17 and IL-22.* Journal of Investigative Dermatology, 2008. **128**(11): p. 2640-2645.
139. Raczkowski, F., et al., *CD39 is upregulated during activation of mouse and human T cells and attenuates the immune response to Listeria monocytogenes.* PLOS ONE, 2018. **13**(5): p. e0197151.
140. Bai, A., et al., *NADH oxidase-dependent CD39 expression by CD8+ T cells modulates interferon gamma responses via generation of adenosine.* Nature Communications, 2015. **6**(1): p. 8819.
141. Strauss, L., et al., *Differential Responses of Human Regulatory T Cells (Treg) and Effector T Cells to Rapamycin.* PLOS ONE, 2009. **4**(6): p. e5994.
142. Long, S.A. and J.H. Buckner, *Combination of rapamycin and IL-2 increases de novo induction of human CD4(+)CD25(+)FOXP3(+) T cells.* Journal of autoimmunity, 2008. **30**(4): p. 293-302.
143. Battaglia, M., et al., *Rapamycin Promotes Expansion of Functional CD4⁺CD25⁺FOXP3⁺ Regulatory T Cells of Both Healthy Subjects and Type 1 Diabetic Patients.* The Journal of Immunology, 2006. **177**(12): p. 8338.
144. Himmel, M.E., et al., *Helios+ and Helios- Cells Coexist within the Natural FOXP3+ T Regulatory Cell Subset in Humans.* The Journal of Immunology, 2013. **190**(5): p. 2001.
145. Corkum, C.P., et al., *Immune cell subsets and their gene expression profiles from human PBMC isolated by Vacutainer Cell Preparation Tube (CPT™) and standard density gradient.* BMC immunology, 2015. **16**: p. 48-48.
146. Nikolaeva, N., et al., *Rapamycin Does Not Induce Anergy but Inhibits Expansion and Differentiation of Alloreactive Human T Cells.* Transplantation, 2006. **81**(3).
147. Powell, J.D., C.G. Lerner, and R.H. Schwartz, *Inhibition of Cell Cycle Progression by Rapamycin Induces T Cell Clonal Anergy Even in the Presence of Costimulation.* The Journal of Immunology, 1999. **162**(5): p. 2775.
148. Lechner, O., et al., *Fingerprints of anergic T cells.* Current Biology, 2001. **11**(8): p. 587-595.
149. Warnes, G., *et. al.*, *Measurement of Autophagy by Flow Cytometry.* Current protocols in cytometry / editorial board, J. Paul Robinson, managing editor., 2014. **68**: p. 9.45.1-9.45.10.
150. Baan, C., et al., *Phospho-specific flow cytometry for pharmacodynamic monitoring of immunosuppressive therapy in transplantation.* Transplantation research, 2012. **1**(1): p. 20-20.
151. Krutzik, P.O., et al., *High-content single-cell drug screening with phosphospecific flow cytometry.* Nature Chemical Biology, 2008. **4**(2): p. 132-142.
152. Lu, Q., et al., *Inhibition of mammalian target of rapamycin improves neurobehavioral deficit and modulates immune response after intracerebral hemorrhage in rat.* Journal of Neuroinflammation, 2014. **11**(1): p. 44.

153. Furukawa, A., S.A. Wisel, and Q. Tang, *Impact of Immune-Modulatory Drugs on Regulatory T Cell.* Transplantation, 2016. **100**(11): p. 2288-2300.
154. Magnusson, L., et al., *Mass Cytometry Studies of Patients With Autoimmune Endocrine Diseases Reveal Distinct Disease-Specific Alterations in Immune Cell Subsets.* Frontiers in immunology, 2020. **11**: p. 288-288.
155. Shultz, L.D., F. Ishikawa, and D.L. Greiner, *Humanized mice in translational biomedical research.* Nature Reviews Immunology, 2007. **7**(2): p. 118-130.
156. Rosenblum, M.D., et al., *Treating human autoimmunity: current practice and future prospects.* Science translational medicine, 2012. **4**(125): p. 125sr1-125sr1.
157. Bendall, S.C., et al., *A deep profiler's guide to cytometry.* Trends in immunology, 2012. **33**(7): p. 323-332.
158. Bendall, S.C., et al., *Single-cell mass cytometry of differential immune and drug responses across a human hematopoietic continuum.* Science (New York, N.Y.), 2011. **332**(6030): p. 687-696.
159. Soloski, M.J. and F.J. Chrest, *Multiparameter flow cytometry for discovery of disease mechanisms in rheumatic diseases.* Arthritis and rheumatism, 2013. **65**(5): p. 1148-1156.

9. Appendix

Table A.1 List of included patients

No.	Sex	Year of birth	Age of debut	Manifestation	AIRE mutation	Autoantibodies
1	Male	1990	1	Candidiasis Adrenocortical failure Hypoparatyroidisme Malarbsoption Alopecia Enamel hypoplasia Keratoconjunctivitis	c.967-979del13/c.967-979del13	Interferon-w 21-hydroxylase 17-hydroprogesterone, Tyrosine hydroxylase
2	Male	1960	43	Hypoparatyroidisme Candidiasis Vitiligo Diabetes mellitus Enamel hypoplasia Hypothyroidism	c.879+1G>A/c.879+1G>A	Interferon-w 21-hydroxylase 17-hydroprogesterone NOD-liker receptor phyrin domain containing 5 Tyrosine hydroxylase Tryptophan hydroxylase Aromatic L-amino acid decarboxylase Glutamic acid decarboxylase
3	Female	1975	23	Adrenocortical failure Candidiasis Enamel hypoplasia	c.879+1G>A/c.879+1G>A	Interferon-w 21-hydroxylase 17-hydroprogesterone NOD-liker receptor phyrin domain containing 5
4	Female	1972	5	Hypoparatyroidisme Hypogonadism Vit. B12 deficiency Malarbsoption Enamel hypoplasia	c.934G>A	Interferon-w NOD-liker receptor phyrin domain containing 5
5	Male	1964	14	Hypoparatyroidisme Candidiasis Diabetes mellitus Keratoconjunctivitis Nail hypotrohia Vitiligo Alopecia Enamel hypoplasia	c.769C>T/c.1249dupC	Interferon-w Aromatic L-amino acid decarboxylase Glutamic acid decarboxylase Tyrosine hydroxylase Tryptophan hydroxylase
6	Male	1986	4	Hypoparatyroidisme Candidiasis Adrenocortical failure Enamel hypoplasia	c.967-979del13/c.967-979del13	Interferon-w 21-hydroxylase Side chain cleavage enzyme Tyrosine hydroxylase
7	Male	1955	12	Adrenocortical failure Hypoparatyroidisme Vit. B12 deficiency	c.967-979del13/c.967-979del13	Interferon-w 17-hydroprogesterone Side chain cleavage enzyme NOD-liker receptor phyrin domain containing 5
8	Male	1948	7	Candidiasis Hypoparatyroidisme Adrenocortical failure Vitiligo	c.769C>T/c.769C>T	Interferon-w 21-hydroxylase Side chain cleavage enzyme Aromatic L-amino acid decarboxylase

				Alopecia Vit. B12 deficiency Enamel hypoplasia		
9	Male	1970	12	Adrenocortical failure Candidiasis	c.967-979del13/c.967-979del13	Interferon-w 21-hydroxylase Side chain cleavage enzyme Glutamic acid decarboxylase
10	Female	1957	1	Candidiasis Hypoparatyroidisme Adrenocortical failure Hypogonadism	c.967-979del13/c.967-979del13	Interferon-w 21-hydroxylase 17-hydroprogesterone Side chain cleavage enzyme Glutamic acid decarboxylase Aromatic L-amino acid decarboxylase Tryptophan hydroxylase Tyrosine hydroxylase
11	Male	1980	9	Hypoparatyroidisme Adrenocortical failure Candidiasis Enamel hypoplasia	c.967-979del13/c.967-979del13	Interferon-w 21-hydroxylase Side chain cleavage enzyme Tyrosine hydroxylase Aromatic L-amino acid decarboxylase Glutamic acid decarboxylase
12	Female	1990	0	Candidiasis Hypoparatyroidisme Adrenocortical failure Enamel hypoplasia	c.769C>T/c.1242_1243insA	Interferon-w 21-hydroxylase 17-hydroprogesterone Side chain cleavage enzyme NOD-liker receptor phyrin domain containing 5

Table A.2 List of included controls

No.	Sex	Year of birth
1	Male	1990
2	Male	1960
3	Female	1971
4	Female	1979
5	Male	1971
6	Male	1986±5 years
7	Male	1955±5 years
8	Male	1948±5 years
9	Male	1970±5 years
10	Femal	1957±5 years
11	Male	1980±5 years
12	Female	1990±5 years
13	Male	1986±5 years
14	Male	1992

Table A.3: Number of live cells before and after isolation.

Samples	Number of live cells before isolation ($\bullet 10_6$)	Number of live cells after isolation ($\bullet 10_6$)
Controls		
Control 1	4.29	3.80
Control 2	6.50	1.97
Control 3	4.66	3.33
Control 4	1.93	1.20
Control 5	3.04	2.70
Patients		
Patient 1	6.70	5.89
Patient 2	2.92	1.87
Patient 3	7.19	1.50
Patient 4	5.60	3.47
Patient 5	7.3	6.84

Table A.4: List of genes in the mTOR signaling pathway included in the qPCR with resting cells

Symbol	Description	Fold change $(\frac{\text{Patient}}{Control})$
AKT1	V-akt murine thymoma viral oncogene homolog 1	0,70
AKT1S1	AKT1 substrate 1 (proline-rich)	0,72
AKT2	V-akt murine thymoma viral oncogene homolog 2	0,84
AKT3	V-akt murine thymoma viral oncogene homolog 3 (protein kinase B, gamma)	0,83
CAB39	Calcium binding protein 39	0,76
CAB39L	Calcium binding protein 39-like	0,98
CDC42	Cell division cycle 42 (GTP binding protein, 25kDa)	0,71
CHUK	Conserved helix-loop-helix ubiquitous kinase	0,82
DDIT4	DNA-damage-inducible transcript 4	**-***
DDIT4L	DNA-damage-inducible transcript 4-like	0,78
DEPTOR	DEP domain containing MTOR-interacting protein	0,75
EIF4B	Eukaryotic translation initiation factor 4B	1,27
EIF4E	Eukaryotic translation initiation factor 4E	0,86
EIF4EBP1	Eukaryotic translation initiation factor 4E binding protein 1	0,83
EIF4EBP2	Eukaryotic translation initiation factor 4E binding protein 2	0,81
FKBP1A	FK506 binding protein 1A, 12kDa	0,82
FKBP8	FK506 binding protein 8, 38kDa	0,90
GSK3B	Glycogen synthase kinase 3 beta	0,88
HIF1A	Hypoxia inducible factor 1, alpha subunit (basic helix-loop-helix transcription factor)	0,96
HRAS	V-Ha-ras Harvey rat sarcoma viral oncogene homolog	1,10

HSPA4	Heat shock 70kDa protein 4	0,62
IGF1	Insulin-like growth factor 1 (somatomedin C)	0,91
IGFBP3	Insulin-like growth factor binding protein 3	0,76
IKBKB	Inhibitor of kappa light polypeptide gene enhancer in B-cells, kinase beta	0,96
ILK	Integrin-linked kinase	**3,41**
INS	Insulin	0,73
INSR	Insulin receptor	0,99
IRS1	Insulin receptor substrate 1	0,86
MAPK1	Mitogen-activated protein kinase 1	0,94
MAPK3	Mitogen-activated protein kinase 3	1,04
MAPKAP1	Mitogen-activated protein kinase associated protein 1	0,93
MLST8	MTOR associated protein, LST8 homolog (S. cerevisiae)	1,22
MTOR	Mechanistic target of rapamycin (serine/threonine kinase)	0,94
MYO1C	Myosin IC	1,43
PDPK1	3-phosphoinositide dependent protein kinase-1	0,94
PIK3C3	Phosphoinositide-3-kinase, class 3	1,06
PIK3CA	Phosphoinositide-3-kinase, catalytic, alpha polypeptide	1,00
PIK3CB	Phosphoinositide-3-kinase, catalytic, beta polypeptide	1,00
PIK3CD	Phosphoinositide-3-kinase, catalytic, delta polypeptide	0,85
PIK3CG	Phosphoinositide-3-kinase, catalytic, gamma polypeptide	0,72
PLD1	Phospholipase D1, phosphatidylcholine-specific	0,91
PLD2	Phospholipase D2	0,94
PPP2CA	Protein phosphatase 2, catalytic subunit, alpha isozyme	0,82
PPP2R2B	Protein phosphatase 2, regulatory subunit B, beta	0,82
PPP2R4	Protein phosphatase 2A activator, regulatory subunit 4	1,02
PRKAA1	Protein kinase, AMP-activated, alpha 1 catalytic subunit	0,95
PRKAA2	Protein kinase, AMP-activated, alpha 2 catalytic subunit	0,86
PRKAB1	Protein kinase, AMP-activated, beta 1 non-catalytic subunit	0,93
PRKAB2	Protein kinase, AMP-activated, beta 2 non-catalytic subunit	0,83
PRKAG1	Protein kinase, AMP-activated, gamma 1 non-catalytic subunit	0,86
PRKAG2	Protein kinase, AMP-activated, gamma 2 non-catalytic subunit	1,47
PRKAG3	Protein kinase, AMP-activated, gamma 3 non-catalytic subunit	0,99
PRKCA	Protein kinase C, alpha	1,89
PRKCB	Protein kinase C, beta	0,90
PRKCE	Protein kinase C, epsilon	0,90
PRKCG	Protein kinase C, gamma	0,94
PTEN	Phosphatase and tensin homolog	1,05
RHEB	Ras homolog enriched in brain	1,27
RHOA	Ras homolog gene family, member A	1,07
RICTOR	RPTOR independent companion of MTOR, complex 2	1,05
RPS6	Ribosomal protein S6	1,03
RPS6KA1	Ribosomal protein S6 kinase, 90kDa, polypeptide 1	1,52
RPS6KA2	Ribosomal protein S6 kinase, 90kDa, polypeptide 2	0,85
RPS6KA5	Ribosomal protein S6 kinase, 90kDa, polypeptide 5	0,80
RPS6KB1	Ribosomal protein S6 kinase, 70kDa, polypeptide 1	0,91

RPS6KB2	Ribosomal protein S6 kinase, 70kDa, polypeptide 2	1,35
RPTOR	Regulatory associated protein of MTOR, complex 1	1,44
RRAGA	Ras-related GTP binding A	0,84
RRAGB	Ras-related GTP binding B	0,66
RRAGC	Ras-related GTP binding C	1,10
RRAGD	Ras-related GTP binding D	1,12
SGK1	Serum/glucocorticoid regulated kinase 1	0,69
STK11	Serine/threonine kinase 11	0,80
STRADB	STE20-related kinase adaptor beta	1,42
TELO2	TEL2, telomere maintenance 2, homolog (S. cerevisiae)	0,96
TP53	Tumor protein p53	1,09
TSC1	Tuberous sclerosis 1	1,37
TSC2	Tuberous sclerosis 2	1,43
ULK1	Unc-51-like kinase 1 (C. elegans)	1,08
ULK2	Unc-51-like kinase 2 (C. elegans)	1,03
VEGFA	Vascular endothelial growth factor A	1,09
VEGFB	Vascular endothelial growth factor B	1,21
VEGFC	Vascular endothelial growth factor C	1,35
YWHAQ	Tyrosine 3-monooxygenase/tryptophan 5-monooxygenase activation protein, theta polypeptide	1,17
ACTB	Actin, beta	1,22
B2M	Beta-2-microglobulin	0,69
GAPDH	Glyceraldehyde-3-phosphate dehydrogenase	0,80
HPRT1	Hypoxanthine phosphoribosyltransferase 1	1,27
RPLP0	Ribosomal protein, large, P0	0,70
HGDC	Human Genomic DNA Contamination	0,72

**The samples were undetectable.*

Table A.5: Titration lines used to determine rapamycin concentration

Concentration (nM)	Frequency of live cells (%)	Proliferation index
Titration line one (control 14)		
0	34,8	2,19
0,05	36,7	1,06
0,1	35,5	1,22
1	47,4	1,56
2	30,7	1,93
Titration line two (control 1)		
0	83,0	2,09
2	78,2	1,65
4	78,5	1,56
Titration line two (patient 1)		
0	76,4	2,27
2	78,5	1,56
4	43,7	1,44

Table A.6: Comparison of live cells with the respective markers for untreated and treated samples in patients and controls.

Markers	Median difference between untreated (-) and treated (+) cells, controls (95% CI)	Median difference between untreated (-) and treated (+) cells, patients (95% CI)	P-value*
$CD3^+$	-0.3 (-2.63, 4.31)	1.4 (-1.90, 3.94)	0.730
$CD3^+CD4^+CD8^-$	2.1 (-2.01, 3.87)	1.6 (-0.98,5.61)	0.548
$CD3^+CD4^+CD25^+$	7.64 (0.50, 18.0)	13.3 (0.61, 27.9)	0.548
Markers within $CD3^+CD4^+CD25^+$			
$CD31^+$	2.18 (-1.09, 8.69)	2.92 (-0.22, 8.41)	>0.999
$CD304^+$	0.56 (-5.27, 3.59)	1.02 (-0.32, 3.62)	0.222
$CD39^+$	3.88 (0.18, 6.91)	10.8 (-0.42, 27.6)	0.151
$CTLA\text{-}4^+$	1.31 (-0.77, 4.97)	2.66 (0.76, 4.01)	0.691
$Helios^+$	1.23 (-0.07, 3.38)	2.66 (0.29, 0.65)	0.897
$FoxP3^+$	1.09 (-1.84, 6.84)	1.36 (-2.35, 10.7)	0.841

**Non-parametric Mann-Whitney test, results were found significant if P < 0.05.*

A.7: Comparison of live cells with the respective markers in T_{reg} for untreated and treated samples in patients and controls.

Markers within $CD25^+$ $FoxP3^+$	Median difference between untreated (-) and treated (+) cells, controls (95% CI)	Median difference between untreated (-) and treated (+) cells, patients (95% CI)	P-value*
$CD31^+$	0.30 (-4.49, 3.15)	0.38 (-0.25, 1.81)	0.548
$CD304^+$	0.51 (-0.31, 2.16)	0.52 (-0.71, 4.17)	0.421
$CD39^+$	0.24 (-6.15, 4.20)	1.69 (-1.34, 7.55)	0.095
$Helios^+$	0.29 (-1.13, 3.14)	0.52 (-0.68, 2.84)	0.691
$CTLA\text{-}4^+$	0.215 (-0.55, 1.93)	0.58 (-0.52, 3.20)	0.421

**Non-parametric Mann-Whitney test, results were found significant if P < 0.05.*